UNIWERSYTET WARMIŃSKO-MAZURSKI W OLSZTYNIE

Wydział Biologii i Biotechnologii

ROZPRAWA DOKTORSKA

MikroRNA i lncRNA jako biomarkery wpływu mikrocystyny-LR na wątrobę i mózg siei *(Coregonus lavaretus)*

w formie trzech spójnych tematycznie artykułów opublikowanych w czasopismach naukowych

mgr Maciej Florczyk
Katedra Biotechnologii w Ochronie Środowiska
Wydział Geoinżynierii

Praca doktorska wykonana w Katedrze Biotechnologii w Ochronie Środowiska
Promotor: prof. dr hab. Paweł Brzuzan

Praca współfinansowana ze środków Narodowego Centrum Nauki przyznanych na podstawie decyzji DEC-2012/07/B/NZ9/01320, DEC-2014/15/N/NZ9/01471, DEC-2016/21/B/NZ9/03566

Olsztyn, 2022

Pragnę złożyć najserdeczniejsze podziękowania

Promotorowi prof. dr hab. Pawłowi Brzuzanowi,
za cierpliwość, opiekę nad rozwojem, przekazaną wiedzę i wiele cennych rad.

Dr hab. inż. Maciejowi Woźnemu,
za cenne wskazówki, pomoc w przygotowaniu pracy oraz wsparcie.

Współpracownikom, Koleżankom i Kolegom z Katedry Biotechnologii w Ochronie Środowiska,
za miłą atmosferę pracy.

Agacie,
za wspólną drogę.

Rodzicom, Dziadkom, Cioci, Wujkowi i Przyjaciołom,
za wsparcie i wytrwałość.

Dziękuję

Spis treści

Spis publikacji wchodzących w skład rozprawy doktorskiej 4

Streszczenie 5

Abstract 6

Wykaz skrótów 7

Opis wyników pracy doktorskiej 8

- Wstęp 8
- Cel badań i hipotezy badawcze 14
- Weryfikacja hipotez 15
  - Zadania badawcze 15
  - Weryfikacja hipotezy 1 16
  - Weryfikacja hipotezy 2 17
  - Weryfikacja hipotezy 3 21
- Stosowane metody 25
- Podsumowanie 27
- Wnioski 28
- Bibliografia 29

Publikacje wchodzące w skład rozprawy doktorskiej 33

Oświadczenia współautorów 79

Spis publikacji wchodzących w skład rozprawy doktorskiej

Publikacja 1: Florczyk M, Brzuzan P, Krom J, Woźny M, Łakomiak A. **miR-122-5p as a plasma biomarker of liver injury in fish exposed to microcystin-LR.** Journal of Fish Diseases. 2016;39:741–51.

IF2016: 2,138; pięcioletni IF2021: 2,689; MNiSW:100 pkt

Praca finansowana ze środków Narodowego Centrum Nauki (DEC-2012/07/B/ NZ9/01320)

Publikacja 2: Florczyk M, Brzuzan P, Łakomiak A, Jakimiuk E, Woźny M. **Microcystin-LR-Triggered Neuronal Toxicity in Whitefish Does Not Involve MiR124-3p.** Neurotoxicity Research. 2019;35:29–40.

IF2019: 2,992; pięcioletni IF2021: 3,771; MNiSW: 70 pkt

Praca finansowana ze środków Narodowego Centrum Nauki (DEC-2014/15/N/NZ9/01471)

Publikacja 3: Florczyk M, Brzuzan P, Woźny M. ***De Novo* Profiling of Long Non-Coding RNAs Involved in MC-LR-Induced Liver Injury in Whitefish: Discovery and Perspectives.** International Journal of Molecular Sciences. 2021;22:941.

IF2021: 4,924; pięcioletni IF2021: 6,132; MNiSW: 140 pkt

Praca finansowana ze środków Narodowego Centrum Nauki (DEC-2016/21/B/NZ9/03566)

Streszczenie

Czynniki antropogeniczne przyczyniają się do wzrostu zakwitów cyjanobakterii (sinic). Większość gatunków sinic produkuje toksyczne dla innych gatunków metabolity wtórne (cyjanotoksyny). Cyjanotoksyny, takie jak mikrocystyny (MC), zagrażają także innym organizmom wodnym i lądowym. MC dostają się do organizmów poprzez absorpcję lub drogą pokarmową. Do wnętrza komórki MC są transportowane aktywnie przez polipeptydy transportujące aniony organiczne (ang. OATP). Skutki toksycznego działania jednego z wariantów MC, mikrocystyny-LR (MC-LR), obserwowane są przede wszystkim w wątrobie. Silna hepatotoksyczność MC-LR wynika m.in. z wysokiej ekspresji OATP w hepatocytach. OATP ulegają ekspresji także w innych narządach, takich jak nerki, mięśnie, czy bariera krew-mózg. W komórce, MC-LR prowadzi m.in. do hiperfosforylacji białek, a nadmierny stres retikulum endoplazmatycznego może uruchamiać cytotoksyczne szlaki sygnałowe. Skutki uszkodzenia wątroby przez MC-LR są porównywalne do skutków jakie powodują inne substancje uszkadzające wątrobę. W farmakologii efekt wywołany przez ogół tych substancji klasyfikowany jest jako DILI (ang. drug-induced liver injury). W diagnostyce uszkodzeń narządów, np. wywołanych DILI, oprócz obserwacji zmian histopatologicznych, wykorzystywane są metody nieinwazyjne. Polegają one na mierzeniu zawartości w płynach ustrojowych cząsteczek specyficznych narządowo - biomarkerów. Powszechnie wykorzystywanymi biomarkerami DILI są enzymy wątrobowe. Jednakże wiele badań zarzuca im brak jednoznacznej specyficzności względem wątroby, a ich liczne izoformy wpływają na trudność w interpretacji wyników. Cząsteczki mające zastąpić wykorzystywane dziś biomarkery, powinny charakteryzować się wyższą specyficznością i czułością, a ich detekcja powinna być możliwa w niewielkiej ilości próby. Z powodu tych cech, biomarkerami nowej generacji mogą stać się niekodujące RNA (ncRNA).

W pracy zbadano wpływ MC-LR na poziomy specyficznych dla wątroby mikroRNA (miRNA) w osoczu siei. Na tle klasycznych metod oceny uszkodzenia wątroby, MiR122-5p wyróżniał się wyższą specyficznością oraz czułością. Ponadto, w pracy zaobserwowano toksyczny dla ośrodkowego układu nerwowego (OUN) przebieg ekspozycji na MC-LR. Zanotowany wzrost ekspresji mRNA glejowego kwaśnego białka włókienkowego (gfap) może wskazywać na indukowane w śródmózgowiu siei zmiany funkcjonalne. Analiza sekwencji nukleotydowej i aminokwasowej gfap siei, wykazała zachowanie elementów struktury ssaczych i rybich odpowiedników. Fragment 3'-UTR mRNA gfap zawierał miejsce rozpoznawane przez MiR124-3p, sugerując zależność funkcjonalną. Jednak badania *in vitro* oparte o system lucyferazowy nie potwierdziły założeń. Nie zaobserwowano również zmian poziomów MiR124-3p w osoczu siei eksponowanej na MC-LR. Dodatkowo, w pracy rozpoczęto badania u siei nad nową klasą biomarkerów - długimi niekodującymi RNA (ang. long noncoding RNA, lncRNA). Te dłuższe niż 200 par zasad niekodujące RNA charakteryzują się zróżnicowaną funkcjonalnością wynikającą z II-rzędowej struktury RNA. W pracy zidentyfikowano sekwencje niekodujące o ekspresji zmienionej przez MC-LR. Toksyna wpłynęła na ekspresję zarówno znanych u innych gatunków lncRNA, jak również nieskatalogowanych dotychczas nowych sekwencji niekodujących. Zależna od czasu ekspozycji na MC-LR zmiana ekspresji lncRNA wskazuje na powiązanie tych cząsteczek z uszkodzeniem i regeneracją wątroby, a także sugeruje możliwość ich potencjalnego wykorzystania w diagnostyce uszkodzenia wątroby. Ponadto, analiza miejsc wiązania MiR122-5p i MiR124-3p w sekwencjach lncRNA, wskazała na możliwe - konieczne do eksperymentalnego potwierdzenia - wzajemne interakcje w przebiegu patogenezy uszkodzenia wątroby i OUN wywołanych MC-LR.

Abstract

Anthropogenic factors contribute to increased blooms of cyanobacteria. Most cyanobacterial species produce secondary metabolites (cyanotoxins) that are toxic to other species. Cyanotoxins, such as microcystins (MCs), also threaten other aquatic and terrestrial organisms. MCs enter organisms through absorption or through the ingestive route. MCs are actively transported into the cell by organic anion transporting polypeptides (OATPs). The toxic effects of microcystin-LR (MC-LR) are observed primarily in the liver. The strong hepatotoxicity of MC-LR is a result of high expression of OATPs in hepatocytes. OATPs are also expressed in other organs such as kidney, muscle, and the blood-brain barrier. In the cell, MC-LR leads to protein hyperphosphorylation, and excessive stress on the endoplasmic reticulum could trigger cytotoxic signaling pathways. The effects of liver damage caused by MC-LR are comparable to those caused by other liver damaging substances. In pharmacology, the effect caused by all these substances is classified as DILI (drug-induced liver injury). For the diagnosis of organ damage, such as that caused by DILI, non-invasive methods are used in addition to the observation of histopathological changes. They are based on measuring the content of organ-specific molecules - biomarkers - in body fluids. Liver enzymes are commonly used as biomarkers of DILI. However, many studies have questioned their lack of clear liver specificity and stated that their multiple isoforms make it difficult to interpret results. The molecules intended to replace the biomarkers used today should have higher specificity and sensitivity and their detection should be possible in a small sample size. Because of these attributes, non-coding RNAs (ncRNAs) may become the next generation biomarkers.

In this thesis, the effect of MC-LR on the levels of liver-specific microRNAs (miRNAs) in whitefish plasma was investigated. Compared to classical methods for assessing liver damage, MiR122-5p was found to have higher specificity and sensitivity. In addition, a central nervous system (CNS) toxicity of MC-LR exposure was observed in this study. The reported increase in mRNA expression of the glial fibrillary acidic protein (gfap) may indicate induced functional changes in the midbrain of whitefish. Nucleotide and amino acid sequence analysis of whitefish gfap, revealed conserved structural elements between mammalian and fish homologs. The 3'-UTR fragment of gfap mRNA contained a site recognized by MiR124-3p, suggesting a functional relationship. However, *in vitro* studies based on the luciferase system did not confirm the hypothesis. Likewise, no changes in MiR124-3p levels were observed in the plasma of whitefish exposed to MC-LR. Additionally, in this thesis, we began studies in whitefish on a new class of biomarkers, long noncoding RNAs (lncRNAs). These noncoding RNAs, which are longer than 200 base pairs, are characterized by diverse functionality resulting from the RNA structure. Noncoding sequences with expression altered by MC-LR were identified. The toxin affected the expression of both lncRNAs known in other species as well as previously uncatalogued novel noncoding sequences. The time-dependent change in lncRNA expression upon exposure to MC-LR indicates a link between these molecules and liver injury and regeneration, and suggests their potential use in the diagnosis of liver injury. Furthermore, analysis of MiR122-5p and MiR124-3p binding sites in lncRNA sequences, indicated possible - needed to be experimentally confirmed - mutual interactions in the pathogenesis of MC-LR-induced liver and CNS damage.

Wykaz skrótów

ALT - aminotransferaza alaninowa

AST - aminotransferaza asparaginianowa

BLAST - ang. Basic Local Alignment Search Tool

ceRNA – ang. competing endogenous RNA

CHOP - ang. C/EBP homologous protein

DILI - ang. Drug-Induced Liver Injury

DLR - system reporterów lucyferazowych (ang. Dual-Luciferase Reporter assay)

GFAP - glejowe kwaśne białko włókienkowe (ang. glial fibrillary acidic protein)

HOTAIR - ang. HOX transcript antisense RNA

HOTTIP - ang. HOXA transcript at the distal tip

HOXA - ang. Homeobox protein Hox-A

HULC - ang. Highly Up-regulated in Liver Cancer

JNK - ang. c-Jun N-terminal kinases

lncRNA - długie niekodujące RNA (ang. long non-coding RNA)

MALAT1 - ang. metastasis associated lung adenocarcinoma transcript 1

miRNA - mikroRNA

MC-LR - mikrocystyna-LR

MFE - minimalna energia swobodna (ang. Minimum Free Energy)

OATP - polipeptydy transportujące aniony organiczne (ang. Organic Anion Transporting Polypeptides)

OUN - Ośrodkowy Układ Nerwowy

RFT - Reaktywne Formy Tlenu

RISC - ang. RNA-induced silencing complex

RNAi - interferencja RNA (ang. RNA interference)

ROC - Receiver Operating Characteristic

UTR - region mRNA niepodlegający translacji, (ang. untranslated region)

Opis wyników pracy doktorskiej

Wstęp

Fotosyntetyczne bakterie prokariotyczne (cyjanobakterie, dawniej sinice), stanowią do 70% całkowitej biomasy fitoplanktonu. Według szacunków, ich wkład w produkcję tlenu przekracza nawet 30% całkowitej produkcji pierwotnej [1], co czyni cyjanobakterie jednym z głównych producentów tlenu. Towarzyszą temu jednak skutki uboczne w postaci toksycznych metabolitów wtórnych - cyjanotoksyn, produkowanych przez niektóre gatunki sinic. Pomimo, że główną przyczyną produkcji cyjanotoksyn jest konkurencja międzygatunkowa, a ich toksyczne efekty wymierzone są przede wszystkim w inne gatunki cyjanobakterii, to nie są one jedynymi wrażliwymi na ich działanie organizmami. Chociaż w naturalnie występujących ekosystemach wodnych ich oddziaływanie na inne organizmy mogłoby pozostać niezauważone, to wywołana przez czynniki antropogeniczne zachwiana równowaga ekosystemów, przenosi skutki działania toksyn także na inne organizmy wodne, a nawet lądowe. Nadmierna eutrofizacja zbiorników wodnych, idąca w parze z podnoszącą się globalną temperaturą, prowadzi do podwyższonej akumulacji produkujących toksyny cyjanobakterii. W rezultacie, zakwity sinic produkujących toksyny (ang. HABs - harmful algal blooms) wpływają pośrednio także na inne organizmy wodne i lądowe, a w skrajnych przypadkach duże stężenia toksyn w zbiornikach wodnych mogą prowadzić do destabilizacji ekosystemów [2].

Cyjanotoksyny, w zależności od wywoływanego efektu toksycznego, klasyfikowane są w czterech głównych kategoriach: hepatotoksyn, cytotoksyn, neurotoksyn oraz dermatotoksyn. Do hepatotoksyn zaliczane są związki, których toksyczne efekty obserwowane są głównie w komórkach wątroby - hepatocytach. Są to na przykład toksyny z grupy mikrocystyn i nodularyna. Natomiast, do cytotoksyn zalicza się na przykład cylindrospermopsynę, wywołującą ogólny toksyczny efekt na narażone na nią komórki (cytotoksyczność). Z kolei neurotoksyny, takie jak anatoksyna lub saxitoksyna, wywołują toksyczny efekt w układzie nerwowym. Do ostatniej kategorii zaliczane są dermatotoksyny, takie jak produkowane przez sinice lipopolisacharydy, które efekt toksyczny wywołują już podczas kontaktu ze skórą.

Zaliczane do hepatotoksyn mikrocystyny (MC), wytwarzane w procesach pozarybosomalnej syntezy białek, przez cyjanobakterie głównie z rodzajów *Microcystis sp.*, *Anabaena sp.*, *Oscillatoria sp.*, *Planktothrix sp*. oraz *Chroococus sp.*, są cyklicznymi heptapeptydami odpornymi na zmienne warunki środowiskowe, jak wysoka temperatura oraz skrajne wartości pH. Okres pół-trwania MC-LR w środowisku wynosi 10 tygodni, a jej rozkład przyspieszyć mogą jedynie wysokie temperatury (powyżej 40 °C) oraz bardzo niskie (<1) i wysokie wartości pH (>9) [3]. Charakterystyczną cechą budowy mikrocystyn, jest obecność dwóch zmiennych oraz pięciu względnie stałych aminokwasów, w tym kluczowym dla biologicznej aktywności, aminokwasem z grupy β-aminokwasów, ADDA [4]. Zmienność aminokwasów, szczególnie w pozycjach drugiej i czwartej, wpływa pośrednio na siłę efektu

toksycznego. Dotychczas zidentyfikowano około 130 wariantów mikrocystyn [5]. Masa cząsteczkowa mikrocystyn, w zależności od wariantu, zawiera się w przedziale od 800 do 1100 Da.

Obecne w środowisku wodnym mikrocystyny dostają się do organizmów poprzez absorpcję lub drogą pokarmową [6]. Ponieważ rozmiar cząsteczki uniemożliwia mikrocystynom pasywne przenikanie przez błony komórkowe, do wnętrza komórki transportowane są przy udziale polipeptydów transportujących aniony organiczne (ang. Organic Anion Transporting Polypeptides, OATP). Wiadomo, że od poziomu ekspresji OATP i związanym z kinetyką transportu typem OATP w komórkach, zależy toksyczność wariantu mikrocystyn, zarówno pod względem narządów dotkniętych toksycznością, rodzajem mechanizmu toksyczności, jak i stopniem wywołanych uszkodzeń [7]. Ekspresja OATP w błonach komórkowych hepatocytów jest na tyle wysoka, że czyni wątrobę głównym celem toksycznego działania mikrocystyn. Obecność leucyny i argininy, odpowiednio, w pozycjach drugiej i czwartej, powoduje, że wariant -LR z powodu swojej budowy łatwiej przenika do hepatocytów, na których błonach komórkowych dominuje typ OATP dobrze odpowiadający hydrofilowej strukturze wariantu -LR [8]. To, jak istotnym elementem toksyczności MC-LR są transportery OATP, sugerują badania prowadzone w zespole profesora Brzuzana, które wskazały, że przerwanie ciągłości syntezy transkryptów OATP może być jednym z mechanizmów obronnych hepatocytów ryb eksponowanych na mikrocystynę-LR (autokleza) [9].

Kanoniczna aktywność (ang. MOA, mode of action) mikrocystyn w komórce polega na wiązaniu fosfataz serynowo-treoninowych PP1 i PP2A. Obecne w komórce mikrocystyny zaburzają mechanizmy regulacyjne oparte na reakcjach fosfo- i defosforylacji [10]. Ponadto, badania nad wpływem mikrocysytny-LR na ludzkie i mysie hepatocyty, dowiodły udział mechanizmów związanych z wywoływaniem w komórce stresu oksydacyjnego [11, 12]. Obserwacje potwierdziły zdolność MC-LR do wiązania dehydrogenazy aldehydowej (ALDH2), co w efekcie prowadzi do nagromadzenia w komórce nadmiernej ilości reaktywnych form tlenu (RFT), których nadmierna akumulacja prowadzi do powstawania stresu oksydacyjnego [11]. Warto zaznaczyć, że oba mechanizmy toksycznego działania mikrocystyn zachodzą jednocześnie, a przewaga jednego mechanizmu nad drugim może zależeć od dawki (narażenie ostre/przewlekłe) oraz od wariantu mikrocystyny [13].

W efekcie, w hepatocytach ssaków i ryb eksponowanych na MC-LR, obserwujemy podobne procesy, obejmujące zarówno produkcję cytokin przeciwzapalnych, deformację cytoszkieletu, uszkodzenie chromatyny, jak i dysfunkcję retikulum endoplazmatycznego [9, 14]. Jednak głównym skutkiem krótkoterminowego, cytotoksycznego działania mikrocystyny-LR obserwowanym na obrazach ultrastruktury komórek wątroby ryb, jest uszkodzenie retikulum endoplazmatycznego oraz cytoszkieletu [9]. Wysoka dawka MC-LR prowadzi do utraty kształtu i morfologii komórek w wyniku inhibicji fosfataz białkowych, co prowadzi do hiperfosforylacji białek, w tym wchodzących w skład cytoszkieletu [15]. Jednocześnie, stres retikulum endoplazmatycznego (wywołany bezpośrednio przez stres oksydacyjny bądź pośrednio przez nadmierne nagromadzenie białek) uruchamia cytotoksyczne szlaki

sygnałowe, prowadząc do aktywacji kinaz JNK i czynnika transkrypcyjnego CHOP. Cytotoksyczne szlaki sygnałowe prowadzą w rezultacie do apoptozy, rzadziej nekrozy, komórek wątroby. W ultrastrukturze wątroby siei potwierdzały to charakterystyczne dla apoptozy zmiany morfologiczne, jak kondensacja chromatyny, pyknoza, karioreksja, fragmentacja DNA, a także obecność ciał apoptotycznych, które występowały bardzo często do drugiego dnia ekspozycji na MC-LR [9].

Obserwacja powyższych wskaźników i procesów przedstawia jednoznaczny obraz hepatotoksycznego działania MC-LR, który powtarza się u różnych gatunków ssaków oraz niższych kręgowców. Owe wskaźniki lub sygnalizatory zdarzeń (signaling events), które w układach biologicznych mogą w mierzalny sposób określać zmiany wywołane ksenobiotykami (tu w znaczeniu substancji, które nie są wytwarzane przez organizm) określa się mianem “biomarkerów”. Obserwacja wywołanych zmian może odbywać się na wielu poziomach: molekularnym, biochemicznym, komórkowym, fizjologicznym, patologicznym lub behawioralnym.

Pomimo, że biopsja i obserwacja zmian histopatologicznych jest uznanym narzędziem diagnostycznym, to w nowoczesnej toksykologii uważana jest już za narzędzie niedopasowane do obecnych standardów i jest, tam, gdzie to możliwe, sukcesywnie zastępowana przez mniej inwazyjne metody. Opublikowane w 2011 roku wspólne stanowisko międzynarodowych towarzystw toksykologicznych Society of Toxicology i EUROTOX przewiduje całkowite zastąpienie tradycyjnej oceny histopatologicznej przez biomarkery oparte na płynach ustrojowych (tzw. płynna biopsja, ang. liquid biopsy). Badanie biomarkerów, zarówno w toksykologii medycznej (na przykład w przypadku testów nowego leku), jak i toksykologii środowiskowej (na przykład w przypadku badania skutków zakwitów sinic), powinno umożliwić przede wszystkim nieinwazyjne, ale też szybkie oraz obarczone małym ryzykiem błędu określenie stanu, w jakim znajduje się badany organizm. Z tego względu, najprostszym sposobem na poszukiwanie nieinwazyjnych biomarkerów uszkodzenia narządów jest poszukiwanie w płynach ustrojowych specyficznych dla danej tkanki składników komórek. Badając ich zmienne poziomy możemy monitorować stan fizjologiczny tych narządów (biomarker monitorujący), jak też diagnozować przyczynę ich odbiegającej od normy ilości (biomarker diagnostyczny).

W diagnozowaniu i monitorowaniu uszkodzeń wątroby, do dziś powszechnie wykorzystywane jest badanie zmian poziomu enzymów wątrobowych, między innymi aminotransferaz alaninowej (ALT) i asparaginianowej (AST), których poziom wzrasta we krwi pod wpływem czynników hepatotoksycznych. Podejście to ma jednak duże ograniczenia. Badania wskazują na brak jednoznacznej specyficzności względem wątroby [16, 17], a także trudności interpretacyjne związane z występowaniem wielu izoform enzymów [18]. Przydatność enzymów wątrobowych w diagnostyce uszkodzenia wątroby często określana jest jako ogólna i pozbawiona dokładności, a w przypadku ostrego uszkodzenia, ich opóźniona detekcja jest niewystarczająca do postawienia szybkiej diagnozy. Przykład wątroby dobrze ilustruje problem, dla rozwiązania którego, badania toksykologiczne nieustannie skupiają się na poszukiwaniach nowej generacji biomarkerów, które będą specyficzne, dokładne oraz czułe.

Dodatkowo, biomarkery nowej generacji powinny być cząsteczkami, które w łatwy i szybki do przeprowadzenia sposób będą mogły informować o stanie fizjologicznym narządów lub stopniu ich uszkodzenia [19].

W ostatnich latach, za cząsteczki, które spełniają wiele z oczekiwanych po biomarkerach nowej generacji założeń, uważa się niekodujące RNA (ang. non-coding RNA, ncRNA). Jest to zróżnicowana pod względem funkcji i długości łańcucha klasa RNA, z której nie powstają klasyczne białka. Niekodujące RNA biorą udział w licznych procesach fizjologicznych oraz patologicznych. Z tego względu, ostatnie dwie dekady przyniosły rosnące zainteresowanie ncRNA, również ze strony toksykologów. Kiedy stało się jasne, że cząsteczki dotychczas uznawane za nieistotne, w rzeczywistości są odpowiedzialne za szereg kluczowych procesów regulacyjnych, zwrócono uwagę na ich zastosowanie w ocenie narażenia i ryzyka ekspozycji na toksyczne substancje [20].

Zróżnicowanie długości sekwencji nukleotydowej jest podstawowym kryterium podziału ncRNA, według którego wyróżnia się krótko- oraz długołańcuchowe cząsteczki. W skład klasy krótkołańcuchowych niekodujących RNA wchodzą między innymi, około 22-nukleotydowe, mikroRNA (ang. microRNA, miRNA). Większość genów kodujących miRNA jest transkrybowana przez polimerazę II, podobnie jak w przypadku mRNA kodujących białka. W uproszczeniu, biologicznie aktywne, dojrzałe miRNA powstają na drodze enzymatycznej obróbki niedojrzałych form (pri-miRNA oraz pre-miRNA) kolejno przez enzymy Drosha oraz Dicer, a następnie, wchodząc w skład kompleksu RISC (ang. RNA-induced silencing complex), stają się biologicznie aktywnymi miRNA. Rola miRNA w kompleksie RISC sprowadza się do rozpoznawania komplementarnej do siebie sekwencji w odcinkach UTR (ang. untranslated region, region nie podlegający translacji) mRNA, tym samym wskazując obecnym w kompleksie białkom z rodziny Argonautów, transkrypt przeznaczony do deadenylacji, i w konsekwencji degradacji całego mRNA przez nukleazy. W przypadku, jeśli komplementarność pomiędzy sekwencjami miRNA a mRNA jest niepełna, kompleks RISC jedynie fizycznie blokuje rybosomowe RNA przed kontynuowaniem translacji, co jednak prowadzi do podobnego efektu wyciszenia ekspresji [21].

Opisany mechanizm jest częścią systemu interferencji RNA (RNAi), zaliczanego do ważnych mechanizmów epigenetycznych. RNAi jest potranskrypcyjnym procesem regulacyjnym, w wyniku którego dochodzi do wyciszenia ekspresji genów, przez promowanie degradacji mRNA lub represję translacji białek. Szacuje się, że tego typu potranskrypcyjnej regulacji może podlegać ponad 60% ludzkich genów kodujących białka [21]. Co ciekawe, według niektórych doniesień, nawet 50% miRNA powstaje z innych niekodujących transkryptów [22], takich jak długie niekodujące RNA (ang. long noncoding RNA, lncRNA).

Te dłuższe niż 200 par zasad niekodujące RNA, dzięki II-rzędowej strukturze RNA, charakteryzują się zróżnicowaną funkcjonalnością. W uproszczeniu, II-rzędowa struktura lncRNA umożliwia interakcje z szeroką gamą zróżnicowanych cząsteczek, przy jednocześnie zachowanej wysokiej specyficzność.

Podobnie, jak w przypadku miRNA, funkcje lncRNA rozpatruje się głównie w ujęciu ich zdolności do regulacji ekspresji genów. W przeciwieństwie jednak do miRNA, regulacja ekspresji genów w przypadku lncRNA odbywa się na wielu poziomach od pre- do post-transkrypcyjnych: poprzez interakcję z DNA, RNA oraz białkami; poprzez zmiany w strukturze i funkcjach chromatyny; poprzez wpływ na splicing RNA, a także jego stabilność oraz translację; wreszcie poprzez interakcje z mikroRNA.

Wzajemne interakcje pomiędzy lncRNA a mikroRNA, przeważnie nie są rozpatrywane jako główne funkcje regulujące ekspresję genów przez lncRNA. Jednak, lncRNA mające możliwość wiązania miRNA są na tyle powszechne, że przyciągają obecnie wiele uwagi. Badania prowadzone w tym kierunku doprowadziły do powstania hipotezy o sieci ceRNA (ang. competing endogenous RNA). Hipoteza zakłada istnienie "sieci", czyli powiązanych na zasadzie sprzężenia zwrotnego, zróżnicowanych ncRNA, które regulują transkrypcję niejako "współzawodnicząc" z mRNA o to, która cząsteczka zwiąże ze sobą miRNA [23]. Na przykład, lncRNA wiążąc miRNA (z języka angielskiego proces ten określany jest potocznie jako "sponging", co w wolnym tłumaczeniu rozumie się jako "pochłanianie" lub też "wsysanie" miRNA przez lncRNA, co w domyśle ma przywoływać obraz gąbki chłonącej wodę) bezpośrednio przyczynia się do zmniejszenia obecnych w puli miRNA, pośrednio tym samym uniemożliwiając degradację mRNA. O powszechności tych procesów, a także możliwości potencjalnego wykorzystania zależności sieci ceRNA w medycynie i diagnostyce, świadczą liczne prace [24–29]. Wśród nich znajdują się także doniesienia o możliwości ograniczania transmisyjności wirusa MERS-CoV (Middle East respiratory syndrome coronavirus), poprzez ingerencję w udział cyrkularnych RNA (circRNA) w procesach propagacji wirusa [30].

Obecność kwasów nukleinowych (w tym niekodujących RNA) we krwi obwodowej związana jest z naturalnymi procesami komórkowymi, od których zależy międzykomórkowa komunikacja i utrzymanie homeostazy. Jak pokazało wiele ostatnich prac, obecność miRNA we krwi obwodowej ssaków wynika głównie z ich stałego transportu w formie związanej z białkami wchodzącymi w skład rodziny argonautów [31, 32]. Te same białka, które wraz z miRNA są składnikami kompleksu RISC, we krwi obwodowej skutecznie chronią miRNA przed degradacją przez licznie występujące we krwi nukleazy. Transport i wymiana materiału komórkowego pomiędzy odległymi komórkami zachodzi też przy wykorzystaniu pęcherzyków zewnątrzkomórkowych, takich jak ektosomy i egzosomy. Egzosomy, których zawartość początkowo uważano za zbędne komórce metabolity, w istocie biorą ważny udział w międzykomórkowej komunikacji, a dużą część ich "ładunku" stanowią niekodujące RNA [33]. Co ciekawe, ekspozycja komórek wątroby na MC-LR wzmaga ekspresję genów związanych z przygotowaniem i wysyłaniem egzosomów do krwioobiegu [34]. Dodatkowo, w przypadku zaprogramowanej lub indukowanej (jak ma to miejsce na przykład po ekspozycji na MC-LR) apoptozy komórek, do krwi obwodowej uwalniane są ciała apoptotyczne zawierające materiał komórkowy obumarłych komórek, który może jeszcze zostać wykorzystany przez inne, zdrowe komórki. Wszystkie

te procesy sprawiają, że stała obecność krążących w krwioobiegu ncRNA, może wzrastać w wyniku zaburzeń i rozwoju chorób.

Początki drogi zmierzającej do wykorzystania krążących we krwi obwodowej miRNA do celów diagnostycznych nie były łatwe. Pierwszy mikroRNA zidentyfikowano i zaklasyfikowano jako niekodujący RNA w 1993 roku [35], natomiast potencjał mikroRNA jako cząsteczek mogących zostać wykorzystanych w diagnostyce, dostrzeżono dopiero w roku 2005 [36]. Jednak użyteczność cyrkulujących w osoczu miRNA jako cząsteczek mogących precyzyjnie określać stan fizjologiczny organizmu, po raz pierwszy zaobserwowano dopiero w 2007 roku. Badanie zmian poziomów miRNA umożliwiło rozróżnienie wariantów chłoniaka B-komórkowego (ang. Diffuse large B-cell lymphoma) [37]. Od tego czasu badania nad funkcjami mikroRNA skupiały się także na ich potencjalnym wykorzystaniu w diagnozowaniu wielu nowotworów, infekcji wirusowych, cukrzycy, chorób metabolicznych i chorób układu krążenia [38].

Prace zespołu profesora Brzuzana dotyczące udziału mikroRNA w regulacji uszkodzenia wątroby ryb przez MC-LR [39–43], doprowadziły do akumulacji wiedzy o wpływie MC-LR na procesy potranskrypcyjnej regulacji genów. Cykl badań poświęcony analizie toksycznego wpływu MC-LR na wątrobę siei *(Coregonus lavaretus)* doprowadził do kompleksowego opracowania miRnomu wątroby siei biorącego udział w odpowiedzi na obecność toksyny [42]. Zidentyfikowano zróżnicowaną gamę miRNA, których ekspresja zmieniała się pod wpływem MC-LR, jednak na szczególną uwagę zasłużyły miRNA biorące udział w rearanżacji cytoszkieletu, metabolizmie komórkowym, regulacji cyklu komórkowego i apoptozy, a także miRNA dla wątroby specyficzne, to znaczy takie, których konstytutywna ekspresja w wątrobie jest na stałym, wysokim poziomie, a ich ekspresja w innych tkankach jest ograniczona.

Cel badań i hipotezy badawcze

Celem rozprawy doktorskiej było określenie możliwości wykorzystania wybranych mikroRNA jako biomarkerów uszkodzenia wątroby (MiR122-5p, MiR92a-3p, let-7c-5p, MiR148a-3p) i mózgu (MiR124-3p) ryb wywołanych mikrocystyną-LR, a także identyfikacja i charakterystyka długich niekodujących RNA biorących udział w uszkodzeniu wątroby ryb wywołanego mikrocystyną-LR.

Przyjęto trzy hipotezy badawcze:

Hipoteza 1: Uszkodzenie wątroby wywołane mikrocystyną-LR przyczyni się do wzrostu ilości krążących we krwi obwodowej mikroRNA, w tym uznawanego za specyficzny i liczny w wątrobie MiR122-5p. Zwiększona ekspresja MiR122-5p wskaże toksyczny dla wątroby przebieg ekspozycji.

Hipoteza 2: Uszkodzenie mózgu wywołane mikrocystyną-LR przyczyni się do wzrostu ilości krążącego we krwi obwodowej uznawanego za specyficzny i liczny w mózgu mikroRNA, MiR124-3p. Związana ze wzrostem ekspresji MiR124-3p we krwi, obniżona ekspresja MiR124-3p w komórkach śródmózgowia siei będzie negatywnie korelować ze zwiększoną ekspresją mRNA gfap, wskazując toksyczny dla mózgu przebieg ekspozycji.

Hipoteza 3: Ekspozycja siei na mikrocystynę-LR przyczyni się do zmian ekspresji profili lncRNA, mogących - poprzez sieć ceRNA - wpływać na przebieg toksycznego uszkodzenia wątroby.

Weryfikacja hipotez

Zadania badawcze

Weryfikacji hipotez podporządkowano następujące zadania badawcze:

Zadanie 1. Profilowanie zmian ekspresji wybranych mikroRNA w osoczu ryb eksponowanych na mikrocystynę-LR i ryb z grupy kontrolnej. Wnioskowanie na temat mocy diagnostycznej wybranych mikroRNA w hepatotoksyczności mikrocystyny-LR u siei.

Zadanie 2. Poznanie sekwencji nukleotydowej cDNA genu *gfap* u siei. W oparciu o uzyskaną sekwencję nukleotydową, wydedukowanie sekwencji aminokwasowej oraz wnioskowanie na temat ewolucji białka. Zdeponowanie sekwencji nukleotydowej i aminokwasowej w bazie banku genów NCBI. Przeprowadzenie analizy *in silico*, w celu wyłonienia potencjalnych miejsc wiązania MiR124-3p do 3'-UTR mRNA gfap.

Zadanie 3. Profilowanie ekspresji mRNA gfap i MiR124-3p w śródmózgowiu ryb eksponowanych na MC-LR i ryb z grupy kontrolnej. Zbadanie regulacyjnych funkcji MiR124-3p względem mRNA gfap, z wykorzystaniem metody podwójnych reporterów lucyferazowych (DLR). Profilowanie ekspresji MiR124-3p w osoczu ryb eksponowanych na MC-LR i ryb z grupy kontrolnej. Wnioskowanie na temat wzajemnych oddziaływań oraz funkcji mRNA gfap i MiR124-3p w mechanizmie neurotoksyczności MC-LR u siei.

Zadanie 4. Poznanie sekwencji długich niekodujących RNA (lncRNA) siei, przez przygotowanie i analizę danych uzyskanych na podstawie sekwencjonowania wysokoprzepustowego (RNA-Seq). Złożenie i analiza jakości uzyskanego transkryptomu referencyjnego. Przeprowadzenie analizy bioinformatycznej, umożliwiającej identyfikację sekwencji lncRNA u siei. Wnioskowanie na temat roli lncRNA w mechanizmie uszkodzenia wątroby przez MC-LR. Zdeponowanie sekwencji transkryptomu referencyjnego oraz wyników analizy bioinformatycznej w bazie NCBI Gene Expression Omnibus.

Weryfikacja hipotezy 1

Jednym z powszechnie występujących miRNA w wątrobie kręgowców jest MiR122-5p [44]. Jak wykazała przekrojowa analiza mikroRNA w transkryptomie myszy, MiR122 stanowił do 70% całej populacji mikroRNA obecnych w wątrobie [45]. U ssaków, MiR122 zaangażowany jest w utrzymanie fenotypu wątroby u dorosłych osobników przez inhibowanie ekspresji genów nie będących genami wątrobowymi [46]. U ludzi MIR122 powiązany jest z ekspresją genów biorących udział w szlakach metabolicznych i związanych z odpowiedzią na stres [47]. Ponieważ utrata funkcji tego mikroRNA prowadzi do procesów nowotworzenia w hepatocytach, jest także klasyfikowany w grupie supresorów nowotworów [48]. U ryb, badania nad MiR122 wykazały jego wysoką konstytutywną ekspresję w wątrobie, a funkcjonalnie, jego zaangażowanie przy wyciszaniu genów biorących udział w degradacji i usuwaniu cholesterolu [44].

Badania na ssakach potwierdziły możliwość wykorzystania MiR122-5p w diagnostyce uszkodzenia wątroby wywołanego przez leki (ang. drug induced liver injury, DILI). DILI to jednostka chorobowa klasyfikująca przypadki uszkodzeń hepatocytów wywołanych ubocznymi skutkami działania leków lub też ich przedawkowania. Do grupy związków chemicznych wywołujących DILI możemy zaliczyć także substancje dostarczane do organizmu z pożywieniem lub wskutek kontaktu ze środowiskiem (ksenobiotyki). Dotychczas, detekcja podwyższonej ekspresji MiR122 we krwi obwodowej gryzoni, umożliwiła diagnostykę DILI wywołaną między innymi acetaminofenem (dostępnym w środkach przeciwbólowych), etanolem, D-galaktozaminą, alkoholem allylowym, α-naftylo isotiocjanatem, trichlorobromometanem i węglanem tetrachlorku [49–52].

Podwyższona ekspresja MiR122-5p we krwi obwodowej ssaków, jest powiązana z często obniżonym poziomem tego miRNA w uszkodzonej wątrobie [44]. Sprzężone z ekspozycją na związki toksyczne, wydostawanie się enzymów wątrobowych (jak na przykład wspomniane ALT, AST) do krwi obwodowej badacze przypisywali nekrozie hepatocytów. Jednak obserwacje ssaczych hepatocytów uszkodzonych pod wpływem stresu oksydacyjnego, rzadko wykazują obecność nekrozy, tym samym sugerując celowy (a na pewno uzasadniony) transport enzymów wątrobowych do krwiobiegu [53]. Podobnie, podwyższona ekspresja kwasów nukleinowych w osoczu, nie musi być jednoznacznie kojarzona z nekrozą. Biorąc pod uwagę, cytowane wyżej, badania nad ultrastrukturą hepatocytów siei po ekspozycji na MC-LR [9], można dostrzec wiele podobieństw w reakcji hepatocytów ssaków i ryb po ekspozycji na MC-LR, także w przypadku przewagi procesów apoptotycznych nad nekrozą. Ponieważ zbliżona wymowa wyników prac innych autorów wskazywała na powiązanie ekspozycji na MC-LR z obniżoną ekspresją specyficznego dla wątroby MiR122-5p w hepatocytach, założono, że podobny mechanizm może także występować u ryb.

Przeprowadzona po raz pierwszy w eksperymencie wchodzącym w skład niniejszej dysertacji doktorskiej, analiza poziomu konstytutywnej ekspresji wybranych miRNA we krwi obwodowej ryb,

wykazała stabilny poziom mikroRNA let-7c-5p, MiR92a-3p, MiR122-5p oraz MiR148-5p u wszystkich ryb z grupy kontrolnej [54] (publikacja 1). Poziom specyficznego dla wątroby MiR122-5p nie był najwyższy wśród wszystkich zbadanych miRNA, jednak jego stała obecność w cyrkulacji, świadczy o jego potencjalnie istotnej roli w utrzymaniu homeostazy, na przykład możliwym wykorzystaniu przez inne niż hepatocyty komórki.

Ekspozycja siei na mikrocystynę-LR, przeprowadzona w tym samym doświadczeniu, spowodowała istotne zwiększenie poziomów badanych miRNA we krwi (Rysunek 2). Najszybsze i najistotniejsze dotyczyło poziomu MiR122-5p. Co ważne, podwyższenie poziomu MiR122-5p we krwi, nastąpiło już w 8 godzinie od podaniu toksyny. Natychmiastowe pojawienie się zwiększonego poziomu MiR122-5p we krwi siei, świadczy o wcześniejszej, niż w przypadku enzymów wątrobowych, możliwości detekcji uszkodzenia wątroby przez MC-LR (podwyższony poziom ALT i AST obserwowano u siei najwcześniej po jednym dniu ekspozycji [9]).

Dalsza, trwająca 24 godziny, ekspozycja ryb na MC-LR, stopniowo zwiększała poziom MiR122-5p cyrkulującego w osoczu. Najwyższy poziom MiR122-5p zaobserwowano po 48 godzinach od podania toksyny. Wzrastający, zależny od czasu narażenia na toksynę, poziom MiR122-5p świadczy o możliwości tej cząsteczki do informowania o przebiegu narażenia. Powyższe wnioski potwierdziła analiza ROC (ang. Receiver Operating Characteristic), która w celu ustalenia wartości decyzyjnej, określa zależność pomiędzy czułością, a swoistością biomarkera (Rysunek 2). Podczas, gdy większość testów używanych w diagnostyce, reprezentuje moc diagnostyczną pomiędzy 0,8 i 0,95, uzyskany wynik (0,976) świadczy o bardzo wysokiej wartości diagnostycznej. **Podsumowując, uzyskane wyniki, pozwoliły pozytywnie zweryfikować pierwszą hipotezę, wskazując także MiR122-5p jako cząsteczkę o potencjalnym zastosowaniu diagnostycznym i monitorującym wpływ MC-LR na wątrobę u ryb.**

Weryfikacja hipotezy 2

Toksyczne działanie mikrocystyn obserwowane u zwierząt, uwidacznia się przede wszystkim w wątrobie. Dlatego, dopiero tragiczne wydarzenia z Caruaru w Brazylii zwróciły uwagę badaczy na inne, niż hepatotoksyczne działanie mikrocystyn. Jak wykazały szczegółowe analizy opublikowane przez Lancet, na skutek wykorzystania zanieczyszczonej mikrocystynami wody, pacjenci lokalnego centrum dializ skarżyli się na zaburzenia widzenia, słuchu, zawroty głowy, wymioty oraz zaburzenia w pracy mięśni. Zatrucie znane jako “Syndrom Caruaru” o symptomach podostej hepatotoksyczności oraz ostrej neurotoksyczności doprowadziło do śmierci 60 osób [55].

Co ciekawe, to w opublikowanej kilka miesięcy wcześniej pracy, zespół badający wpływ zanieczyszczenia wody mikrocystyną-LR na zachowanie danio pręgowanego (*Danio rerio*), po raz pierwszy opisał możliwe, neurotoksyczne działanie toksyny. Jak wykazano, mikrocystyna-LR w naturalnie występujących stężeniach powodowała nie tylko zaburzenia w aktywności i motoryce oraz

obniżoną reakcję na bodźce, ale także obserwowano odległe w czasie skutki, jak na przykład negatywny wpływ na sukces reprodukcyjny [56]. W kolejnych latach, podejrzewany przez badaczy, neurotoksyczny efekt działania MC-LR, obserwowano także w aktywności poruszania się słonecznicy pospolitej (*Leucaspius delineatus*) oraz gatunku z rodzaju *Jenynsia*, *Jenynsia multidentata* [57, 58].

Tak, jak w przypadku wątroby, za obecnością MC-LR w OUN, stoją transportery OATP, obecne w barierze pomiędzy naczyniami krwionośnymi, a tkanką nerwową (tak zwaną barierą krew-mózg). Ich ekspresję potwierdzono u ssaków [7], a także i u ryb [59]. Pomimo, że ta fizyczna i metaboliczna bariera, umożliwiając selektywny transport substancji z krwi do płynu mózgowo-rdzeniowego, przyczynia się do zabezpieczenia układu nerwowego przed szkodliwymi czynnikami [60], nie jest w stanie zapewnić ochrony przed mikrocystynami wykorzystującymi obecne w niej transportery.

Indukowane toksycznym działaniem MC-LR, zwiększone powstawanie RFT, jest szczególnie niebezpieczne dla ośrodkowego układu nerwowego (OUN; ang. central nervous system, CNS). Zwiększona podatność na RFT wynika, między innymi, z dużej zawartość nienasyconych kwasów tłuszczowych, jak również intensywnego metabolizmu tlenowego połączonego ze, stosunkowo małą, aktywnością enzymów antyoksydacyjnych [61]. Ośrodkowy układ nerwowy wraz z obwodowym układem nerwowym, przekazuje informacje z wewnątrz i z zewnątrz ciała, kieruje funkcjami motorycznymi, integruje procesy myślowe, uczenie się oraz pamięć. Złożoność tych funkcji, a także niektóre cechy układu, jak na przykład niezdolność dojrzałych neuronów do podziału oraz silna zależność od glukozy i tlenu, czynią go niezwykle wrażliwym na uszkodzenia [62].

W kontekście badań toksykologicznych, obserwacja zmian zachowania danio pręgowanego, jest powszechnie wykorzystywanym, podstawowym biomarkerem. Pomimo, że jest to, względnie prosta, metoda oceny wpływu badanej substancji na OUN, jest narzędziem etycznie wątpliwym. Nie odpowiada też na podstawowe pytanie, jakie stawia sobie współczesna diagnostyka: w jaki sposób potencjalny biomarker zaangażowany jest w procesy, które pozwala zidentyfikować? *Podejście funkcjonalne* do rozwoju diagnostyki, opiera się na poszukiwaniu takich biomarkerów, których użycie będzie wynikało ze zrozumienia funkcji oraz procesów, w wyniku których obserwuje się pojawienie się biomarkera [63]. Dzięki temu, można nie tylko lepiej poznać mechanizmy zachodzące pod wpływem badanych substancji, ale - jednocześnie rozumiejąc zależności łączące biomarker z procesami - można lepiej projektować rozwiązania łagodzące wpływ substancji, lub odwracać negatywne skutki ich działania.

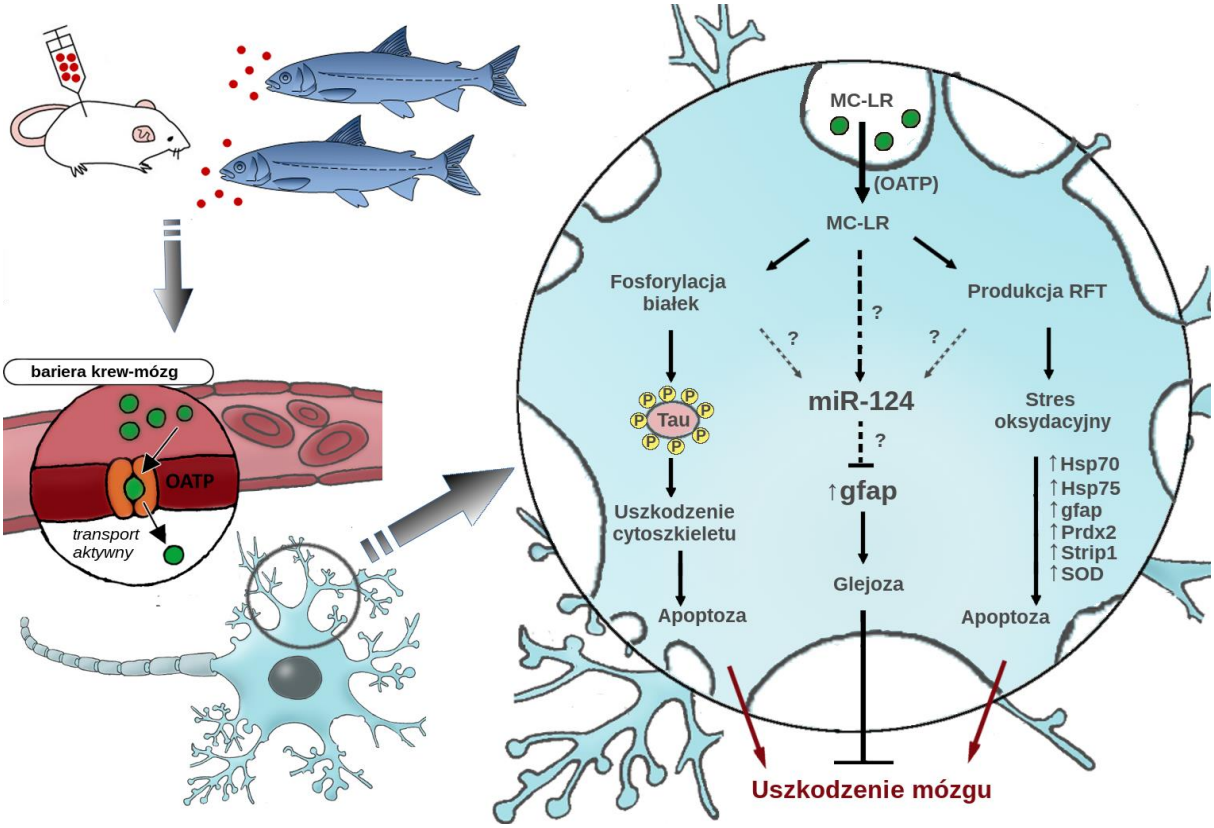
U ssaków, MC-LR wykazuje działanie cytotoksyczne we wszystkich typach komórek mózgu [7], prowadząc do apoptozy oraz degradacji połączeń neuronów [64]. Na poziomie molekularnym, w komórkach OUN kręgowców, białkiem wskaźnikowym m.in. stresu oksydacyjnego jest glejowe kwaśne białko włókienkowe (ang. Glial fibrillary acidic protein, GFAP/Gfap/). Białko GFAP/Gfap jest białkiem filamentów pośrednich, ulegającym ekspresji w licznych komórkach OUN, głównie w astrocytach [65]. U ssaków, zwiększona ekspresja białka GFAP/Gfap jest wskaźnikiem aktywacji komórek gleju gwiaździstego (astrocytów). Aktywacja wywoływana jest czynnikami mogącymi

negatywnie wpłynąć na funkcjonowanie neuronów, takich, jak ksenobiotyki mające działanie neurotoksyczne [66]. W wyniku aktywacji astrocytów, dochodzi do nienowotworowego przerostu i rozrostu astrocytów - glejozy (inaczej zwanej blizną glejową). Aktywne astrocyty uwalniają zarówno cytokiny prozapalne, jak i te, które uczestniczą w procesach naprawczych [67].

Wywołaną podaniem MC-LR, zwiększoną ilość białka Gfap w OUN, po raz pierwszy zaobserwowano u szczurów [68]. Szczury iniekowowane mikrocystyną miały zaniki pamięci, a także obserwowano zaburzenia w nauce. Analiza proteomu oraz ekspresji genów, ujawniła, że na poziomie molekularnym efektem ekspozycji były zmiany w ekspresji oraz ilości białek zaangażowanych w budowę cytoszkieletu (np. białka Tau), rozwój i przeciwdziałanie stresowi oksydacyjnemu (białka szoku cieplnego Hsp70, Hsp75, peroksydazy Prdx2, SOD) oraz apoptozę (Rysunek 1). Aktywację astrocytów zaobserwowała także inna grupa badaczy, podająca szczurom mikrocystyny drogą pokarmową [66].

Skutki toksycznego uszkodzenia komórek OUN przez MC-LR, wynikają z tego samego podłoża molekularnego, co skutki hepatotoksyczności i, być może, prowadzą do nich te same ścieżki sygnałowe. Na powiązania pomiędzy wpływem MC-LR na układ nerwowy, a zaburzoną ekspresją mikroRNA, wskazały doświadczenia przeprowadzone u nicienia, *Caenorhabditis elegans* [69]. Brak wątroby u nicieni powoduje, że wywołana przez MC-LR neurotoksyczność uwidacznia się najwyraźniej. Analiza ekspresji genów wykazała, że zmianom poziomów licznych miRNA, towarzyszyły zmiany ekspresji genów uczestniczących w procesach związanych z zachowaniem neurologicznym (ang. neurological behavior), rozwojem neuronów, transdukcją sygnałów komórkowych oraz transportem międzybłonowym.

Prowadząc badania doktorskie nad cząsteczkami miRNA mogącymi stać się biomarkerami uszkodzenia mózgu siei przez MC-LR, w pracy skupiono się na mikroRNA uznawanych za specyficzne dla układu nerwowego. Jedną z hipotez pracy dotyczącej wpływu MC-LR na mózg siei [70] (publikacja 2), było założenie, że wysoka konstytutywna ekspresja miRNA w OUN utrzymuje mRNA gfap na niskim poziomie, a wzrost ekspresji gfap w mózgu siei po ekspozycji na MC-LR może wynikać ze spadku poziomu ekspresji miRNA (Rysunek 1). Wśród kandydatów założenia spełnił m.in. MiR124-3p, którego konstytutywna ekspresja w mózgu szczurów była 260-krotnie większa niż w pozostałych tkankach [52]. Ponadto, jak wykazała wstępna analiza bioinformatyczna przeprowadzona na sekwencji mRNA gfap innego gatunku ryby (łosoś atlantycki, *Salmo salar*), gfap ma w swojej sekwencji nukleotydowej potencjalne miejsce wiązania MiR124-3p. Dodatkowo, MiR124 wielokrotnie pojawiał się na listach mikroRNA, których ekspresja ulegała zmianie pod wpływem czynników uszkadzających ośrodkowy układ nerwowy [71].



Rysunek 1. Prawdopodobne drogi pobierania i toksyczności mikrocystyny w komórkach nerwowych kręgowców. Mikrocystyna na drodze transportu aktywnego (białkowe przenośniki OATP) przenika barierę krew-mózg i wnika do komórek nerwowych. Niepożądane działania mikrocystyny wynikają ze sprzężonych mechanizmów prowadzących do apoptozy komórek i, w następstwie, uszkodzenia mózgu. Inhibicja fosfataz prowadzi do hiperfosforylacji białek biorących udział w budowie cytoszkieletu (np. białka Tau). Powoduje to zaburzenia w strukturze komórkowej, utratę kształtu komórek i, w konsekwencji, apoptozę. Nagromadzenie reaktywnych form tlenu (RFT) prowadzi do stresu oksydacyjnego, przed którym komórka broni się m.in. zwiększając ekspresję białek (SOD, Prdx2) odpowiedzialnych za eliminację wolnych rodników. Następuje także indukcja ekspresji białek biorących udział w odpowiedzi na stres (Hsp70, Hsp75 oraz glejowego kwaśnego białka włókienkowego - gfap). Hipoteza jednej z prac wchodzących w skład rozprawy, zakładała, że niektóre miRNA (np. MiR124) mogłyby uczestniczyć w regulacji procesów obronnych komórek, np. negatywnej modulacji białka gfap, w celu utrzymania homeostazy.

W drugiej z prac wchodzących w skład rozprawy doktorskiej ustalono, że **gfap siei zachowuje elementy struktury ssaczych i rybich odpowiedników** (Rysunek 2) oraz potwierdzono wstępne analizy bioinformatyczne, że **fragment 3'-UTR mRNA gfap siei zawiera miejsce rozpoznawane przez MiR124-3p.** Przeprowadzone badania dostarczyły nowych informacji na temat struktury i potencjalnych mechanizmów regulujących ekspresję białka wskaźnikowego uszkodzenia komórek nerwowych u siei. Wykonanie badań z wykorzystaniem modelu innego niż ssaczy dodatkowo pozwoliło na wnioskowanie o ewolucji analizowanego białka. W pracy wykazano, że uzyskana sekwencja nukleotydowa gfap siei zawiera w swoim regionie 3'-UTR potencjalny element rozpoznawany przez MiR124-3p. Otrzymane sekwencje zostały zdeponowane w nukleotydowej i białkowej bazach danych NCBI (numery akcesyjne: MG182670 oraz AUM86163). Otrzymany fragment 3'-UTR z wyłonionym miejscem wiązania, posłużył następnie do skonstruowania wektorów plazmidowych, wykorzystanych

w technice biologii molekularnej opartej na badaniu poziomu bioluminescencji w systemie lucyferazowym DLR (ang. Dual-Luciferase Reporter) (Rysunek 2).

Ustalenie sekwencji mRNA białka gfap siei umożliwiło profilowanie zmian ekspresji mRNA gfap siei w śródmózgowiu ryb eksponowanych na MC-LR w porównaniu do ryb z grup kontrolnych. W grupie eksponowanej na MC-LR wykazano **podwyższoną ekspresję mRNA gfap** zaczynającą się od siódmego dnia trwania eksperymentu. **Sugeruje to, że u siei, oprócz działania hepatotoksycznego, MC-LR wywołuje skutki toksyczne dla układu nerwowego.**

Jednakże, podwyższony poziom mRNA gfap, nie był powiązany ze spadkiem poziomu ekspresji MiR124-3p w śródmózgowiu siei. Jednocześnie, poziom ekspresji MiR124-3p w osoczu ryb eksponowanych nie różnił się od poziomu ekspresji w osoczu ryb z grupy kontrolnej. Wreszcie, brak negatywnej korelacji pomiędzy mRNA gfap, a MiR124-3p potwierdziły eksperymenty *in vitro* oparte na badaniu poziomu bioluminescencji w systemie lucyferazowym (DLR). **Uzyskane wyniki doprowadziły do odrzucenia hipotezy o mechanizmie supresji mRNA gfap przez MiR124-3p (hipoteza druga).**

Weryfikacja hipotezy 3

Pomimo, że wiedza o sekwencjach i funkcjach poszczególnych lncRNA u ludzi i organizmów modelowych katalogowana jest w licznych bazach danych, to badacze chcący rozbudowywać bazy o sekwencje nowych gatunków, muszą zmierzyć się z istotnym problemem: w przeważającej większości sekwencje lncRNA nie są, bądź są bardzo słabo zachowane pomiędzy gatunkami [72]. Dlatego, choć badacze dzięki rozwojowi technik sekwencjonowania, są w stanie w szybkim tempie charakteryzować nowe sekwencje u kolejnych organizmów, to poznanie funkcji poszczególnych transkryptów pozostaje daleko w tyle za tempem deponowania nowych transkryptów. Pionierzy nie mogą porównywać swoich sekwencji z sekwencjami zdeponowanymi w bazach danych innych gatunków, a niejednokrotnie zdarza się tak, że np. lncRNA o podobnych funkcjach u człowieka i u myszy mogą mieć sekwencje odmienne, bądź podobne tylko w małym fragmencie [72].

Z tego powodu, w badaniach nad lncRNA tak, jak w przypadku strategii poszukiwania nowych biomarkerów, rozsądnym jest wykorzystanie *podejścia funkcjonalnego*, tzn. nastawionego, najpierw na poznanie funkcji danej sekwencji niekodującej, a następnie zakatalogowaniu jej wraz z sekwencjami o podobnych, bądź identycznych funkcjach u innych organizmów. Dlatego, w ostatniej z prac wchodzących w skład dysertacji, pierwszym krokiem było wyłonienie sekwencji lncRNA biorących udział w mechanizmie uszkodzenia wątroby siei przez MC-LR (publikacja 3). Do realizacji tego celu, ekspozycję siei na MC-LR prowadzono przez 9 dni. Próby pobierano w dniu 1, 6 oraz 9. Wyizolowane RNA sekwencjonowano z wykorzystaniem sekwenatora Illumina HiSeq4000 (Rysunek 2).

Analiza danych RNA-Seq jest szczególnie trudna i obarczona większym prawdopodobieństwem błędu u taksonów bez ustalonego genomu referencyjnego, takich jak sieja. Z tego powodu w pracy zastosowano metodę alternatywną, polegającą na złożeniu (*de novo*), na podstawie sekwencjonowanych

prób, transkryptomu (genomu) referencyjnego. Analiza kompletności uzyskanego genomu referencyjnego, wykazała najwyższą uzyskaną do tej pory, wśród transkryptomów referencyjnych siei, kompletność z sekwencjami zdeponowanymi w bazie OrthoDB [73]. Uzyskany genom referencyjny, udostępniono w publicznie dostępnej bazie danych Dryad pod numerem DOI: 10.5061/dryad.tb2rbnzz4.

Sekwencje pozostałe po odfiltrowaniu transkryptów kodujących, sklasyfikowano w trzech kategoriach. Pierwszą grupę stanowiły transkrypty niekodujące posiadające podobieństwo z transkryptami zdeponowanymi w bazach danych sekwencji niekodujących (grupa znanych ncRNA). Wśród konserwowanych u siei sekwencjach transkryptów niekodujących, zidentyfikowano 94 transkrypty lncRNA, których ekspresja uległa zmianie pod wpływem ekspozycji na MC-LR. Znalazły się tutaj na przykład transkrypty takich lncRNA, jak **HOXA, HOTTIP, HOTAIR** oraz **HULC**, natomiast ekspresja transkryptu rozpoznanego jako **MALAT1** była obniżona. Weryfikacja ich ekspresji za pomocą Real-Time PCR potwierdziła obserwowane w analizie bioinformatycznej zmiany. Wymienione lncRNA od lat pojawiają się w literaturze w kontekście procesów nowotworzenia u ssaków. Na przykład, podwyższoną ekspresję lncRNA MALAT1 obserwowano w przypadku raka płuc oraz raka wątrobowokomórkowego, natomiast jego obniżoną ekspresją charakteryzują się rak jelita grubego oraz rak piersi [74], wskazując na to, że swoją obecnością - w zależności od zaburzenia - może hamować bądź wspomagać rozwój nowotworów.

Jak wspomniano we wstępie, badanie sieci ceRNA w uszkodzeniach wywołanych MC-LR może przyczynić się do głębszego zrozumienia procesów wynikających z interakcji pomiędzy lncRNA, miRNA i mRNA, jak też wykorzystania tych zależności w projektowaniu nowych biomarkerów. Do sprawdzenia hipotezy o potencjalnym udziale sieci ceRNA w uszkodzeniu wątroby przez MC-LR, wykorzystano narzędzie RNAhybrid [75]. Uzyskane sekwencje konserwowanych u siei lncRNA przeanalizowano pod kątem obecności miejsc wiązania MiR122-5p. Wśród transkryptów z przynajmniej jednym miejscem wiązania znajdował się transkrypt o podwyższonej ekspresji - lncRNA HULC. U ssaków, wyciszenie MiR122-5p przez lncRNA HULC obserwowane było w rozwoju kostniakomięsaka [76]. Co ciekawe, jak stwierdzono w innej pracy, intensywny rozwój komórek raka wątrobowokomórkowego zachodził tylko przez kooperację lncRNA HULC z lncRNA MALAT1. Autorzy wykazali, że tylko podwyższona ekspresja obu tych lncRNA prowadziła do opisanego efektu [77], nie wyjaśnili jednak molekularnych zależności leżących u podstaw tej kooperacji. Być może obserwowane efekty mogły wynikać z zależności łączącej lncRNA HULC z MiR122-5p, którego obniżoną ekspresję również obserwowano w rozwoju komórek raka wątrobowokomórkowego [78]. Co więcej, podwyższona ekspresja cyrkulującego we krwi MALAT1 została niedawno zaobserwowana u pacjentów cierpiących na choroby nowotworowe wywodzące się z układu chłonnego [79], wskazując na możliwość wykrycia tej cząsteczki w krwioobiegu i potencjalnego wykorzystania jako narzędzia diagnostycznego.

Drugą grupę stanowiły transkrypty, które nie miały potencjału kodującego lub otwartej ramki

odczytu, natomiast narzędzie BLAST (ang. Basic Local Alignment Search Tool) odnalazło ich sekwencje we fragmentach 3'-UTR zdeponowanych w banku genów sekwencjach mRNA. Grupa obejmowała niezależne od sekwencji kodujących fragmenty niekodujące, w literaturze określane jako autonomiczne transkrypty 3'-UTR. Do rozdzielenia cząsteczki mRNA na niezależne od siebie fragmenty zawierające część kodującą oraz część niekodującą 3'-UTR, dochodzi na drodze potranskrypcyjnego cięcia mRNA [80]. W pracy, do tej grupy zaklasyfikowano tylko te transkrypty niekodujące, które posiadały swój odpowiednik wśród rozpoznanych transkryptów kodujących białka (odfiltrowanych na początku analizy). Pozwoliło to na porównanie profili ekspresji obu grup transkryptów wywodzących się z tego samego mRNA.

Porównanie ekspresji par transkryptów wykazało przeważnie ten sam kierunek zmian. Na przykład, jeśli transkrypty zidentyfikowane jako autonomiczne 3'-UTR miały podwyższoną ekspresję po ekspozycji na MC-LR, to odpowiadające temu samemu mRNA transkrypty kodujące, również miały podwyższoną ekspresję. Ponadto, analiza zróżnicowanej ekspresji w trzech punktach poboru prób (1, 6 i 9 dni od rozpoczęcia ekspozycji) pokazała podobieństwa pomiędzy szóstym, a dziewiątym dniem ekspozycji, w których kierunek i rozkład zmian ekspresji był podobny. Również analiza wyrażeń ontologii genów (ang. GO terms) potwierdziła podobieństwa funkcjonalne pomiędzy profilem ekspresji dni szóstego i dziewiątego.

Natomiast, na tym tle wyróżniał się dzień pierwszy ekspozycji, w którym jednoczesną podwyższoną ekspresję zaobserwowano aż u 82% transkryptów, a obniżoną jedynie u 11%. Pod względem ontologii genów, dzień pierwszy, w porównaniu do dnia szóstego i dziewiątego, charakteryzował się zwiększoną ekspresją transkryptów zaangażowanych w regulację transkrypcji oraz obniżonym poziomem transkryptów zaangażowanych w regulację aktywności enzymatycznej. **Powyższe różnice świadczą o odwzorowaniu w profilach ekspresji niekodujących transkryptów, przynajmniej dwóch etapów przebiegu uszkodzenia wątroby siei wywołanego przez ekspozycję na MC-LR: początkowego uszkodzenia i następującej po nim regeneracji**. Te obserwacje pokrywają się z obserwacjami ultrastruktury hepatocytów siei eksponowanych na MC-LR [9] i **świadczą o potencjalnej wysokiej specyficzności lncRNA w diagnozowaniu przebiegu uszkodzenia i regeneracji wątroby.**

Co ciekawe, poziom ekspresji części par wywodzących się z tego samego mRNA zmieniał się w przeciwnych kierunkach. Biorąc pod uwagę hipotezę mówiącą o regulatorowej roli mechanizmu skracania mRNA [81], na uwagę zasłużyły pary, gdzie ekspresja autonomicznych transkryptów 3'-UTR była podwyższona, a ekspresja transkryptów zawierających sekwencje kodujące obniżona lub nie uległa zmianie. Uważa się, że dzięki mechanizmowi skracania mRNA, komórka, usuwając z mRNA miejsca wiązania miRNA, chroni przed zmniejszeniem puli kodujących białka mRNA [81]. Jak poprzednio, analiza ontologii genów w parach o przeciwstawnym kierunku ekspresji, wykazała wyraźną różnicę pomiędzy pierwszym, a szóstym i dziewiątym dniem ekspozycji.

Ostatnią grupę analizowanych lncRNA stanowiły sekwencje niekodujące, które nie posiadały

podobieństwa z żadną sekwencją wśród sekwencji zdeponowanych w wykorzystanych w analizie bazach danych. Zaklasyfikowano je jako nowe, niepoznane u innych gatunków sekwencje niekodujące. W celu potwierdzenia różnic pomiędzy uzyskanymi transkryptami niekodującymi, a transkryptami zawierającymi sekwencje kodujące, transkrypty porównano pod względem najmniejszej energii swobodnej (ang. minimum free energy, MFE), zawartości par GC oraz długości sekwencji. Porównanie wykazało istotne różnice we wszystkich trzech parametrach. **Strukturalne różnice pomiędzy transkryptami niekodującymi, a transkryptami zawierającymi sekwencje kodujące, uwiarygodniły przyjętą w pracy nową metodę identyfikacji sekwencji niekodujących u gatunków bez genomu referencyjnego.** Wśród nowych transkryptów lncRNA, ekspozycja na MC-LR spowodowała zmianę ekspresji 4 429 transkryptów, z czego podwyższoną ekspresję miało 1 739 transkryptów, natomiast obniżoną ekspresję miało 2 689 transkryptów. Analiza Real-Time PCR potwierdziła zmiany ekspresji wybranych transkryptów nowych lncRNA.

Wśród sekwencji zaklasyfikowanych jako nowe lncRNA, narzędzie RNAhybrid odnalazło 142 sekwencje posiadające przynajmniej jedno silne miejsce wiązania MiR122-5p. Jeżeli uszkodzenie wątroby przez MC-LR prowadzi do wiązania MiR122-5p przez tak liczne lncRNA, może to stanowić jedną z przyczyn tłumaczących obniżanie poziomu tego mikroRNA w wątrobie pod wpływem MC-LR. Co więcej, zrozumienie aktywnego zaangażowania sieci ceRNA w regulację uszkodzenia wątroby przez MC-LR może prowadzić do pełniejszego zrozumienia mechanizmów działania mikrocystyn, ale też i innych ksenobiotyków. Zanim jednak do tego dojdzie, w pierwszej kolejności powinniśmy skupić się na możliwości zrozumienia i wykorzystania sieci ceRNA do poznania nowych biomarkerów procesów, które chcielibyśmy regulować [79, 82]. Eksperymentalne potwierdzenie związku pomiędzy poziomami ekspresji poszczególnych składników sieci zaangażowanej w procesy uszkodzenia wątroby przez MC-LR, a następnie potwierdzenie ich obecności we krwi obwodowej, powinno być następstwem prac stanowiących niniejszą rozprawę.

Zależności pomiędzy miRNA, a lncRNA obserwowane w wątrobie, mogą dotyczyć również mózgu. Wśród sekwencji nowych lncRNA o zmienionej ekspresji w wątrobie znalazły się 84 sekwencje posiadające przynajmniej jedno silne miejsce wiązania z MiR124-5p. Być może stabilny poziom MiR124-3p w mózgu siei po ekspozycji na MC-LR, po części kontrolowany jest przez niektóre z nowych lncRNA. Chociaż wytypowane w wątrobie lncRNA nie muszą ulegać ekspresji w mózgu, to biorąc pod uwagę kompletność uzyskanego *de novo* transkryptomu wątroby z sekwencjami zdeponowanymi w bazie OrthoDB, jest prawdopodobne, że część zidentyfikowanych lncRNA będzie ulegać zróżnicowanej ekspresji także w innych tkankach siei, w tym w mózgu. Założenie to dodatkowo uprawdopodabniają badania przeprowadzone na ssakach, z których wynika, że nawet 40% znanych u ssaków lncRNA ulega ekspresji w mózgu [83].

Stosowane metody

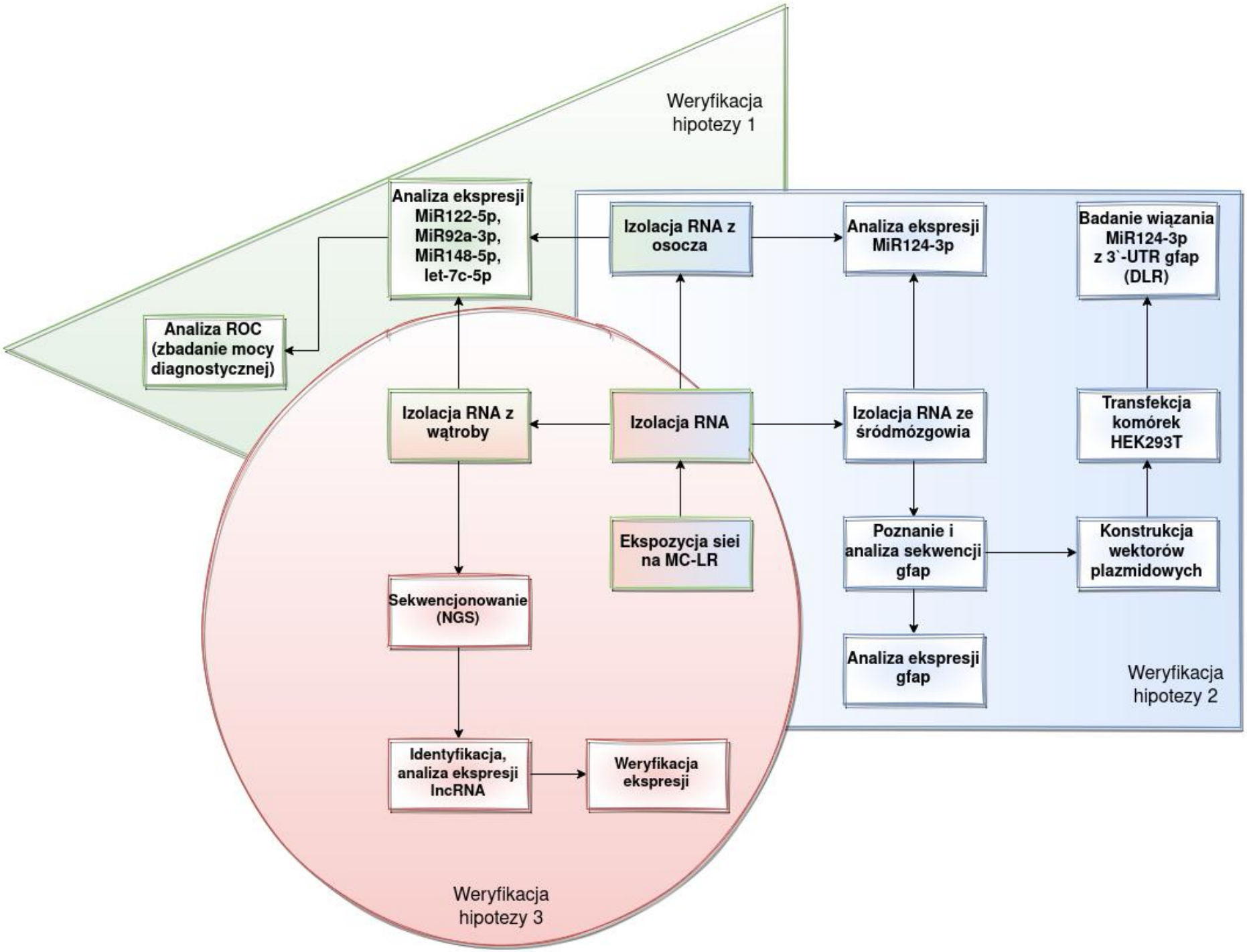
Schematyczną reprezentację metod stosowanych przy realizacji celu badań przedstawiono na Rysunku 2 (rysunek zamieszczono na następnej stronie).

Metodologia badawcza obejmowała między innymi:

* ekspozycję ryb na mikrocystynę-LR,
* izolację całkowitego RNA z wątroby, śródmózgowia i osocza,
* otrzymywanie cDNA z mRNA, lncRNA i miRNA,
* profilowanie ekspresji mRNA, lncRNA i miRNA z wykorzystaniem Real-Time PCR,
* konstrukcję wektorów plazmidowych,
* hodowlę *in vitro* komórek HEK-293T,
* transfekcję komórek HEK-293T z wykorzystaniem plazmidów z system podwójnych reporterów lucyferazowych (DLR),
* identyfikację długich niekodujących RNA siei na podstawie procesowania i analizy danych NGS.

Szczegółową metodologię zamieszczono w załączonych publikacjach.

Rysunek 2. Graficzne przedstawienie metod stosowanych przy realizacji celu badań oraz weryfikacji hipotez badawczych. Każda z figur geometrycznych reprezentuje jedną z trzech hipotez badawczych. W obrębach figur geometrycznych przedstawiono metodologie badawcze wspólne przy weryfikacji wszystkich hipotez (fragmenty nakładających się na siebie figur), jak i specyficzne dla celów weryfikacji poszczególnych hipotez.


Weryfikacja hipotezy 1
Analiza ekspresji MiR122-5p, MiR92a-3p, MiR148-5p, let-7c-5p
Izolacja RNA z osocza
Analiza ekspresji MiR124-3p
Badanie wiązania MiR124-3p z 3`-UTR gfap (DLR)
Analiza ROC (zbadanie mocy diagnostycznej)
Izolacja RNA z wątroby
Izolacja RNA
Izolacja RNA ze śródmózgowia
Transfekcja komórek HEK293T
Ekspozycja siei na MC-LR
Poznanie i analiza sekwencji gfap
Konstrukcja wektorów plazmidowych
Sekwencjonowanie (NGS)
Analiza ekspresji gfap
Weryfikacja hipotezy 2
Identyfikacja, analiza ekspresji lncRNA
Weryfikacja ekspresji
Weryfikacja hipotezy 3

Podsumowanie

Uszkodzenie wątroby siei przez MC-LR spowodowało wzrost krążących we krwi obwodowej specyficznych dla wątroby mikroRNA. Wśród nich MiR122-5p może być rozważony jako cząsteczka o potencjalnym zastosowaniu diagnostycznym i monitorującym wpływ MC-LR na wątrobę ryb. W drugiej z prac wchodzących w skład rozprawy doktorskiej ustalono, że gfap siei zachowuje elementy struktury ssaczych i rybich odpowiedników oraz potwierdzono, że fragment 3'-UTR mRNA gfap siei zawiera miejsce rozpoznawane przez MiR124-3p. Profilowanie zmian ekspresji mRNA gfap siei w śródmózgowiu ryb eksponowanych na MC-LR w porównaniu do ryb z grup kontrolnych wykazało, że w grupie eksponowanej na MC-LR obserwowano podwyższoną ekspresję mRNA gfap zaczynającą się od siódmego dnia trwania eksperymentu. Sugeruje to, że u siei, oprócz działania hepatotoksycznego, MC-LR wywołuje skutki toksyczne dla układu nerwowego. Jednakże, podwyższony poziom mRNA gfap, nie był powiązany ze spadkiem poziomu ekspresji MiR124-3p w śródmózgowiu siei. Jednocześnie, poziom ekspresji MiR124-3p w osoczu ryb eksponowanych nie różnił się od poziomu ekspresji w osoczu ryb z grupy kontrolnej. Wreszcie, brak negatywnej korelacji pomiędzy mRNA gfap, a MiR124-3p potwierdziły eksperymenty in vitro oparte na badaniu poziomu bioluminescencji w systemie lucyferazowym (DLR). W trzeciej z prac wchodzących w skład rozprawy doktorskiej zidentyfikowano transkrypty lncRNA, których ekspresja uległa zmianie pod wpływem ekspozycji na MC-LR. Zmiana ekspresji dotyczyła na przykład transkryptów takich lncRNA, jak HOXA, HOTTIP, HOTAIR, HULC oraz MALAT1. Ponadto, w profilach ekspresji niekodujących transkryptów zaobserwowano przynajmniej dwa etapy przebiegu uszkodzenia wątroby siei wywołanego przez ekspozycję na MC-LR: początkowego uszkodzenia i następującej po nim regeneracji. Te obserwacje pokrywają się z obserwacjami ultrastruktury hepatocytów siei eksponowanych na MC-LR i świadczą o potencjalnej wysokiej specyficzności lncRNA w diagnozowaniu przebiegu uszkodzenia i regeneracji wątroby.

Wnioski

1. Uszkodzenie wątroby wywołane mikrocystyną-LR przyczyniło się do wzrostu ilości krążących we krwi obwodowej cząsteczek MiR122-5p, MiR92a-3p oraz MiR148a-3p, wskazując toksyczny dla wątroby przebieg ekspozycji. Wśród badanych mikroRNA, wzrost ilości krążących cząsteczek MiR122-5p nastąpił najszybciej. Analiza ROC potwierdziła wysoką czułość i specyficzność cząsteczki MiR122-5p w diagnozowaniu uszkodzenia wątroby u siei.
2. Uszkodzenie mózgu wywołane mikrocystyną-LR przyczyniło się do wzrostu ekspresji mRNA gfap w śródmózgowiu siei, wskazując na toksyczny dla mózgu przebieg ekspozycji. Wzrost ekspresji mRNA gfap nie był związany z obniżoną ekspresją MiR124-3p, wskazując na brak regulacji ekspresji mRNA gfap przez MiR124-3p. Brak regulacji potwierdziły badania oparte o system lucyferazowy. Ilość krążącego we krwi MiR124-3p pozostała stała przez cały okres prowadzenia ekspozycji, wykluczając wykorzystanie tej cząsteczki jako biomarkera uszkodzenia mózgu u siei.
3. Ekspozycja siei na mikrocystynę-LR przyczyniła się do zmian ekspresji profili lncRNA, wskazując na powiązanie tych cząsteczek z uszkodzeniem i regeneracją wątroby siei. Odnalezione w sekwencjach zidentyfikowanych lncRNA miejsca wiązania MiR122-5p i MiR124-3p wskazują na potencjalny – konieczny do eksperymentalnego potwierdzenia – udział sieci ceRNA w patogenezie narządów wywołanej MC-LR.

Bibliografia

1. Paerl HW, Fulton RS, Moisander PH, Dyble J. Harmful freshwater algal blooms, with an emphasis on cyanobacteria. TheScientificWorldJournal. 2001;1:76–113.

2. Christoffersen K. Ecological implications of cyanobacterial toxins in aquatic food webs. Phycologia. 1996;35:42–50.

3. Harada K-i, Tsuji K, Watanabe MF, Kondo F. Stability of microcystins from cyanobacteriaIII. Effect of pH and temperature. Phycologia. 1996;35:83–8.

4. Dawson RM. Review article the toxicology of microcystins. 1998;36:953–62.

5. Rinehart KL, Namikoshi M, Choi BW. Structure and biosynthesis of toxins from blue-green algae (cyanobacteria). Journal of Applied Phycology. 1994;6:159–76.

6. Cazenave J, Wunderlin DA, Krause E, Pflugmacher S, Wiegand C. Uptake, tissue distribution and accumulation of microcystin-RR in Corydoras paleatus, Jenynsia multidentata and Odontesthes bonariensis: A field and laboratory study. 2005;75:178–90.

7. Feurstein D, Holst K, Fischer a, Dietrich DR. Oatp-associated uptake and toxicity of microcystins in primary murine whole brain cells. Toxicology and applied pharmacology. 2009;234:247–55.

8. Greer B, Meneely JP, Elliott CT. Uptake and accumulation of Microcystin-LR based on exposure through drinking water: An animal model assessing the human health risk. Scientific Reports. 2018;8:4913.

9. Woźny M, Lewczuk B, Ziółkowska N, Gomułka P, Dobosz S, Łakomiak A, et al. Intraperitoneal exposure of whitefish to microcystin-LR induces rapid liver injury followed by regeneration and resilience to subsequent exposures. Toxicology and Applied Pharmacology. 2016;313:68–87.

10. Mackintoshl C, Beatti A, Fujiki H. Cyanobacterial microcystin-LR is a potent and specific inhibitor of protein phosphatases 1 and 2A from both mammals and higher plants. 1990;264:187–92.

11. Chen T, Cui J, Liang Y, Xin X, Owen Young D, Chen C, et al. Identification of human liver mitochondrial aldehyde dehydrogenase as a potential target for microcystin-LR. Toxicology. 2006;220:71–80.

12. Weng D, Lu Y, Wei Y, Liu Y, Shen P. The role of ROS in microcystin-LR-induced hepatocyte apoptosis and liver injury in mice. Toxicology. 2007;232:15–23.

13. McLellan NL, Manderville RA. Toxic mechanisms of microcystins in mammals. Toxicology Research. 2017;6:391–405.

14. Xie LC and P. Mechanisms of Microcystin-induced Cytotoxicity and Apoptosis. Mini-Reviews in Medicinal Chemistry. 2016.

15. Zhou M, Tu W-w, Xu J. Mechanisms of microcystin-LR-induced cytoskeletal disruption in animal cells. Toxicon. 2015;101:92–100.

16. Nathwani RA, Pais S, Reynolds TB, Kaplowitz N. Serum alanine aminotransferase in skeletal muscle diseases. Hepatology. 2005;41:380–2.

17. Burhop K, Gordon D, Estep T. Review of hemoglobin-induced myocardial lesions. Artificial cells, blood substitutes, and biotechnology. 2004;32:353–74.

18. Yang R-Z, Blaileanu G, Hansen BC, Shuldiner AR, Gong D-W. cDNA Cloning, Genomic Structure, Chromosomal Mapping, and Functional Expression of a Novel Human Alanine Aminotransferase. Genomics. 2002;79:445–50.

19. Ganzleben C, Antignac J-P, Barouki R, Castaño A, Fiddicke U, Klánová J, et al. Human biomonitoring as a tool to support chemicals regulation in the European Union. International Journal of Hygiene and Environmental Health. 2017;220 2 Pt A:94–7.

20. Dempsey JL, Cui JY. Long Non-Coding RNAs: A Novel Paradigm for Toxicology. Toxicological Sciences. 2017;155:3–21.

21. Lewis BP, Burge CB, Bartel DP. Conserved seed pairing, often flanked by adenosines, indicates that thousands of human genes are microRNA targets. Cell. 2005;120:15–20.

22. Saini HK, Griffiths-Jones S, Enright AJ. Genomic analysis of human microRNA transcripts. Proceedings of the National Academy of Sciences of the United States of America. 2007;104:17719–24.

23. Salmena L, Poliseno L, Tay Y, Kats L, Pandolfi PP. A ceRNA hypothesis: The Rosetta Stone of a hidden RNA language? Cell. 2011;146:353–8.

24. Qi X, Zhang D-H, Wu N, Xiao J-H, Wang X, Ma W. ceRNA in cancer: Possible functions and clinical implications. Journal of Medical Genetics. 2015;52:710–8.

25. Bai Z, Sun H, Li X, Wu J, Yuan H, Zhang G, et al. Time-ordered dysregulated ceRNA networks reveal disease progression and diagnostic biomarkers in ischemic and dilated cardiomyopathy. Cell Death Discovery. 2021;7:296.

26. Guan X, Yao Y, Bao G, Wang Y, Zhang A, Zhong X. Diagnostic model of combined ceRNA and DNA methylation related genes in esophageal carcinoma. PeerJ. 2020;8:e8831.

27. Zhang J, Lou W. A Key mRNA-miRNA-lncRNA Competing Endogenous RNA Triple Sub-network Linked

to Diagnosis and Prognosis of Hepatocellular Carcinoma. Frontiers in Oncology. 2020;10:340.

28. Long J, Bai Y, Yang X, Lin J, Yang X, Wang D, et al. Construction and comprehensive analysis of a ceRNA network to reveal potential prognostic biomarkers for hepatocellular carcinoma. Cancer Cell International. 2019;19:90.

29. Yang L, Lu P, Yang X, Li K, Chen X, Qu S. Excavating novel diagnostic and prognostic long non-coding RNAs (lncRNAs) for head and neck squamous cell carcinoma: An integrated bioinformatics analysis of competing endogenous RNAs (ceRNAs) and gene co-expression networks. Bioengineered. 2021;12:12821–38.

30. Zhang J, Han C, Song K, Chen W, Ungerleider N, Yao L, et al. The long-noncoding RNA MALAT1 regulates TGF-β/Smad signaling through formation of a lncRNA-protein complex with Smads, SETD2 and PPM1A in hepatic cells. PLOS ONE. 2020;15:e0228160.

31. Arroyo JD, Chevillet JR, Kroh EM, Ruf IK, Pritchard CC, Gibson DF, et al. Argonaute2 complexes carry a population of circulating microRNAs independent of vesicles in human plasma. Proceedings of the National Academy of Sciences. 2011;108:5003–8.

32. Florijn BW, Duijs JMGJ, Levels JH, Dallinga-Thie GM, Wang Y, Boing AN, et al. Diabetic Nephropathy Alters the Distribution of Circulating Angiogenic MicroRNAs Among Extracellular Vesicles, HDL, and Ago-2. Diabetes. 2019;68:2287–300.

33. Xie Y, Dang W, Zhang S, Yue W, Yang L, Zhai X, et al. The role of exosomal noncoding RNAs in cancer. Molecular Cancer. 2019;18:37.

34. Biales AD, Bencic DC, Flick RW, Delacruz A, Gordon DA, Huang W. Global transcriptomic profiling of microcystin-LR or -RR treated hepatocytes (HepaRG). Toxicon: X. 2020;8:100060.

35. Lee RC, Feinbaum RL, Ambros V. The C. Elegans heterochronic gene lin-4 encodes small RNAs with antisense complementarity to lin-14. Cell. 1993;75:843–54.

36. Calin GA, Ferracin M, Cimmino A, Di Leva G, Shimizu M, Wojcik SE, et al. A microRNA signature associated with prognosis and progression in chronic lymphocytic leukemia. New England Journal of Medicine. 2005;353:1793–801.

37. Lawrie CH, Soneji S, Marafioti T, Cooper CDO, Palazzo S, Paterson JC, et al. MicroRNA expression distinguishes between germinal center B cell-like and activated B cell-like subtypes of diffuse large B cell lymphoma. International Journal of Cancer. 2007;121:1156–61.

38. Wang J, Chen J, Sen S. MicroRNA as Biomarkers and Diagnostics. Journal of Cellular Physiology. 2016;231:25–30.

39. Brzuzan P, Woźny M, Ciesielski S, Łuczyński MK, Góra M, Kuźmiński H, et al. Microcystin-LR induced apoptosis and mRNA expression of p53 and cdkn1a in liver of whitefish (Coregonus lavaretus L.). Toxicon: Official Journal of the International Society on Toxinology. 2009;54:170–83.

40. Brzuzan P, Wony M, Woliska L, K. uczyski M. Discovering the Role of MicroRNAs in Microcystin-Induced Toxicity in Fish. In: Radis-Baptista G, editor. An Integrated View of the Molecular Recognition and Toxinology - From Analytical Procedures to Biomedical Applications. InTech; 2013.

41. Łakomiak A, Brzuzan P, Jakimiuk E, Florczyk M, Woźny M. miR-34a and bcl-2 expression in whitefish (Coregonus lavaretus) after microcystin-LR exposure. Comparative Biochemistry and Physiology Part B: Biochemistry and Molecular Biology. 2016;193:47–56.

42. Brzuzan P, Florczyk M, Łakomiak A, Woźny M. Illumina Sequencing Reveals Aberrant Expression of MicroRNAs and Their Variants in Whitefish (Coregonus lavaretus) Liver after Exposure to Microcystin-LR. PloS One. 2016;11:e0158899.

43. Łakomiak A, Brzuzan P, Jakimiuk E, Florczyk M, Woźny M. Molecular characterization of the cyclin-dependent protein kinase 6 in whitefish (Coregonus lavaretus) and its potential interplay with miR-34a. Gene. 2019;699:115–24.

44. Thakral S, Ghoshal K. miR-122 is a unique molecule with great potential in diagnosis, prognosis of liver disease, and therapy both as miRNA mimic and antimir. Current Gene Therapy. 2015;15:142–50.

45. Lagos-Quintana M, Rauhut R, Yalcin A, Meyer J, Lendeckel W, Tuschl T. Identification of Tissue-Specific MicroRNAs from Mouse. Current Biology. 2002;12:735–9.

46. Coulouarn C, Factor VM, Andersen JB, Durkin ME, Thorgeirsson SS. Loss of miR-122 expression in liver cancer correlates with suppression of the hepatic phenotype and gain of metastatic properties. Oncogene. 2009;28:3526–36.

47. Girard M, Jacquemin E, Munnich A, Lyonnet S, Henrion-Caude A. miR-122, a paradigm for the role of microRNAs in the liver. Journal of Hepatology. 2008;48:648–56.

48. Hsu S-h, Wang B, Kota J, Yu J, Costinean S, Kutay H, et al. Essential metabolic, anti-inflammatory, and anti-tumorigenic functions of miR-122 in liver. The Journal of Clinical Investigation. 2012;122:2871–83.

49. Wang K, Zhang S, Marzolf B, Troisch P, Brightman A, Hu Z, et al. Circulating microRNAs, potential biomarkers for drug-induced liver injury. Proceedings of the National Academy of Sciences. 2009;106:4402–7.

50. Zhang S, Chen L, Jung EJ, Calin GA. Targeting microRNAs with small molecules: Between Dream and Reality. Clinical pharmacology and therapeutics. 2010;87:754–8.

51. Starckx S, Batheja A, Verheyen GR, Jonghe SD, Steemans K, Dijck BV, et al. Evaluation of miR-122 and other biomarkers in distinct acute liver injury in rats. Toxicologic pathology. 2013;41:795–804.

52. Laterza OF, Lim L, Garrett-Engele PW, Vlasakova K, Muniappa N, Tanaka WK, et al. Plasma microRNAs as sensitive and specific biomarkers of tissue injury. Clinical Chemistry. 2009;55:1977–83.

53. Contreras-Zentella ML, Hernández-Muñoz R. Is Liver Enzyme Release Really Associated with Cell Necrosis Induced by Oxidant Stress? Oxidative Medicine and Cellular Longevity. 2016;2016.

54. Florczyk M, Brzuzan P, Krom J, Woźny M, Łakomiak A. miR-122-5p as a plasma biomarker of liver injury in fish exposed to microcystin-LR. Journal of Fish Diseases. 2016;39:741–51.

55. Pouria S, de Andrade a, Barbosa J, Cavalcanti R, Barreto V, Ward C, et al. Fatal microcystin intoxication in haemodialysis unit in Caruaru, Brazil. The Lancet. 1998;352:21–6.

56. Baganz D, Staaks G, Steinberg C. Impact of the cyanobacteria toxin, microcystin-lr on behaviour of zebrafish, danio rerio. Water Research. 1998;32:948–52.

57. Baganz D, Staaks G, Pflugmacher S, Steinberg CEW. Comparative study of microcystin-LR-induced behavioral changes of two fish species, Danio rerio and Leucaspius delineatus. Environmental toxicology. 2004;19:564–70.

58. Cazenave J, Nores ML, Miceli M, Díaz MP, Wunderlin D a, Bistoni M a. Changes in the swimming activity and the glutathione S-transferase activity of Jenynsia multidentata fed with microcystin-RR. Water research. 2008;42:1299–307.

59. Steiner K, Zimmermann L, Hagenbuch B, Dietrich D. Zebrafish Oatp-mediated transport of microcystin congeners. Archives of Toxicology. 2015;1–11.

60. Ballabh P, Braun A, Nedergaard M. The blood-brain barrier: An overview: Structure, regulation, and clinical implications. Neurobiology of Disease. 2004;16:1–13.

61. Watts ME, Pocock R, Claudianos C. Brain Energy and Oxygen Metabolism: Emerging Role in Normal Function and Disease. Frontiers in Molecular Neuroscience. 2018;11:216.

62. Purves D, Williams SM. Neuroscience. 2nd edition. Sinauer Associates 2001; 2001.

63. Califf RM. Biomarker definitions and their applications. Experimental Biology and Medicine. 2018;243:213–21.

64. Feurstein D, Stemmer K, Kleinteich J, Speicher T, Dietrich DR. Microcystin congener- and concentration-dependent induction of murine neuron apoptosis and neurite degeneration. Toxicological sciences : an official journal of the Society of Toxicology. 2011;124:424–31.

65. Middeldorp J, Hol EM. GFAP in health and disease. Progress in Neurobiology. 2011;93:421–43.

66. Li X-B, Zhang X, Ju J, Li Y, Yin L, Pu Y. Alterations in neurobehaviors and inflammation in hippocampus of rats induced by oral administration of microcystin-LR. Environmental Science and Pollution Research. 2014;21:12419–25.

67. Li K, Li J, Zheng J, Qin S. Reactive Astrocytes in Neurodegenerative Diseases. Aging and Disease. 2019;10:664–75.

68. Li G, Cai F, Wang J. A Proteomic Analysis of MCLR-induced Neurotoxicity: Implications for Alzheimer's Disease. 2012;127:485–95.

69. Saul N, Chakrabarti S, Stürzenbaum SR, Menzel R, Steinberg CEW. Neurotoxic action of microcystin-LR is reflected in the transcriptional stress response of Caenorhabditis elegans. Chemico-Biological Interactions. 2014;223:51–7.

70. Florczyk M, Brzuzan P, Łakomiak A, Jakimiuk E, Woźny M. Microcystin-LR-Triggered Neuronal Toxicity in Whitefish Does Not Involve MiR124-3p. Neurotoxicity Research. 2019;35:29–40.

71. Sun P, Liu DZ, Jickling GC, Sharp FR, Yin K-J. MicroRNA-based therapeutics in central nervous system injuries. Journal of Cerebral Blood Flow & Metabolism. 2018;38:1125–48.

72. Wang J, Zhang J, Zheng H, Li J, Liu D, Li H, et al. Neutral evolution of "non-coding" complementary DNAs. Nature. 2004;431:1–2.

73. Kriventseva EV, Kuznetsov D, Tegenfeldt F, Manni M, Dias R, Simão FA, et al. OrthoDB v10: Sampling the diversity of animal, plant, fungal, protist, bacterial and viral genomes for evolutionary and functional annotations of orthologs. Nucleic Acids Research. 2019;47:D807–11.

74. Sun Y, Ma L. New Insights into Long Non-Coding RNA MALAT1 in Cancer and Metastasis. Cancers. 2019;11.

75. Krüger J, Rehmsmeier M. RNAhybrid: microRNA target prediction easy, fast and flexible. Nucleic Acids Research. 2006;34 Web Server issue:W451–454.

76. Kong D, Wang Y. Knockdown of lncRNA HULC inhibits proliferation, migration, invasion, and promotes apoptosis by sponging miR-122 in osteosarcoma. Journal of Cellular Biochemistry. 2018;119:1050–61.

77. Wu M, Lin Z, Li X, Xin X, An J, Zheng Q, et al. HULC cooperates with MALAT1 to aggravate liver cancer

stem cells growth through telomere repeat-binding factor 2. Scientific Reports. 2016;6.

78. Kishikawa T, Otsuka M, Tan PS, Ohno M, Sun X, Yoshikawa T, et al. Decreased miR122 in hepatocellular carcinoma leads to chemoresistance with increased arginine. Oncotarget. 2015;6:8339–52.

79. Fernandes M, Marques H, Teixeira AL, Medeiros R. ceRNA Network of lncRNA/miRNA as Circulating Prognostic Biomarkers in Non-Hodgkin Lymphomas: Bioinformatic Analysis and Assessment of Their Prognostic Value in an NHL Cohort. International Journal of Molecular Sciences. 2021;23:201.

80. Navarro E, Mallén A, Hueso M. Dynamic Variations of 3′UTR Length Reprogram the mRNA Regulatory Landscape. Biomedicines. 2021;9:1560.

81. Malka Y, Steiman-Shimony A, Rosenthal E, Argaman L, Cohen-Daniel L, Arbib E, et al. Post-transcriptional 3-UTR cleavage of mRNA transcripts generates thousands of stable uncapped autonomous RNA fragments. Nature Communications. 2017;8.

82. Ye C, Zhu S, Yuan J. Construction of ceRNA Network to Reveal Potential Biomarkers in Crohn's Disease and Validation in a TNBS Induced Mice Model. Journal of Inflammation Research. 2021;14:6447–59.

83. Briggs JA, Wolvetang EJ, Mattick JS, Rinn JL, Barry G. Mechanisms of Long Non-coding RNAs in Mammalian Nervous System Development, Plasticity, Disease, and Evolution. Neuron. 2015;88:861–77.

Publikacje wchodzące w skład rozprawy doktorskiej

Journal of Fish Diseases 2016, **39**, 741–751 doi:10.1111/jfd.12406



miR-122-5p as a plasma biomarker of liver injury in fish exposed to microcystin-LR

M Florczyk[1], P Brzuzan[1], J Krom[2], M Woźny[1] and A Łakomiak[1]

1 Department of Environmental Biotechnology, Faculty of Environmental Sciences, University of Warmia and Mazury in Olsztyn, Olsztyn, Poland

2 Department of Salmonid Research in Rutki, Inland Fisheries Institute in Olsztyn, Olsztyn, Poland

Abstract

Recent studies have shown the presence of large amounts of microRNAs (miRNAs; miRs) from damaged cells in the peripheral blood. In this study, we investigated the levels of miRNAs circulating in the blood plasma of whitefish (*Coregonus lavaretus*) after exposure to microcystin-LR. We used real-time PCR to examine the relative expression of plasma levels of 4 miRNAs (miR-122-5p and let-7c-5p, the liver-enriched microRNAs, miR-148a-3p which promotes the hapatospecific phenotype in mammals, and miR-92a-3p, a cell proliferation and angiogenesis promoter, potentially hepatocarcinogenic) during the first 48 h after exposure to MC-LR. We observed a rapid increase of miR-122-5p levels 8 h after exposure ($P < 0.05$), which continued to the end of the experiment. Our results demonstrated that the plasma miR-122-5p was indicative of MC-LR-induced liver injury, exhibiting areas under the curve close to 1 in ROC analysis (AUC = 0.976, $P < 0.001$). Although plasma levels of miR-148a-3p and miR-92a-3p were significantly elevated by the end of the experiment, their discriminative power was lower than reported for the miR-122-5p. Based on these results and reports on miRNA-based diagnosis of liver injuries in mammals, plasma miR-122-5p could be considered as a robust, new generation diagnostic biomarker in fish, helpful for the non-invasive diagnosis of liver damage.

Correspondence *M Florczyk, Department of Environmental Biotechnology, Faculty of Environmental Sciences, University of Warmia and Mazury in Olsztyn, Słoneczna 45G, 10-709 Olsztyn, Poland (e-mail: maciej.florczyk@uwm.edu.pl)*

Keywords: circulating microRNA, fish, hepatotoxicity, microcystin-LR.

Introduction

Exposure to toxic chemicals often leads to cellular damage. One of the most common causes of hepatocytes contents escaping into the bloodstream is liver injury caused by various compounds. Drug-induced liver injury (DILI) is a serious concern for public health as well as for drug development and approval (Kaplowitz 2001; Lee 2003; Senior 2007) and remains a leading cause of acute liver injury in many parts of the world. Due to lack of reliable biomarkers for early detection, the mechanisms involved in DILI are still not fully understood (Urban, Daly & Aithal 2014).

Blood levels of alanine aminotransferase (ALT) and aspartate aminotransferase (AST) are the two most important indicators of liver injury, in addition to a variety of other non-routine predictive biomarkers (Ozer *et al.* 2008). Under normal conditions, blood levels of ALT and AST are low, but they can become significantly elevated as a result of exposure to hepatotoxic compounds. Measurement of enzyme activity is generally a reliable method; however, there are several limitations to the use of blood levels of ALT and AST as biomarkers in liver injury. They cannot fully meet the needs of diagnosis because their specificity is not limited to the liver. ALT activity is also associated with muscle necrosis (Nathwani *et al.* 2005) and elevated AST activity with heart and skeletal muscle injury (Burhop, Gordon & Estep 2004). Although ALT and AST activity is increased in cases of drug- or alcohol-induced liver

© 2015 John Wiley & Sons Ltd

Journal of Fish Diseases

toxicity, alcohol consumption, hepatitis or metastatic carcinoma, both enzymes have multiple isoforms, which makes them harder to identify (Panteghini, Renze & van Solinge 2006). Moreover, serum activity levels of ALT and AST do not always correlate with histomorphological changes (Ozer *et al.* 2008). In spite of their limitations, ALT and AST are still commonly used as predictors of hepatocytes damage.

Despite much research, no novel biomarkers of liver injuries have yet been found, mainly due to a failure to meet the requirements of sensitivity and accuracy, which are critical aspects for novel biomarker discovery. MicroRNAs are a class of endogenously expressed, small, single-stranded, non-coding RNAs that play key roles in the regulation of gene expression in a broad spectrum of biological processes. miRs mediate post-transcriptional gene regulation by binding to and repressing specific messenger RNA targets. Interestingly, a number of microRNAs have been found in the blood stream of many organisms, including humans (Gilad *et al.* 2008). These findings triggered interest in their use as potential diagnostic tools. To date, most studies on circulating miRNAs have focused on identification and discrimination between human diseases. However, the success in identifying circulating miRNAs related with cancer, hepatitis or heart condition, raised interest in utilizing circulating miRNAs in toxicant-induced toxicity. Although it has been found that plasma/serum levels of miRNA expression change in response to exposure to diverse toxicants (Sonkoly & Pivarcsi 2011; Yokoi & Nakajima 2011), little is known about circulating miRNAs in drug-induced liver toxicity. The first studies conducted with rodents reported alterations in the serum of liver-enriched miRNAs as a result of liver damage caused by toxicants (Wang *et al.* 2009). These alterations not only paralleled changes in the activity of the aminotransferases that are commonly used to diagnose liver damage, but also occurred much earlier than changes in aminotransferase activity (Laterza *et al.* 2009; Wang *et al.* 2009). Recent studies have reported that plasma or serum liver-enriched microRNAs could be used as precocious, sensitive biomarkers for liver injuries caused by various pharmaceutical compounds (Zhang *et al.* 2010; Su *et al.* 2012).

Despite the potential application of circulating microRNAs as biomarkers of tissue injury in mammals, there is still a lack of research on the use of miRNAs to diagnose liver damage in non-mammalian species such as fish. This seems crucial as fishes are exposed to various naturally occurring compounds, many of which are potent toxins. This is important from the analytical point of view to obtain samples for monitoring MC-LR-induced damages with non-invasive procedure. MicroRNAs, along with other parameters determined in plasma, could be useful as biomarkers. Being easy to collect and study in large populations, they could be helpful in screening or epidemiological studies (Sedan *et al.* 2013).

Therefore, in this study, we selected four abundant liver miRNAs, which have been implicated in various biological processes and considered previously as biomarkers of liver injury in mammals (Table 1). The miR-122-5p is expressed mainly in the liver at very high levels and was found to be a more specific indicator of liver lesions than traditional liver enzymes, AST or ALT. Following liver injury by prolonged graft warm ischaemia times, miR-122-5p and miR-148a-3p expression significantly decreased in the liver and increased in serum (Farid *et al.* 2012). The miR-92a-3p expression is implicated in hepatocellular carcinoma development in humans, and the miR levels in the plasma show a high diagnostic value (Shigoka *et al.* 2010). Finally, the let-7c expression was found to be significantly upregulated in whitefish liver after microcystin-LR treatment (Brzuzan *et al.* 2012). We

Table 1 Details of selected microRNAs of this study. The miRNA nomenclature followed the miRBase v. 21 (ssa; *Salmo salar*)

miRNA	miRNA sequence	Putative biological process[a]	miRNA reference
ssa-miR-122-5p	uggagugugacaaugguguuug	Fatty-acid metabolism, maintenance of adult liver phenotype	MIMAT0032301
ssa-miR-148a-3p	ucagugcauuacagaacuuugu	Promotes the hepatospecific phenotype, tumour suppressor	MIMAT0032380
ssa-miR-92a-3p	uauugcacuugucccggccugu	Cell proliferation, angiogenesis promoter	MIMAT0032708
ssa-let-7c-5p	ugagguaguagguuguaugguu	Signal transduction	MIMAT0032265

[a]Based on the literature review; see text for details.

© 2015 John Wiley & Sons Ltd

aimed first at detecting these miRNAs in the plasma of whitefish (*C. lavaretus*) and then asked whether the microRNAs could serve as biomarkers of MC-LR-induced liver injury in fish exposed to MC-LR, a known hepatotoxic compound widely occurring in marine and fresh waters (Dawson 1998; Lee *et al.* 2015). Using quantitative method (Real-Time PCR), we investigated changes in the levels of the four microRNAs in the peripheral blood of whitefish treated with sublethal dose of MC-LR for 8, 24 and 48 h. We found miR-122-5p to be a very sensitive and robust indicator of MC-LR-induced liver damage, after 8 h of the treatment. Moreover, we observed altered levels of plasma miR-148a-3p and miR-92a-3p at the end of the experiment; however, both miRs showed less discriminative power than miR-122-5p.

Materials and methods

Fish exposure to MC-LR

Hatchery-reared juveniles of European whitefish (*Coregonus lavaretus*, 98.8 ± 8.5 g mean weight, 24.0 ± 0.7 cm mean length) were held at the Department of Salmonid Research in Rutki (Inland Fisheries Institute in Olsztyn, Poland). The fish were acclimated for 2 weeks at 10 °C. During the acclimation period, the whitefish were fed four times a day (Skretting). After acclimatization, the fish were deprived of food for 2 days, then anaesthetized by immersion in etomidate solution (Kazuń & Siwicki 2012) prior to injection. The MC-LR dosage was selected based on our earlier study in whitefish (Brzuzan *et al.* 2009). Chemical standard of MC-LR (purity ≥95%; HPLC) was obtained from Enzo Life Sciences (Enzo Biochem, Inc.) and dissolved in saline solution (0.8% NaCl) as a vehicle solvent. The prepared solution contained 10 μg of MC-LR per 200 μL of volume set for each intraperitoneal injection. Fifteen (Exposed) whitefish individuals received single intraperitoneal injections (0.5 × 25 mm needle) of MC-LR (100 μg kg^{-1} body wt.; 10 μg•200 μL^{-1} of 0.8% NaCl), and in the same way, 11 control fish were injected with an equal volume of saline solution alone. Following injection, the fish were placed in separate single-pass flow-through tanks supplied with system (surface) water for 48 h (pH 7.5; oxygen saturation >90%; ammonium <0.134 mg L^{-1}). Finally, 5 whitefish sampled immediately prior to placing in flow-through tanks were taken as an initial control (0 h) and were used for measuring constitutive expression levels of the miRs in the plasma. Water temperature was measured once a day. The 95% confidence interval of the temperature in the tanks with exposed and control fish was 8–9 °C.

Collection of fish plasma samples

At the times of collection (0 h and after 8, 24 and 48 h), the fishes were anesthetized (Kazuń & Siwicki 2012) and around 2 mL of whole blood was taken from the caudal vein using S-Monovette® K3 EDTA (Sarstedt). Then, the fish were killed and the liver was dissected out to examine if gross changes of the organ occurred, being indicative of the hepatotoxic effect of MC-LR (Ashworth & Mason 1946). After collection, the blood was mixed by gently inverting the tube several times and immediately centrifuged at 13 000 ***g*** at room temperature for 5 min. The plasma layer (approximately 300 μL) from the top of the tube was transferred into a fresh tube. Plasma was stored at −20 °C during sample collection, shipped on dry ice and stored at −80 °C in the laboratory until RNA extraction. All animals used in this study were handled in accordance with the regulations set forth by the Local Ethical Commission in No. 100/2011 issued on 23 November 2011.

Total RNA extraction and reverse transcription using the modified stem-loop method

Total RNA was extracted from 80 μL of plasma from control and MC-treated whitefish using a mirVana isolation kit (Life Technologies) according to the manufacturer's protocol with modifications. After thawing, samples were briefly centrifuged and 10 volumes of lysis/binding Buffer were added. Samples were vortexed vigorously for 1 min. For total RNA extraction from plasma, we used a method recently published by (Roberts, Coenen-Stass & Wood 2014). To normalize sample-to-sample variation in the RNA isolation procedure, an exogenous spike-in control of 3 μL of synthetic 5 nM cel-miR-39-3p (5′-UCACCGGGUGUAA AUCAGCUUG-3′) was added. Then, 80 μL of homogenate additive was added and mixed by inverting the tube several times before it was left on ice for 10 min. Next, 800 μL of acid phenol: chloroform was added and the mixture was vortexed for 1 min. To separate the aqueous and organic

© 2015 John Wiley & Sons Ltd

phases, the tubes were centrifuged for 5 min at maximum speed (13 000 ***g***) at room temperature. About 300 μL of upper phase was then transferred into a fresh tube. Next, 1.25 volumes of 99.8% ethanol at room temperature were added, and the entire solution was transferred into individual filter cartridges before centrifugation for 30 s at 10 000 ***g***. Initial washing was conducted with 700 μL of washing buffer 1, followed by two washes with 500 μL of washing buffer 2/3. RNA was eluted from the washed filter cartridges with 50 μL of preheated (95 °C) elution solution. The extracted RNA was immediately used in the next step and stored at −80 °C.

To study miRNA expression, we adapted the stem-loop RT-PCR method (Xue *et al.* 2008). Specific stem-loop reverse transcription primers were designed (Table 2). Each primer consisted of 8 nucleotides specific to the 3′ end of a miRNA and nucleotides complementary to the universal reverse primer. Reverse transcription (RT) was performed using a RevertAid™ First Strand cDNA Synthesis Kit (Thermo Scientific). Each reaction mixture for cDNA synthesis contained 8 μL of extracted RNA and 1 μL of a 100 μM solution of stem-loop RT primer that was specific to the microRNA (Table 2). Then, the remaining reagents were added in the following order: 4 μL of 5× reaction buffer, 1 μL of RiboLock RNase inhibitor (20 μ μL^{-1}), 2 μL of dNTP mix and 1 μL of RevertAid M-MuLV Reverse Transcriptase (200 μ μL^{-1}). To check for possible DNA contamination, two additional control reactions were run, one with all RT components except the enzyme and the other without DNAse-treated RNA but with all other reagents (NTC). The reaction proceeded for 5 min at 25 °C, followed by 60 min at 42 °C and was terminated by heating at 70 °C for 5 min. The RT product was diluted (20×) with RNase-free water, stored at −80 °C and thawed only once, just before qPCR amplification.

microRNAs expression analysis using real-time PCR

Real-time PCR primers were designed based on the conserved 5′-ends of the microRNA sequences (Table 2). Each primer consisted of 15 nucleotides from the 5′-end of the miRNA and additional nucleotides to increase melting temperatures (Xue *et al.* 2008). Real-time PCR was performed with an ABI 7500 real-time PCR system (Applied

Table 2 Sequences of primers used for stem-loop reverse transcription and real-time PCR. Primers were designed according to Xue *et al.* (2008). Each RT stem-loop primer consisted of 8 nucleotides specific to the 3′-end of a miRNA (boldunderlined) and nucleotides complementary to the universal reverse primer (boldtalic). Real-time PCR forward primers (...) consisted of 15 nucleotides from the 5′-end of the miRNA and additional nucleotides (boldunderlined) to increase melting temperatures

miRNA	Primer sequence [5′–3′]		Length (bp)	microRNA MiRBase acc. no.
ssa-miR-122-5p	RT stem-loop primer	GTCGTATCCAGT***GCAGGGTCCGAGGTATTC***GCACTGGATACGAC***AAACACCA***	52	MIMAT0032301
	Forward primer	**ATCGTACGTGGG**TGGAGTGTGACAATG	27	
ssa-let-7c-5p	RT stem-loop primer	GTCGTATCCAGT***GCAGGGTCCGAGGTATTC***GCACTGGATACGAC***AACTATAC***	52	MIMAT0032265
	Forward primer	**ATCGTACGTGGG**TGAGGTAGTAGGTTG	27	
ssa-miR-148a-3p	RT stem-loop primer	GTCGTATCCAGT***GCAGGGTCCGAGGTATTC***GCACTGGATACGAC***ACAAAGTT***	52	MIMAT0032380
	Forward primer	**ATCGTACGTGGG**TCAGTGCATTACAGA	27	
ssa-miR-92a-3p	RT stem-loop primer	GTCGTATCCAGT***GCAGGGTCCGAGGTATTC***GCACTGGATACGAC***ACAGGCCG***	52	MIMAT0032708
	Forward primer	**ATCGTACGTGGG**TATTGCACTTGTCCC	27	
cel-miR-39-3p	RT stem-loop primer	GTCGTATCCAGT***GCAGGGTCCGAGGTATTC***GCACTGGATACGAC***CAAGCTGA***	52	MIMAT0000010
	Forward primer	**ATCGTACGTGGG**TCACCGGGTGTAAAT	27	
Universal reverse primer		GCAGGGTCCGAGGTATTC	18	

© 2015 John Wiley & Sons Ltd

Biosystems) in singleplex mode. For miRNA quantification, each reaction mixture consisted of 7.5 μL of 2× FastStart SYBR Green Master ROX mix (Roche), 0.65 μM forward primer, 0.65 μM universal reverse primer (Table 2), 1 μL of 20× diluted RT product and 4.5 μL of PCR grade water, for a final volume of 15 μL. The reaction was performed in triplicate in a 96-well plate in standard thermal conditions: 95 °C for 10 min, followed by 40 cycles of 95 °C for 15 s and 60 °C for 1 min. A melting curve analysis followed by agarose gel electrophoresis was performed to verify the quality of the obtained PCR products. Finally, the specificity of the primer pairs was confirmed by sequencing the PCR products that were obtained (Genomed).

Statistical analysis

Data obtained from the real-time PCR assay was used to compute the normalized ratio of microRNA levels in the plasma of the MC-LR-treated group relative to the control group of whitefish (expression ratio, R) at respective time points. The calculations were performed with REST©2009 software (Pfaffl, Horgan & Dempfle 2002). Synthetic exogenous cel-miR-39-3p was used as a reference microRNA in normalization. Differences between groups (control vs. treated) were assessed for statistical significance using a randomization test calculated with REST©2009 software (Pfaffl *et al.* 2002) with 5000 iterations performed for each microRNA.

Receiver operating characteristic (ROC) curve test was used to evaluate diagnostic performances of the examined serum miRNAs. $P < 0.05$ of the area under the curve (AUC) was considered significant. The ROC curve analysis was conducted with MedCalc Statistical software version 15.2 (MedCalc software bvba; http://www.medcalc.org; 2015). For the ROC analysis, raw Ct values for the miRNAs and cel-miR-39 normalizing gene, for each of the control and treated whitefish, were exported to and the relative expression was calculated individually in GenEx 5 Professional software (MultiD Analyses AB). The serum miRNA expression levels of control fish from 8, 24 and 48 h of the experiment ($n = 11$) were considered as taken from a sample of 'healthy' fish. Accordingly, the serum expression values for miRs of the whitefish challenged for 8, 24 and 48 h ($n = 15$) were treated as those which were 'not healthy'.

Results

Gross observations

No fish died during anaesthesia. During the entire study, there were no discernible differences in the swimming behaviour of exposed fish and control fish. No gross changes were observed in the livers of the control fish; the liver was reddish brown and had tender structure. In contrast, the enlarged liver of the MC-LR-challenged fish was readily apparent throughout the whole exposure period. At 8 h post-injection, the livers were slightly redder than these from the control group. However, a progressive development of discoloration of this organ was observed after 24 and 48 h of the exposure (Fig. 1a). In some cases, the liver structure of the exposed fish was partially liquefied.

qPCR accuracy

All indicators of the quality of the PCR analysis appeared to be good. Dissociation curves in the SYBR Green real-time PCRs presented as a single, sharp peak. Analysis of a single band of appropriate size (approximately 65 bp) on 1.2% agarose gel showed specificity and sensitivity for detection of miRNAs. Among the performed runs, no appreciable target detection (Cq > 40) occurred with the negative template controls, as well as those in which reverse transcriptase was omitted (data not shown).

Constitutive levels of examined miRNAs in plasma of the control fish (0 h)

There is no information defining miRNA expression in fish blood and a complete screen of known miRNAs has not been reported. Of the four miRNAs measured in plasmas of whitefish, the abundance of the expressed miRs was based on their Cq (with standard deviation SD; $n = 5$); data for which higher value indicates lower expression. The plasma miRNA order was as follows: let-7c-5p (Cq = 24.37; SD = 0.40) > miR-92a-3p (Cq = 26.33; SD = 0.46) > miR-122-5p (Cq = 27.14; SD = 0.10) > miR-148a-5p (Cq = 32.16; SD = 0.75).

Levels of 3 microRNAs were significantly elevated in whitefish blood plasma 48 h after exposure to MC-LR

From the previous study of miRNA expression in whitefish liver exposed to MC-LR (Brzuzan *et al.*

© 2015 John Wiley & Sons Ltd

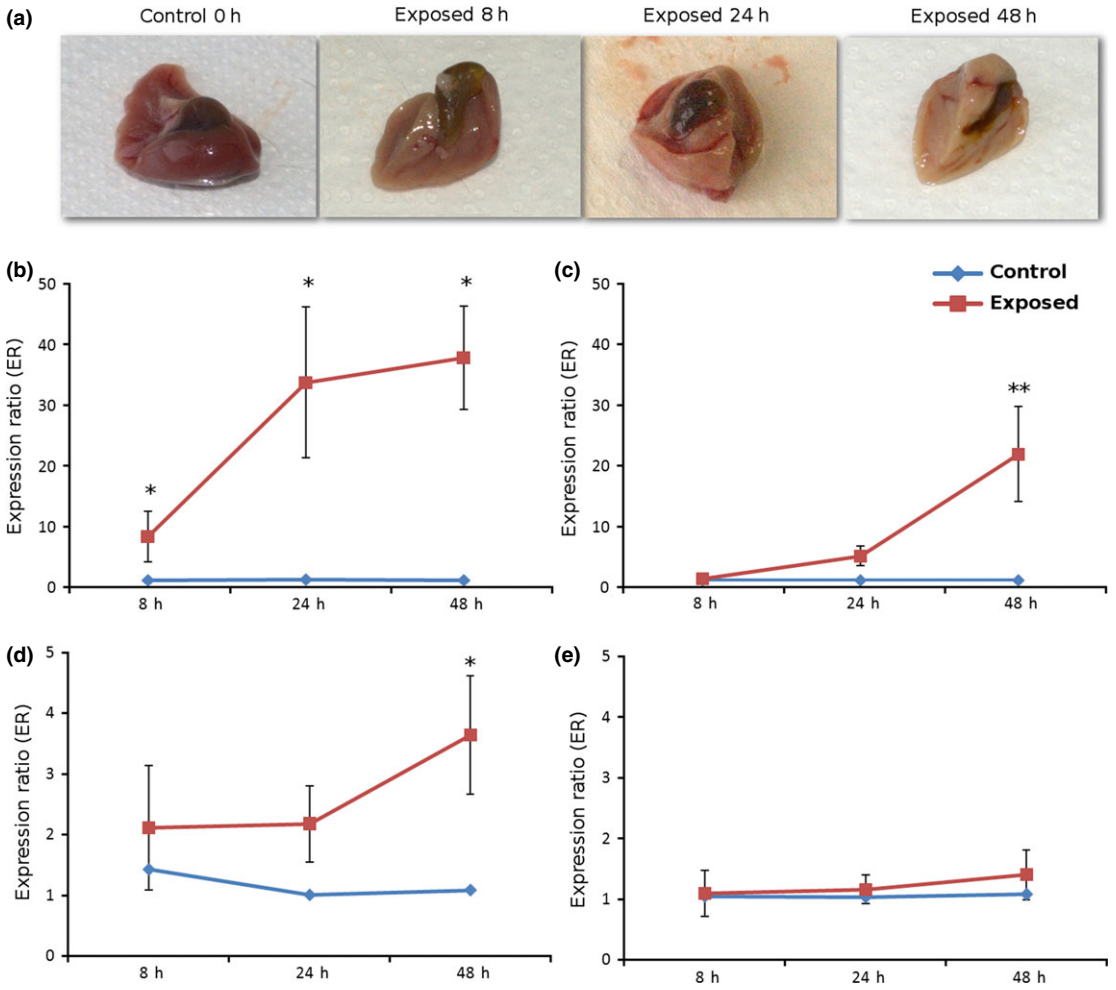


Figure 1 Gross appearance of whitefish liver and changes in plasma levels of four miRNA examined in the study. (a) The appearance of normal whitefish liver (0 h) and discolorated, swollen and haemorrhagic livers from whitefish due to microcystin intoxication, after 8, 24 and 48 h of the treatment. (b) miR-122-5p, (c) miR-148a-3p, (d) miR-92a-3p and (e) let-7c-5p in whitefish exposed to microcystin-LR (100 μg kg^{-1} body weight) for 8 h, 24 h and 48 h. Markers represent mean values ($n = 5$, except for control sample at 24 h and 48 h where $n = 3$) of expression ratios (R ± SE), normalized by cel-miR-39-3p as reference microRNA at each respective time of the experiment. Data were analysed using REST 2009 software. Asterisks denote exposure group means that are significantly different from control group using a randomization test (REST; *$P < 0.05$; **$P < 0.01$).

2012), it appeared that it was necessary to determine the profile of miRNAs in MC-LR-induced hepatoxicity by measuring the miRNA levels in the peripheral blood over the first 48 h of exposure. Fig. 1b through e shows expression patterns of whitefish miRNAs in the plasma of the control and treated fish after 8 h, 24 h and 48 h of exposure to 100 μg MC-LR kg^{-1} body weight. After 8 h and 24 h, compared to controls, only the miR-122-5p plasma levels of treated fish were increased significantly (8 h: R = 8.27, SE = 4.17832, $P < 0.05$; 24 h: R = 33.64, SE = 12.41, $P < 0.05$). Compared to the respective controls, the challenge to MC-LR for 48 h resulted in elevation of 3 miRNAs levels: miR-122-5p (R = 37.72, SE = 8.53, $P < 0.05$), miR-148a-3p (R = 21.82, SE = 7.84; $P < 0.05$) and miR-92a-3p (R = 3.64, SE = 0.97; $P < 0.01$). During the treatment, no changes of the let-7c-5p plasma levels occurred in the treated fish compared to controls (Fig. 1e).

The diagnostic performance of microRNAs

The ROC curve analysis was performed to study the diagnostic performance of each of these miRNAs for whitefish. As can be observed in Fig. 2,

© 2015
John Wiley & Sons Ltd

the miRNAs presented different areas under the curve (AUC) values, between 0.606 for let-7c ($P = 0.353$) and 0.976 for miR-122-5p ($P < 0.001$). The serum miR-122 showed the highest sensitivity and specificity, 86.7% and 100%, respectively, at the expression level criterion of $R > 2.198$. These data demonstrate that the serum miR-122 could be used for diagnosis of liver injury with nearly 90% sensitivity and 100% specificity in this cohort of fish. The diagnostic performance of two other serum miRNAs, miR-148a-5p and miR-92a-3p, although statistically significant, was lower than that of miR-122-5p, with respective sensitivity/specificity values of 80.0/90.9% and 73.3/81.8%.

Discussion

Detecting and quantifying miRNAs in the fish body fluids is an important initial step in investigating their possible biological functions, for example as mediators in cell-to-cell communication networks (Creemers, Tijsen & Pinto 2012). In the current study, we determined the constitutive expression levels of four selected miRNAs in whitefish plasma using real-time PCR. The presence of the 4 miRNAs in the circulation system of whitefish may suggest that they may be functionally involved in regulation of gene expression of recipient cells, as it is being uncovered in mammals (Creemers *et al.* 2012). As the precise source of miRNAs in plasma is not yet known, there is particular interest in comparing the expression between plasma and cellular miRNA patterns. Our data demonstrate that the release of miRNAs from the liver into the bloodstream might be uneven, at least with regard to miR-122-5p which is the most abundant miR in whitefish liver (Brzuzan *et al.* 2012); Brzuzan *et al.* unpublished), but its constitutive levels in the plasma were lower than those of let-7c-5p. Further studies on the release mechanisms and kinetics, the stability of circulating miRNAs, as well as their target cells, should reveal the connectivity grid of the miRNAs in the circulation system of fish.

Microcystin toxicity is a multipathway process that results in severe liver injury in both mammals and fish. In this study, we designated 3 miRNAs (miR-122-5p, miR-148a-3p and miR-92a-3p) as potential plasma biomarkers with high sensitivity and specificity for liver injury. Remarkably, the circulating miRNA-122-5p could predict liver cell damage caused by MC-LR in whitefish very soon after exposure (8 h). Moreover, the increased plasma levels of miR-122-5p continued to increase

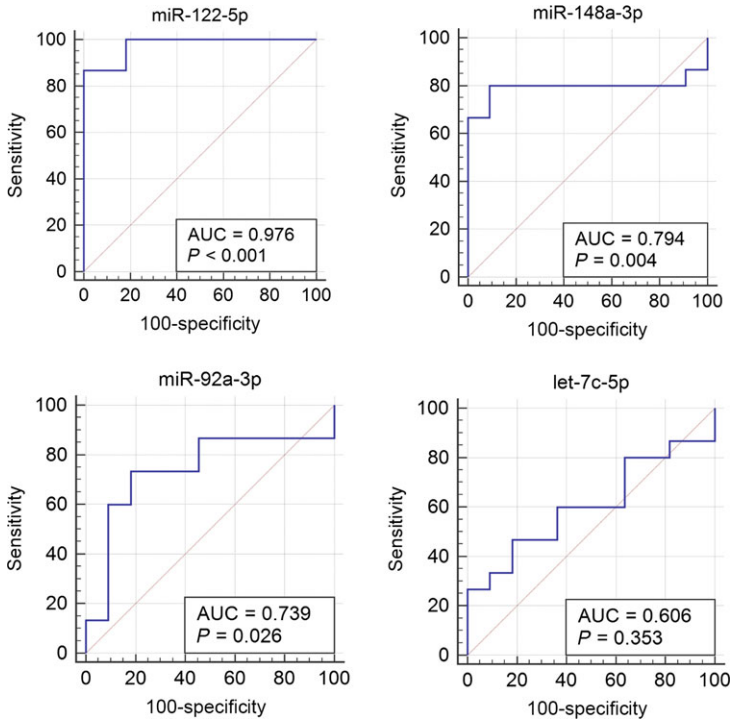


Figure 2 Receiver operating characteristics (ROC) analysis of serum miRNAs as liver injury risk biomarkers in whitefish exposed to MC-LR. ROC curves of miR-122-5p, miR-148a-3p, miR-92a-3p and let-7c-5p expression levels in plasma, determined by qPCR, in samples obtained after the treatment experiment. Shown is also a ROC curve (diagonal) for an uninformative test (sensitivity + specificity = 1). AUC, area under the curve.

© 2015 John Wiley & Sons Ltd

Table 3 Effects of various DILI factors on blood biomarkers

DILI factor	Biomarker	Main finding	Organism	Reference
Acetaminophen	miR-122 miR-192 ALT	Elevation of miRNA levels was observed in the plasma as early as 1 h after exposure	Mouse	Wang *et al.* (2009)
Allyl alcohol	miR-122 ALT AST	All measured hepatocellular biomarkers, in addition to miR-122, were already elevated at 6 h indicating the induction of toxicity	Rat	Starckx *et al.* (2013)
Alpha-naphthyl isothiocyanate	miR-122 α-GST	The 6-h time point changes coincided with minimal to moderate increases in miR-122 and α-GST	Rat	Starckx *et al.* (2013)
Ethanol	miR-122 ALT	miR-122 concentration and ALT activity in the plasma showed similar time-dependent increases, but miR-122 with higher fold change	Mouse	Zhang *et al.* (2010)
Lipopolysaccharide	miR-122 ALT	Both miR-122 concentration and ALT activity in plasma showed a time-dependent change, the miR-122 concentration increased much more rapidly than ALT activity	Mouse	Zhang *et al.* (2010)
Trichlorobromomethane	miR-122 ALT AST	Slight increases in AST or ALT in most animals with hepatocellular degeneration/necrosis in the liver; a few animals with liver histopathology showed no change in these conventional biomarkers. In contrast, increases in miR-122 were observed in all animals and the magnitude of the change was greater than that seen with ALT and AST (100-fold)	Rat	Laterza *et al.* (2009)
Carbon tetrachloride	miR-122 ALT	miR-122 concentration in animals treated with $CBrCl_3$ was approximately 6000-fold higher than the baseline values for the control group. Changes in ALT were 75-fold higher	Rat	Laterza *et al.* (2009)
MC-LR	ALT AST LDH	Increased activity of ALT, AST and LDH after injection at a dose 150 μg kg^{-1} body weight	Fish	Råbergh, Bylund & Eriksson (1991)
MC-LR	ALT AST	Increased activity of AST and ALT after injection at dose 100 μg kg^{-1} body weight, accordingly 48 h and 72 h after exposure	Fish	Brzuzan *et al.* (2009)
MC-LR	ALT, ALP, Bb, MetHb, ROOHs, glutathione, α-tocopherol levels, SOD	ALT, ALP, Bb, MetHb, ROOHs, glutathione, α-tocopherol levels, SOD activity and plasma lipid profile alternated after 30 days of treatment	Mouse	Sedan *et al.* (2013)
Microcystis bloom	ALT AST GGT LDH ALP	ALT and AST activities were significantly higher after oral 4 weeks feeding with blooms	Fish	Li *et al.* (2004)

at the end of experiment (48 h), confirming its high diagnostic value. The other plasma miRs, miR-148a-5p and miR-92a-3p, have less potential for use as early biomarkers of liver injury, as their plasma levels were increased only after 48 h after exposure to MC-LR.

To our knowledge, this is the only study reporting elevated levels of microRNAs in fish plasma after exposure to microcystin-LR. However, this corresponds well with previous studies, where miR-122 levels were elevated due to drug-induced hepatocellular injury (Table 3). To date, studies on the detection and validation levels of the circulating miR-122 in animal blood have been conducted on rodents. For example, Wang *et al.* (2009) observed an elevation of miR-122 in mouse plasma as early as 1 h after exposure to acetaminophen, a common drug known for liver damage. Similar results were shown in treatment with D-galactosamine or ethanol (Zhang *et al.*

© 2015 John Wiley & Sons Ltd

2010), as well as after administration of allyl alcohol or α-naphthyl isothiocyanate (Starckx *et al.* 2013). Laterza *et al.* (2009) showed increased levels of miR-122 in rats' plasma after administration of trichlorobromomethane and carbon tetrachloride. In all cases, elevated levels of plasma miR-122 resulted from the liver cell damage.

Our data demonstrate that our panel of miRNAs shows a high diagnostic value with AUC values between 0.739 and 0.0976 in ROC analysis. This discriminative power is higher than those reported for other liver injury biomarkers currently in development, including today's gold standard biomarkers of drug-induced liver injury, ALT and AST. Several reports on circulating miRNAs point to their precocious level changes compared to the ALT or AST (Table 3). For example, our previous study on whitefish treated with the same dose of MC-LR (100 μg kg^{-1} body weight) showed that AST and ALT levels were not elevated in MC-LR-challenged whitefish until, 48 and 72 h after the exposure, respectively (Brzuzan *et al.* 2009). Moreover, while elevated ALT or AST levels in plasma usually indicate liver injury, plasma ALT activity originating from extra-hepatic sources has also been reported from patients with burns, muscle inflammation, hypothyroidism or myopathies (Mazer & Perrone 2008). On the other hand, AST is localized also in heart, brain and skeletal muscle. This makes the use of ALT or AST levels alone in diagnosis of liver diseases unreliable, whereas the expression of miR-122 is fairly restricted to liver. Thus, miRNA-based method is more sensitive and probably more reliable than the current serological method, plasma ALT or AST level, to detect and monitor toxin-induced liver injuries.

Unfortunately, all previous studies were concerned with the use of circulating microRNAs in diagnosis of liver injury in response to various drugs and substances which are a potential direct threat to human health. As microRNAs expressed in the liver are conserved among different vertebrate lineages and their levels are changed as a result of liver injury, it raised a question as to whether circulating microRNAs can be used as a biomarker in environmental studies. MC-LR is known to disturb liver metabolism (e.g. Wang *et al.* 2010). As MC-LR may also affect the quantity of several functional proteins involved in organic acid metabolism in fish (Wang *et al.* 2010), it is likely that the liver metabolic networks are evolutionarily conserved and connected by tissue-specific miRNAs, such as miR-122 (Brzuzan *et al.* 2012). This potential diagnostic tool may have various applications in those environmental sciences which deal with pollution of both anthropogenic and natural origin, particularly in environmental toxicology. Epidemiological studies on rodents show that prolonged exposure to sublethal doses of MCs is often unnoticed and such signs as body weight or behaviour do not differ from control groups (Guzman & Solter 2002; Andrinolo *et al.* 2008). This is why subchronic intoxication of humans and livestock is undetected. This increases the need to discover sensitive biomarkers for prolonged MC-LR exposure (Sedan *et al.* 2013; Singh & Asthana 2014). Whether the observed increase of miRNA-122-5p in MC-LR-challenged fish plasma remains stable in terms of weeks rather than hours after exposure should be investigated in further studies.

To sum up, the results of our study suggest that miRNA-122 can be used in environmental studies as a non-invasive biomarker to detect liver damage in fish, as a promising alternative to today's gold standard hepatotoxicity markers. Plasma levels of miRNA-122-5p in whitefish are elevated within 8 h of exposure to MC-LR and show high specificity, with an AUC value of 0.976 ($P < 0.001$). miR-148a-3p and miR-92a-3p, although they respond more slowly to exposure to MC-LR and have lower AUC values, also show potential and are worth further investigating.

Acknowledgements

We thank Dr. Stefan Dobosz from the Department of Salmonid Research in Rutki, Inland Fisheries Institute in Olsztyn, Poland, for his excellent technical assistance during hatchery operations. The authors also thank Trev Hill and Mark Leonard for proofreading the manuscript. The study was supported by research grant from National Science Centre (Poland) No. DEC-2012/07/B/NZ9/01320.

References

Andrinolo D., Sedan D., Telese L., Aura C., Masera S., Giannuzzi L., Marra C.A. & de Alaniz M.J.T. (2008) Hepatic recovery after damage produced by sub-chronic intoxication with the cyanotoxin microcystin LR. *Toxicon* **51**, 457–467.

© 2015 John Wiley & Sons Ltd

Ashworth C.T. & Mason M.F. (1946) Observations on the pathological changes produced by a toxic substance present in blue-green algae (*Microcystis aeruginosa*). *The American Journal of Pathology* **22**, 369–383.

Brzuzan P., Woźny M., Ciesielski S., Łuczyński M.K., Góra M., Kuźmiński H. & Dobosz S. (2009) Microcystin-LR induced apoptosis and mRNA expression of p53 and cdkn1a in liver of whitefish (*Coregonus lavaretus* L.). *Toxicon: Official Journal of the International Society on Toxinology* **54**, 170–183.

Brzuzan P., Woźny M., Wolińska L. & Piasecka A. (2012) Expression profiling in vivo demonstrates rapid changes in liver microRNA levels of whitefish (*Coregonus lavaretus*) following microcystin-LR exposure. *Aquatic Toxicology* **122–123**, 188–196.

Burhop K., Gordon D. & Estep T. (2004) Review of hemoglobin-induced myocardial lesions. *Artificial Cells, Blood Substitutes, and Biotechnology* **32**, 353–374.

Creemers E.E., Tijsen A.J. & Pinto Y.M. (2012) Circulating microRNAs: novel biomarkers and extracellular communicators in cardiovascular disease? *Circulation Research* **110**, 483–495.

Dawson R.M. (1998) The toxicology of microcystins. *Toxicon* **36**, 953–962.

Farid W.R.R., Pan Q., van der Meer A.J.P., de Ruiter P.E., Ramakrishnaiah V., de Jonge J., Kwekkeboom J., Janssen H.L.A., Metselaar H.J., Tilanus H.W., Kazemier G. & van der Laan L.J.W. (2012) Hepatocyte-derived microRNAs as serum biomarkers of hepatic injury and rejection after liver transplantation. *Liver Transplantation* **18**, 290–297.

Gilad S., Meiri E., Yogev Y., Benjamin S., Lebanony D., Yerushalmi N., Benjamin H., Kushnir M., Cholakh H., Melamed N., Bentwich Z., Hod M., Goren Y. & Chajut A. (2008) Serum microRNAs are promising novel biomarkers. *PLoS ONE* **3**, e3148.

Guzman R.E. & Solter P.F. (2002) Characterization of sublethal microcystin-LR exposure in mice. *Veterinary Pathology* **39**, 17–26.

Kaplowitz N. (2001) Drug-induced liver disorders: implications for drug development and regulation. *Drug Safety* **24**, 483–490.

Kazuń K. & Siwicki A.K. (2012) Propiscin – a safe new anaesthetic for fish. *Archives of Polish Fisheries* **20**, 173–177.

Laterza O.F., Lim L., Garrett-Engele P.W., Vlasakova K., Muniappa N., Tanaka W.K., Johnson J.M., Sina J.F., Fare T.L., Sistare F.D. & Glaab W.E. (2009) Plasma microRNAs as sensitive and specific biomarkers of tissue injury. *Clinical Chemistry* **55**, 1977–1983.

Lee W.M. (2003) Drug-induced hepatotoxicity. *The New England Journal of Medicine* **349**, 474–485.

Lee T.A., Rollwagen-Bollens G., Bollens S.M. & Faber-Hammond J.J. (2015) Environmental influence on cyanobacteria abundance and microcystin toxin production in a shallow temperate lake. *Ecotoxicology and Environmental Safety* **114**, 318–325.

Li X.-Y., Chung I.-K., Kim J.-I. & Lee J.-A. (2004) Subchronic oral toxicity of microcystin in common carp (*Cyprinus carpio* L.) exposed to Microcystis under laboratory conditions. *Toxicon* **44**, 821–827.

Mazer M. & Perrone J. (2008) Acetaminophen-induced nephrotoxicity: pathophysiology, clinical manifestations, and management. *Journal of Medical Toxicology* **4**, 2–6.

Nathwani R.A., Pais S., Reynolds T.B. & Kaplowitz N. (2005) Serum alanine aminotransferase in skeletal muscle diseases. *Hepatology (Baltimore, MD)* **41**, 380–382.

Ozer J., Ratner M., Shaw M., Bailey W. & Schomaker S. (2008) The current state of serum biomarkers of hepatotoxicity. *Toxicology* **245**, 194–205.

Panteghini M., Renze B. & van Solinge W.W. (2006) Enzymes. In: *Tietz textbook of clinical chemistry and molecular diagnostics* (ed. by C.A. Burtis, E.R. Ashwood & D.E. Bruns), pp. 597–643. St. Louis, Elsevier Saunders.

Pfaffl M.W., Horgan G.W. & Dempfle L. (2002) Relative expression software tool (REST) for group-wise comparison and statistical analysis of relative expression results in real-time PCR. *Nucleic Acids Research* **30**, e36.

Råbergh C.M.I., Bylund G. & Eriksson J.E. (1991) Histopathological effects of microcystin-LR, a cyclic peptide toxin from the cyanobacterium (blue-green alga) *Microcystis aeruginosa* on common carp (*Cyprinus carpio* L.). *Aquatic Toxicology* **20**, 131–145.

Roberts T.C., Coenen-Stass A.M.L. & Wood M.J.a. (2014) Assessment of RT-qPCR normalization strategies for accurate quantification of extracellular microRNAs in murine Serum. *PLoS ONE* **9**, e89237.

Sedan D., Giannuzzi L., Rosso L., Marra C.A. & Andrinolo D. (2013) Biomarkers of prolonged exposure to microcystin-LR in mice. *Toxicon* **68**, 9–17.

Senior J.R. (2007) Drug hepatotoxicity from a regulatory perspective. *Clinics in Liver Disease* **11**, 507–524, vi.

Shigoka M., Tsuchida A., Matsudo T., Nagakawa Y., Saito H., Suzuki Y., Aoki T., Murakami Y., Toyoda H., Kumada T., Bartenschlager R., Kato N., Ikeda M., Takashina T., Tanaka M., Suzuki R., Oikawa K., Takanashi M. & Kuroda M. (2010) Deregulation of miR-92a expression is implicated in hepatocellular carcinoma development: miR-92a in hepatocellular carcinogenesis. *Pathology International* **60**, 351–357.

Singh S. & Asthana R.K. (2014) Assessment of microcystin concentration in carp and catfish: a case study from Lakshmikund pond, Varanasi, India. *Bulletin of Environmental Contamination and Toxicology* **92**, 687–692.

Sonkoly E. & Pivarcsi A. (2011) MicroRNAs in inflammation and response to injuries induced by environmental pollution. *Mutation Research/Fundamental and Molecular Mechanisms of Mutagenesis* **717**, 46–53.

Starckx S., Batheja A., Verheyen G.R., Jonghe S.D., Steemans K., Dijck B.V., Singer M., Bogdan N., Snoeys J., Vinken P., Sasaki J.C., Gompel J.V., Guzzie-Peck P., Lampo A. & Lammens L. (2013) Evaluation of miR-122 and other biomarkers in distinct acute liver injury in rats. *Toxicologic Pathology* **41**, 795–804.

Su Y.W., Chen X., Jiang Z.Z., Wang T., Wang C., Zhang Y., Wen J., Xue M., Zhu D., Zhang Y., Su Y.J., Xing T.Y., Zhang C.Y. & Zhang L.Y. (2012) A panel of serum

© 2015 John Wiley & Sons Ltd

microRNAs as specific biomarkers for diagnosis of compound- and herb-induced liver injury in rats. *PLoS ONE* **7**, e37395.

Urban T., Daly A. & Aithal G. (2014) Genetic basis of drug-induced liver injury: present and future. *Seminars in Liver Disease* **34**, 123–133.

Wang K., Zhang S., Marzolf B., Troisch P., Brightman A., Hu Z., Hood L.E. & Galas D.J. (2009) Circulating microRNAs, potential biomarkers for drug-induced liver injury. *Proceedings of the National Academy of Sciences* **106**, 4402–4407.

Wang M., Chan L.L., Si M., Hong H. & Wang D. (2010) Proteomic analysis of hepatic tissue of zebrafish (*Danio rerio*) experimentally exposed to chronic microcystin-LR. *Toxicological Sciences: An Official Journal of the Society of Toxicology* **113**, 60–69.

Xue X., Sun J., Zhang Q., Wang Z., Huang Y. & Pan W. (2008) Identification and characterization of novel microRNAs from *Schistosoma japonicum*. *PLoS ONE* **3**, e4034.

Yokoi T. & Nakajima M. (2011) Toxicological implications of modulation of gene expression by microRNAs. *Toxicological Sciences* **123**, 1–14.

Zhang Y., Jia Y., Zheng R., Guo Y., Wang Y., Guo H., Fei M. & Sun S. (2010) Plasma microRNA-122 as a biomarker for viral-, alcohol-, and chemical-related hepatic diseases. *Clinical Chemistry* **56**, 1830–1838.

Received: 14 April 2015
Revision received: 12 June 2015
Accepted: 26 June 2015

© 2015
John Wiley & Sons Ltd

Neurotoxicity Research (2019) 35:29–40
https://doi.org/10.1007/s12640-018-9920-4

ORIGINAL ARTICLE

Microcystin-LR-Triggered Neuronal Toxicity in Whitefish Does Not Involve MiR124-3p

Maciej Florczyk[1] · Paweł Brzuzan[1] · Alicja Łakomiak[1] · Ewa Jakimiuk[2] · Maciej Woźny[1]

Received: 25 February 2018 / Revised: 28 May 2018 / Accepted: 30 May 2018 / Published online: 7 June 2018
© The Author(s) 2018

Abstract

Microcystin-LR (MC-LR) is a potent hepatotoxin that has also been pointed out of causing neurotoxicity, but the exact mechanisms of action still remain ambiguous and need to be elucidated. Data from studies on mammals show that pathology of astrocyte cells points to perturbations of microRNA signaling. Glial fibrillary acidic protein (GFAP), a neuronal cell/astrocyte-specific protein, and a microRNA-124-3p (MiR124-3p) are among putative triggers and regulators of neuronal cell/astrocyte reactivity. In the present study on whitefish (*Coregonus lavaretus*), we found that *gfap* mRNA contains a putative target site for MIR124-3p, to potentially affect its expression changes. qPCR expression study of *gfap*:MiR124-3p pair in the midbrain of juvenile whitefish, during 28 days of exposure to a repeated subacute dose of MC-LR (100 μg kg^{-1} body mass), showed marginally significant up-regulation of *gfap* only on the 7th day of exposure period which suggests neuronal toxicity. During the whole exposure period, neither midbrain nor blood plasma levels of MiR124-3p were changed. Furthermore, double luciferase gene reporter assay confirmed the lack of MiR124-3p involvement in mediating control over *gfap* mRNA expression. These data show that, although MC-LR may trigger neuronal toxicity in whitefish, this does not involve MiR124-3p in response to the treatment.

Keywords microRNA · Neurotoxicity · Gliosis · Circulating microRNA

Introduction

Microcystins (MCs) are a challenging group of cyclic heptapeptide hepatotoxins for which a substantial gap in knowledge persists regarding the underlying molecular mechanisms of organ toxicity and injury. Microcystin-LR (MC-LR) is a commonly acting potent environmental agent that has gained a role in causing neurotoxicity. The adverse effects entailed by MC-LR exposure include both behavioral changes, such as different swimming habits and uncommon daily activity (Baganz et al. 1998, 2004; Cazenave et al. 2008), and altered brain physiology (i.e., altered levels of proteins involved in the cytoskeleton assemblage, dysregulated signal transduction, protein degradation, metabolism, transport, apoptosis, and translation) (Wang et al. 2010). In mammals, damage to the central nervous system (CNS) is reflected by increased expression of glial fibrillary acidic protein (GFAP). GFAP/Gfap is an intermediate filament protein expressed by numerous cells in the CNS, including mature astrocytes (Middeldorp and Hol 2011). Following various kinds of injury to the CNS, including chemical insult, astrocytes become reactive and respond in a typical manner termed astrogliosis (Sofroniew and Vinters 2010). Astrogliosis is characterized by rapid synthesis of *gfap* resulting in the formation of a glial scar, a common marker of damage to the CNS (Brenner 2014).

Although the exact mechanisms of action still remain ambiguous, the range of observed neuronal defects points to perturbations of epigenetic factors such as microRNA (miRNA) signaling. MiRNAs are small (19–23 nucleotides), single-stranded non-coding RNAs that act as post-transcriptional regulators of gene expression (Moxon et al. 2008). They negatively modulate up to 60% of mammalian protein-coding genes by interacting with response elements in the 3′ untranslated regions (3′UTRs)

Electronic supplementary material The online version of this article (https://doi.org/10.1007/s12640-018-9920-4) contains supplementary material, which is available to authorized users.

✉ Maciej Florczyk
maciej.florczyk@uwm.edu.pl

[1] Department of Environmental Biotechnology, Faculty of Environmental Sciences, University of Warmia and Mazury in Olsztyn, ul. Słoneczna 45G, 10-709 Olsztyn, Poland

[2] Division of Veterinary Prevention and Feed Hygiene, Faculty of Veterinary Medicine, University of Warmia and Mazury in Olsztyn, ul. Oczapowskiego 13, 10-950 Olsztyn, Poland

of mRNAs and target the mRNAs for degradation and/or inhibit their translation (Bartel 2004; Friedman et al. 2009). Our previous studies on MC-LR effects on fish miRnome have revealed that MC-LR was capable of modulating expression of several microRNAs, members of RNA interference system, in the liver of challenged fish (Brzuzan et al. 2012, 2016; Łakomiak et al. 2016), which points out their mechanistic involvement in the toxicity mechanism. Since molecular background of MC-LR toxicity seems to be similar in different tissues, it was reasonable to assume that similar effects will emerge in the brain. MiRNA profiling of experimental stroke brains has shown alterations in many individual miRNAs, and bioinformatics tools revealed putative functional miRNA:mRNA pairs (Saul et al. 2014). The observation that miRNA levels in the nervous system were changed by MC-LR (Saul et al. 2014) prompted us to investigate the role of fish microRNAs in the context of brain-specific MC-LR toxicity. Moreover, recent studies have shown that disrupted expression of GFAP is associated with altered levels of miRNAs such as MiR125b (Pogue et al. 2010) and MiR145 (Wang et al. 2015). MiR3099 has been shown to target GFAP in the mouse brain (Abidin et al. 2017).

The possibility that MiR124 is able to induce proliferation of reactive astrocytes has recently been demonstrated in mice (Hamzei Taj et al. 2016). MiR124 is the most abundant miRNA in the nervous system of mammals and fish, and it is considered as a nervous system-specific miRNA (Kapsimali et al. 2007; Mishima et al. 2007). Noteworthy, the MIR124 family members were detected in 46 animal species, from *Caenorhabditis* to *Homo sapiens* (Guo et al. 2009). Their abundance in embryonic and adult cortical tissues of various mammalian species range from 5 to 48% of all miRNAs expressed, suggesting that it has a key function in the CNS (Lagos-Quintana et al. 2002; Landgraf et al. 2007). MiR124 was proven to regulate brain development, as well as it is enriched in mature brain tissue, where it plays important roles in neuronal regulation. MiR124 has been shown to be downregulated in CNS pathologies, such as glioma and medulloblastoma, suggesting its possible involvement in brain tumor progression. On the other hand, MiR124 was found to increase neuronal survival and functional improvement of the neurological deficits (Hamzei Taj et al. 2016) and enhance brain repair in Parkinson's disease (Saraiva et al. 2016). Mammals treated with MiR124 developed a significantly reduced glial scar area after occlusion of the right middle cerebral artery (Doeppner et al. 2013). More recently, it has been shown that MIR124-3p target sequence in mediated gene transfer restored astrocyte activity in rats, thus showing its utility in studying the miRNA contribution to physiological and pathophysiological processes in the brain (Taschenberger et al. 2017).

Since the above studies link changes in brain GFAP and miRNA expression in mammals, the goals of this study were to dissect involvement of this miRNA:mRNA pair in fish exposed to known neurotoxic environmental agent microcystin-LR (Li et al. 2014). First, we were curious whether there is a functional relationship between expression of MiR124-3p and *gfap* mRNA in vitro, thereby suggesting the possibility of interaction and involvement of this miRNA-mRNA pair in vivo in response to neuronal cells to stressing conditions. To address this issue, we determined nucleotide sequence of the whitefish *gfap* mRNA. Then, using computational approach, we revealed that the 3′UTR of whitefish *gfap* mRNA contains one putative MiR124-3p response element. Secondly, we investigated whether long-term exposure of whitefish to MC-LR would cause alterations in the expression of either molecule in brains similar to those observed in mammals. To this end, we profiled expression levels of MiR124-3p and *gfap* mRNA in the brains of whitefish treated for 1/3, 1, 2, 7, 14, and 28 days with a subacute dose of MC-LR. Additionally, we examined whether plasma levels of MiR124-3p could relate to disrupted *gfap* expression in the brain and possibly serve as a biomarker of MC-LR exposure. Finally, to confirm the functional involvement of MiR124-3p:*gfap* pair, a dual-luciferase reporter assay was performed.

Material and Methods

Determining *gfap* cDNA Sequence of European Whitefish

We first obtained a partial *gfap* cDNA sequence of European whitefish, using a designed set of primers (Cla-gfap-F1, Cla-gfap-R1; Supplementary File 1) based on the *S. salar* EST sequence available at GenBank (accession no. GE794087.1). Initial PCR amplification of a starting DNA sequence was conducted using Phusion Flash PCR Master Mix (Thermo Scientific) with the following cycling conditions: 98 °C for 10 s; 30 cycles at 98 °C for 1 s, 60 °C for 5 s, 72 °C for 10 s; followed by 72 °C for 1 min. Following electrophoresis, a band observed at the expected size was cut out and purified using the PureLink™ Quick Gel Extraction and PCR Purification Combo Kit (Invitrogen). The putative cDNA fragment of *gfap* mRNA was then sequenced under contract (Genomed).

The partial *gfap* cDNA sequence was subsequently used as a query in a BLAST search against the sequence deposited in sequence read archive (SRA), accession no. SRX465095, obtained from three pooled normal embryos of lake whitefish (*Coregonus clupeaformis*). The revealed sequence of putative *gfap* of lake whitefish was used as a template to design other sets of primers: Cla-gfap-2-F2 and Cla-gfap-2-R2, Cla-gfap-2-F3 and Cla-gfap-2-R3, and Cla-gfap-2-F4 and Cla-gfap-2-R4 (Supplementary File 1). These primers were used to amplify the partial 5′UTR, entire coding sequence, and partial 3′

UTR of European whitefish *gfap*, respectively. PCR was carried out in a final volume of 25 μL as follows: 1 μL of cDNA as template, 12.5 μL of 2 × DreamTaq Green PCR Master Mix (Thermo Scientific), 0.5 μM of forward and reverse primers (Cla-gfap-2-F2 and Cla-gfap-2-R2, or Cla-gfap-2-F3 and Cla-gfap-2-F3, or Cla-gfap-2-F4 and Cla-gfap-2-R4), and 9.5 μL of nuclease-free water. The PCR conditions were 1 cycle at 95 °C for 3 min followed by 30 cycles at 95 °C for 30 s, optimal annealing temperature (as indicated in Supplementary File 1) for 30 s and 72 °C for 1 min. Final extension was carried out at 72 °C for 30 min. The PCR products were cloned using the InsTAclone PCR Cloning Kit (Thermo Scientific) according to the manufacturer's protocol, with some modifications. PCR amplicons were ligated into pTZ57R/T vector, afterwards the ligation mixtures were transformed into the JM109 competent *Escherichia coli* cells (Promega, USA) using a heat shock (42 °C) transformation method. The resulting transformants were spread on LB agar plates containing X-gal (40 μg/mL), IPTG (40 μg/mL), and ampicillin (100 μg/mL) and incubated overnight at 37 °C. Insert-positive colonies were picked and inoculated into 4 mL of LB with 100 μg/mL of ampicillin. After incubation at 37 °C for 16 h, the plasmids DNA were isolated using a Plasmid Mini Kit (A&A Biotechnology) and sequenced (Genomed). Nucleotide sequences were then assembled using Clustal X 2.1 software into a cDNA sequence of 2160-bp length. This allowed further MiR124-3p target site identification with Segal Lab software.

The obtained *gfap* cDNA sequence was further analyzed by RegRNA 2.0 web server (Chang et al. 2013) to identify the homology of functional RNA motifs and sites, and to align with *gfap* transcript of zebrafish (Ensembl accession no. ENSDART00000028270.6) to predict potential exon–exon junction. In order to find the open reading frame and to acquire the amino acid sequence, cDNA sequence was subjected to the ORF finder software (Wheeler et al. 2004). To identify the domain organization of deduced Gfap protein sequence, the InterPro v. 53 (Mitchell et al. 2015), SMART (Letunic et al. 2015), and Conserved Domains Search (Marchler-Bauer et al. 2015) were used. The molecular weight (MW) and isoelectric point (pI) were determined using the Compute pI/Mw tool (Gasteiger et al. 2005). The sequence of whitefish *gfap* has been deposited in GenBank under accession no. MG182670.

Phylogenetic Analysis of Whitefish Gfap

To gain insight into the evolutionary relationship of Gfap, the deduced amino acid sequence was compared with those of other vertebrates deposited in NCBI database: XP_02141413 (*O. mykiss*), XP_01404923 (*S. salar*), AAH68410.1 (*D. rerio*), AAB22581.1 (*H. sapiens*), and P03995.4 (*M. musculus*). The sequences were aligned using Clustal W (Larkin et al. 2007) and the output was visualized using BoxShade 3.21 software (www.ch.embnet.org/software/BOX_ form.html). The sequences were also compared using Clustal X 2.1 software to create the percent identity matrix. The phylogenetic tree was constructed using the neighbor-joining method implemented in MEGA 6.06 software (Tamura et al. 2013) with default settings and 1000 bootstrap replicates. The tree was rooted with CED-9 sequences from *Caenorhabditis elegans* (GenBank accession no. NP_499284).

Construction of Luciferase Reporter Plasmids for Luciferase Assay

To investigate whether MiR124-3p can regulate the expression of whitefish *gfap*, three types of luciferase reporter plasmids were prepared based on the pmirGLO Dual-Luciferase miRNA Target Expression Vector (Promega). To construct the gfap-3′UTR-wt plasmid, the entire 3′UTR region of whitefish gfap, obtained in this study, which contains putative MiR124-3p response element(s), was amplified by PCR using 1 μL of cDNA template, 12.5 μL of 2× Phusion Flash PCR Master Mix (Thermo Scientific), 0.5 μM of gfap-3′UTR-F-DraI and gfap-3′UTR-R-XbaI primers, and 9.5 μL of nuclease-free water. Cycling conditions were as follows: 98 °C for 10 s; 30 cycles at 98 °C for 1 s, 62 °C for 5 s, and 72 °C for 25 s; followed by 72 °C for 2 min. The gel-purified (Invitrogen) product was double digested with *XbaI* and *DraI* restriction enzymes (Thermo Scientific) and cloned into a multiple cloning site of the pmirGLO downstream of the firefly luciferase gene (gfap-3′UTR-wt). Additionally, plasmids containing mutations in the sequence complementary to the seed region of *gfap* (gfap-3′UTR-mut, positive control) were also generated. The resulting plasmids were used to transform the competent *E. coli* JM109 cells (Promega) via the heat shock method. All subsequent steps up to isolation of plasmids from the liquid bacterial culture were carried out as described in the "Determining *gfap* cDNA sequence of European whitefish" section. All plasmids were confirmed by sequencing (Genomed). Sequences of each oligonucleotides used for generation of luciferase reporter plasmids are provided in Supplementary File 1.

Cell Culture

Human Embryonic Kidney 293T (HEK-293T) cells were purchased from the American Type Culture Collection (ATCC, USA) and maintained in Dulbecco's Modified Eagle's Medium/Nutrient Mixture F-12 Ham (DMEM/F12, Sigma-Aldrich) supplemented with 10% heat-inactivated fetal bovine serum, 2 mM L glutamine, 100 U/mL penicillin, and 100 μg/mL streptomycin (Sigma-Aldrich). HEK-293T cells were incubated at 37 °C in a humidified 5% CO_2 incubator.

Cell Transfection and Dual-Luciferase Reporter Assay

At 24 h prior to transfection, the HEK-293T cells were plated at 8×10^4 cells per well in 24-well dishes. Transient transfection was performed at ~ 80% confluence using the FuGENE HD transfection reagent (Promega) according to the manufacturer's protocol. For each transfection experiment, 500 ng of the appropriate reporter construct (gfap-3′UTR-wt, gfap-3′ UTR-mut, or unmodified pmirGLO vector) and 60 nM of MiR124-3p mimic or Negative Control (Dharmacon, USA) were used. For each plasmid, three independent transfection experiments were performed and each was done in quadruplicate. Twenty-four hours after, transfection cells were harvested and assayed for firefly and Renilla luciferase activities by the Dual-Luciferase Reporter Assay System (Promega) in a GloMax-Multi+ Microplate Multimode Reader (Promega), according to the manufacturer's instruction. Relative luciferase activity was compared using the ratio of firefly and Renilla luciferase activity (F/R) of MiR124-3p to the Negative Control ratio of firefly and Renilla luciferase activity (F/R).

Cell Viability Assay

To measure cell viability, CellTiter-Glo Luminescent Cell Viability Assay was used (Promega). It measures the viability of cells based upon the quantification of cellular ATP levels. The assay relies upon the generation of a luminescent signal which is proportional to the amount of ATP and thus the number of cells that are present. For each plasmid, one additional transfection experiment was performed in quadruplicate. To obtain a value for background luminescence, control wells containing medium without cells were prepared. After transfection procedure, the volume of CellTiter-Glo Reagent equal to the volume of cell culture medium present in each well was added. Contents were mixed for 2 min to induce cell lysis and incubated at room temperature for 10 min. Luminescence signal was measured in GloMax-Multi+ Microplate Multimode Reader (Promega).

Fish Handling and Exposure

Hatchery-reared juveniles of whitefish (*Coregonus lavaretus*, 98.8 ± 8.5 g mean weight, 24.0 ± 0.7 cm mean length) were held at the Department of Salmonid Research in Rutki (Inland Fisheries Institute in Olsztyn, Poland). The fish were acclimated for 2 weeks at 10 °C. During the acclimation period, the whitefish were fed four times a day (Skretting). After acclimatization, the fish were deprived of food for 2 days, then anesthetized by immersion in etomidate solution prior to injection. The MC-LR dosage was selected based on our earlier studies in whitefish (Brzuzan et al. 2016; Woźny et al. 2016). Chemical standard of MC-LR (purity ≥ 95%; HPLC) was obtained from Enzo Life Sciences (Enzo Biochem, Inc.) and dissolved in saline solution (0.8% NaCl) as a vehicle solvent. The prepared solution contained 10 μg of MC-LR per 200 μL of volume set for each intraperitoneal injection. Exposed whitefish individuals received single intraperitoneal injections (0.5 × 25 mm needle) of MC-LR (100 μg kg^{-1} body wt.; 10 μg per 200 μL^{-1} of 0.8% NaCl), and in the same way, control fish were injected with an equal volume of saline solution alone. Following injection, the fish were placed in separate single-pass flow-through tanks supplied with system (surface) water for 48 h (pH 7.5; oxygen saturation > 90%; ammonium < 0.134 mg L^{-1}). The intraperitoneal injections of MC-LR or saline were repeated on days 7, 14, and 21. Finally, six whitefish sampled immediately prior to placing in flow-through tanks were taken as an initial control (0 h). Water temperature was measured once a day. The 95% confidence interval of the temperature in the tanks with exposed and control fish was 8–9 °C. All animals used in this study were handled in accordance with the regulations set forth by the Local Ethical Commission in Olsztyn (resolution No. 100/2011 issued on 23rd of November 2011).

Collection of Fish Tissue and Plasma Samples

At the times of collection (0 h and after 1/3 days, 1 days, 2 days, 7 days, 14 days, 28 days), the fishes were anesthetized with etomidate solution and around 2 mL of whole blood was taken from the caudal vein using S-Monovette K3 EDTA (Sarstedt). Then, the fish were killed and the brain was dissected out and preserved in RNAlater (Sigma-Aldrich). After collection, the blood was mixed by gently inverting the tube several times and immediately centrifuged at 4000×*g* at room temperature for 5 min. The plasma layer (approximately 400 μL) from the top of the tube was transferred into a fresh tube. Plasma was stored at − 20 °C during sample collection, shipped on dry ice, and stored at − 80 °C in the laboratory until next procedures.

Extraction and Reverse Transcription of Total RNA from Brain Tissue

Total RNA was extracted from the midbrain (approximately 20 mg) from control and MC-treated whitefish using a mirVana isolation kit (Life Technologies) according to the manufacturer's protocol. Briefly, 200 μL of Lysis/Binding Buffer was added. Samples were vortexed vigorously for 1 min. Then, 20 μL of miRNA Homogenate Additive was added and mixed by inverting the tube several times before it was left on ice for 10 min. Next, 200 μL of Acid-Phenol:Chloroform was added and the mixture was vortexed for 1 min. To separate the aqueous and organic phases, the tubes were centrifuged for 5 min at maximum speed (10,000×*g*).

About 200 μL of upper phase was then transferred into a fresh tube. Next, 1.25 volumes of 99.8% ethanol at room temperature were added, and the entire solution was transferred into individual filter cartridges before centrifugation for 30 s at 10000×*g*. Initial washing was conducted with 700 μL of Washing Buffer 1, followed by two washes with 500 μL of Washing Buffer 2/3. RNA was eluted from the washed filter cartridges with 40 μL of preheated (95 °C) Elution Solution. The extracted RNA was immediately used in the next step. For mRNA expression studies, total RNA was DNAse treated, according to the manufacturer's protocol (Turbo DNAse; Ambion; USA). Reverse transcription (RT) was then directly carried out using a RevertAid First Strand cDNA synthesis kit (Thermo Scientific; USA). The cDNA synthesis reaction contained 1 μg of DNAse-treated total RNA and 5 μM of oligo(dT)$_{18}$ primer. After optional incubation (65 °C for 5 min), the samples were chilled on ice and the following components were added: 4 μL of 5× Reaction Buffer, 20 U of RiboLock RNase Inhibitor, 1 mM of dNTP mix, and 200 U of RevertAid M-MuLV Reverse Transcriptase. To check for DNA contamination, two additional control reactions were run, one with all RT components except the enzyme (RT-), and the other with DNAse-treated RNA and no other reagents (NTC). The reaction was carried out at 42 °C for 60 min, and then terminated by heating at 70 °C for 5 min. Synthesized cDNA samples were stored at − 80 °C and thawed only once, just before amplification.

To profile MiR124-3p expression, we designed a protocol based on polyadenylated RNA and stem-loop reverse transcription (Biggar et al. 2014; Brzuzan et al. 2016). miRNA polyadenylation was performed using a polymerase tailing kit (Epicentre). Reactions were prepared with 1 μL of 10× polyadenylate polymerase buffer, 1 μL of adenosine triphosphate (ATP, 10 mM), 0.5 μL of *Escherichia coli* poly(A)polymerase (4 U), 1 μg of total RNA, and RNase-free water to a final volume of 10 μL. Reaction mixtures were incubated at 37 °C for 30 min, followed by 95 °C for 5 min to terminate the adenylation, and then transferred directly to ice. Reverse transcription was performed as described above, with one modification. Instead of using oligo(dT)18 primer, an aliquot of 10 μL of polyadenylated RNA from the previous step was incubated with 1 μL of 100 μM universal stem-loop RT primer (5′-CTC ACA GTA CGT TGG TAT CCT TGT GAT GTT CGA TGC CAT ATT GTA CTG TGA GTT TTT TTT TVN-3′), followed by already described procedure. Synthesized cDNA samples were diluted (20×) stored at − 80 °C and thawed only once, just before amplification.

miRNA Extraction from Plasma

Total RNA was extracted from 80 μL of plasma from control and MC-treated whitefish using a mirVana isolation kit (Life Technologies) according to the manufacturer's protocol with modifications. After thawing, samples were briefly centrifuged and 10 volumes of Lysis/Binding Buffer were added. Samples were vortexed vigorously for 1 min. To normalize sample-to-sample variation in the RNA isolation procedure, an exogenous spike-in control of 3 μL of synthetic 5 nM cel-MiR39-3p (5′-UCACCGGGUGUAA AUCAGCUUG-3′) was added. Then, 80 μL of miRNA Homogenate Additive was added and mixed by inverting the tube several times before it was left on ice for 10 min. Next, 800 μL of Acid-Phenol:Chloroform was added and the mixture was vortexed for 1 min. To separate the aqueous and organic phases, the tubes were centrifuged for 5 min at maximum speed (10,000×*g*) at room temperature. About 300 μL of upper phase was then transferred into a fresh tube. Next, 1.25 volumes of 99.8% ethanol at room temperature were added, and the entire solution was transferred into individual filter cartridges before centrifugation for 30 s at 10000×*g*. Initial washing was conducted with 700 μL of Washing Buffer 1, followed by two washes with 500 μL of Washing Buffer 2/3. RNA was eluted from the washed filter cartridges with 40 μL of preheated (95 °C) Elution Solution. The extracted RNA was immediately used in the next steps described above.

qPCR Analysis

Real-time PCR was used to determine *gfap* mRNA and MiR124-3p levels in midbrain and plasma of control and MC-LR-treated whitefish. Reactions were carried out in final volumes of 20 μL, consisting of 10 μL of Power SYBR Green PCR Master Mix (Life Technologies, USA), 0.25 μM of each primer (forward and reverse; Supplementary File 1), 1 μL of cDNA template (see "Determining *gfap* cDNA Sequence of European Whitefish" and "Phylogenetic Analysis of Whitefish Gfap"), and 7 μL of PCR-grade water. Amplification was performed on an ABI 7500 Real-time PCR System thermocycler (Applied Biosystems; USA) with the following conditions: 95 °C for 10 min, then 45 cycles of 95 °C for 15 s and 60 °C for 1 min. The reaction for each sample was carried out in duplicates. No template controls (NTCs) were included to test for the possibility of cross-contamination. To check the quality of each PCR products, melting curve analyses were additionally performed after each run.

Quantitative cycle (Cq) values obtained from qPCR were converted into template concentration using a standard curve plot (Cq versus log DNA concentration), following the approach of Arukwe (2006) as described by Spachmo and Arukwe (2012). To generate the standard curve, plasmids with target sequences were used to prepare a series of six tenfold dilutions and then served as the template in qPCR. Cq values obtained for each dilution were plotted against the log of the DNA concentration and then used to extrapolate the unknown samples to absolute numbers. In order to calculate relative expression, the absolute numbers of all analyzed samples

were divided by the geometric mean obtained from the control group; and these values were further presented as the expression ratio (R). Based on the results obtained for the standard curve, PCR efficiency was also calculated according to the following equation: $E = 10^{[-1/\text{slope}]}$ (Pfaffl et al. 2002).

Statistical Analysis

The gene (*gfap*; MiR124-3p) expression data obtained from the treatment study was tested for statistical differences using an unpaired t test (two-tailed) to compare the values determined in control fish cohort with those of the exposed whitefish at the respective time points. To test for normality of the distribution of the samples compared, the non-parametric Kolmogorov-Smirnov (K-S) test was used. In cases where the K-S test failed, two-sample Mann-Whitney test was applied. The correlation between expression of MiR124-3p in the brain and peripheral blood serum was analyzed using the Pearson method. All calculations and statistical analyses were performed using GenEx 5 Professional software (MultiD Analyses).

Results

Gfap in Whitefish Is a Structurally Conserved Protein

The obtained cDNA sequence of whitefish *gfap* comprised 2160 base pairs, including partial 5′UTR (38 bp) and partial 3′UTR (748 bp) (Fig. 1). The cDNA of *gfap* encoded a Kozak consensus sequence gccAUGG (Fig. 1; nucleotides from − 3 to + 4). The open reading frame encodes 457 amino acids long protein. The analysis showed also that the estimated molecular weight of the putative protein is 52.1 kDa with a theoretical isoelectric point of 5.26. The predicted protein contains one putative functional Gfap homology intermediate filament domain: 90–398 aa (E value = $1.83e^{-126}$). The length of the full deduced amino acid sequence of whitefish Gfap (457 aa) differs from the compared species' aa sequences by 27 (*M. musculus*), 25 (*H. sapiens*), 14 (*D. rerio*), or is the same (*O. mykiss* and *S. salar*). A multiple alignment of the deduced whitefish Gfap protein sequence with those of other species retrieved from GenBank (Fig. 2) allowed the calculation pairwise identity score matrix which demonstrated that the whitefish Gfap protein shared 98% identity with salmon and trout, 81% with zebrafish, and 63% with human and mouse. In addition, the neighbor-joining tree showed that whitefish Gfap clustered together with salmon and trout (100% of bootstrap value) and then coalesced with zebrafish (87%). The second group consisted of human and mouse, which formed another cluster with 100% frequency of occurrence. Together, these data suggest that whitefish Gfap is a structurally conserved protein, which retains functional features characteristic for intermediate filament protein.

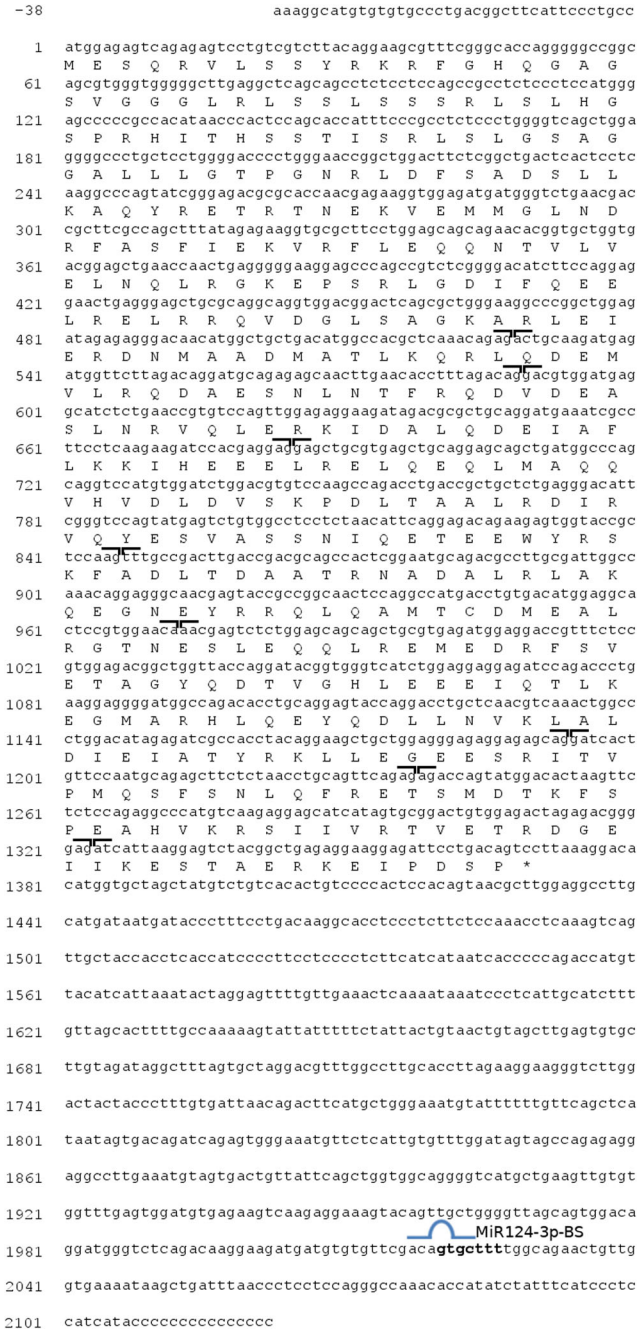


Fig. 1 Nucleotide sequence of cDNA of whitefish *gfap* aligned with deduced amino acid sequence (GenBank accession no. MG182670). Predicted exon–exon junctions and predicted MiR124-3p binding site (MiR124-3p-BS) are indicated

A MiR124-3p Target Site Is Present in the 3′UTR of *gfap* in Whitefish

One of the objectives of our study was to investigate whether the 3′UTR of *gfap* in whitefish contains a putative MiR124-3p

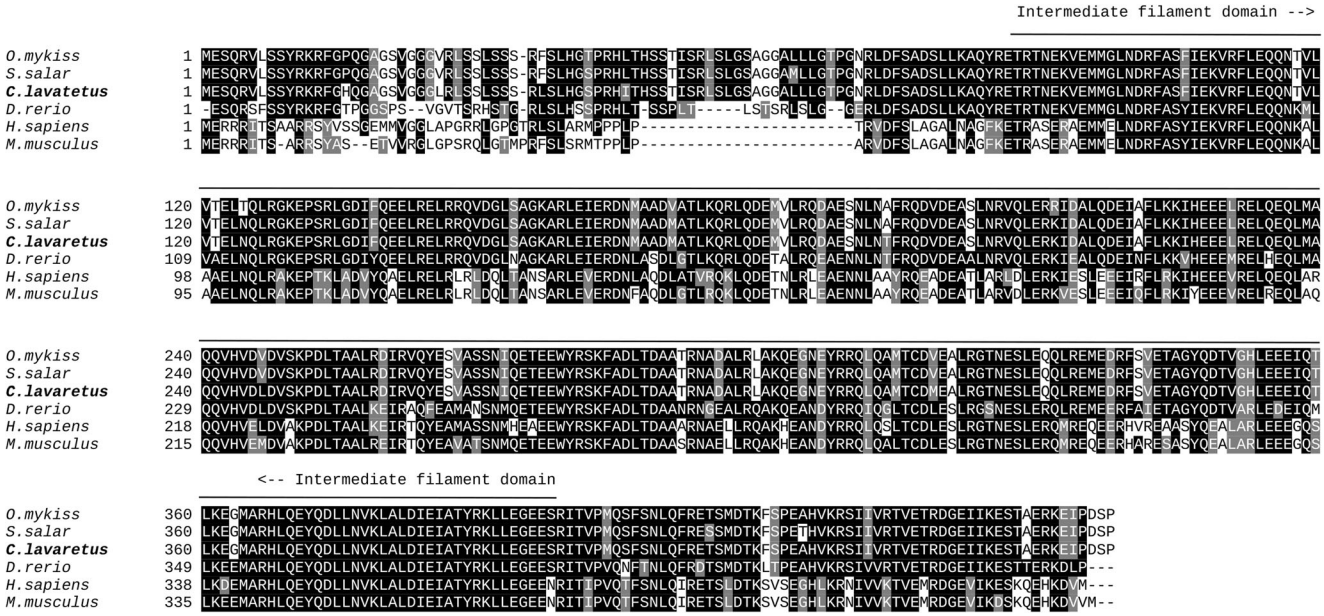


Fig. 2 Multiple alignment of deduced amino acid sequence for whitefish Gfap with those for other species. The alignment was built using Clustal W and presented using BoxShade. Identical residues are white letters in black boxes, while conservative substitutions are shaded in gray. The Gfap-conserved functional domains are indicated on the top of the region

response element(s). In silico analysis, using Segal Lab software identified one MiR124-3p target site within the analyzed 3′UTR sequence (Fig. 1). The strength of the potential miRNA:mRNA interaction could be estimated in terms of the minimum free energy for hybridization (ΔG), which for the predicted target site equals − 14.9 mol^{-1}. Figure 3a shows the putative base-pairing between mature MiR124-3p and its predicted target region within the 3′UTR of whitefish *gfap* mRNA. The degree of complementarity to the seed region (nucleotides 2, 3, 5, 6, and 7 of microRNA) classifies this target site into the so-called *GUT moderate-stringent* seed class, which contains one G:U wobble with the uracil on the target site of mRNA (Saito and Sætrom 2010).

gfap Is Up-regulated from the 7th Day of Exposure to MC-LR

Starting on the 7th day of exposure, we observed up-regulation of *gfap* expression relative to the untreated control groups (Fig. 4a). While the differences between gfap expression levels were significant at 7 days after injection ($p = 0.016$), those observed until the last day of experiment were not: 14 days ($p = 0.065$) and 28 days ($p = 0.084$). This up-regulation of *gfap* expression may serve as a defense mechanism against MC-LR.

At the same time, MiR124-3p levels in the whitefish brains remained unchanged (Fig. 4b) so as plasma levels of this miRNA (Fig. 4c), which suggest no functional correlation between *gfap* and MiR124-3p expression levels in MC-LR triggered toxicity in whitefish.

The 3′UTR of Whitefish *gfap* Is Not a Functional Target of MiR124-3p In Vitro

In order to verify the findings from in vivo experiment, we performed dual-luciferase reporter assay. This is the first study to investigate whether *gfap* is negatively regulated by MiR124-3p. Cotransfection of HEK-293T with the gfap-3′ UTR-wt luciferase reporter plasmid and MiR124-3p mimic did not lead to any inhibition of luciferase activity. The same results were observed with gfap-3′UTR-mut construct. These data show that studied *gfap* 3′UTR was not a direct target for MiR124-3p in vitro (Fig. 3b).

Discussion

This study investigates the possibility of functional correlation between *gfap* and MiR124-3p expression in MC-LR-exposed whitefish, and the suitability of plasma MiR124-3p as a potential biomarker of brain injury. We found that MC-LR induced the expression of *gfap* mRNA from the 7th day of the exposure period and kept it slightly elevated to the end of the treatment. This indicates that MC-LR may induce functional changes in the brain of whitefish that could be caused due to injury of that organ. Although MCs are primarily considered to be hepatotoxins, several studies have demonstrated that MC exposure causes a variety of symptoms related to neurotoxic effects (reviewed in Florczyk et al. 2014). For example, MC-LR exposure produced inflammatory effects in rat brains: astrocyte hyperplasia

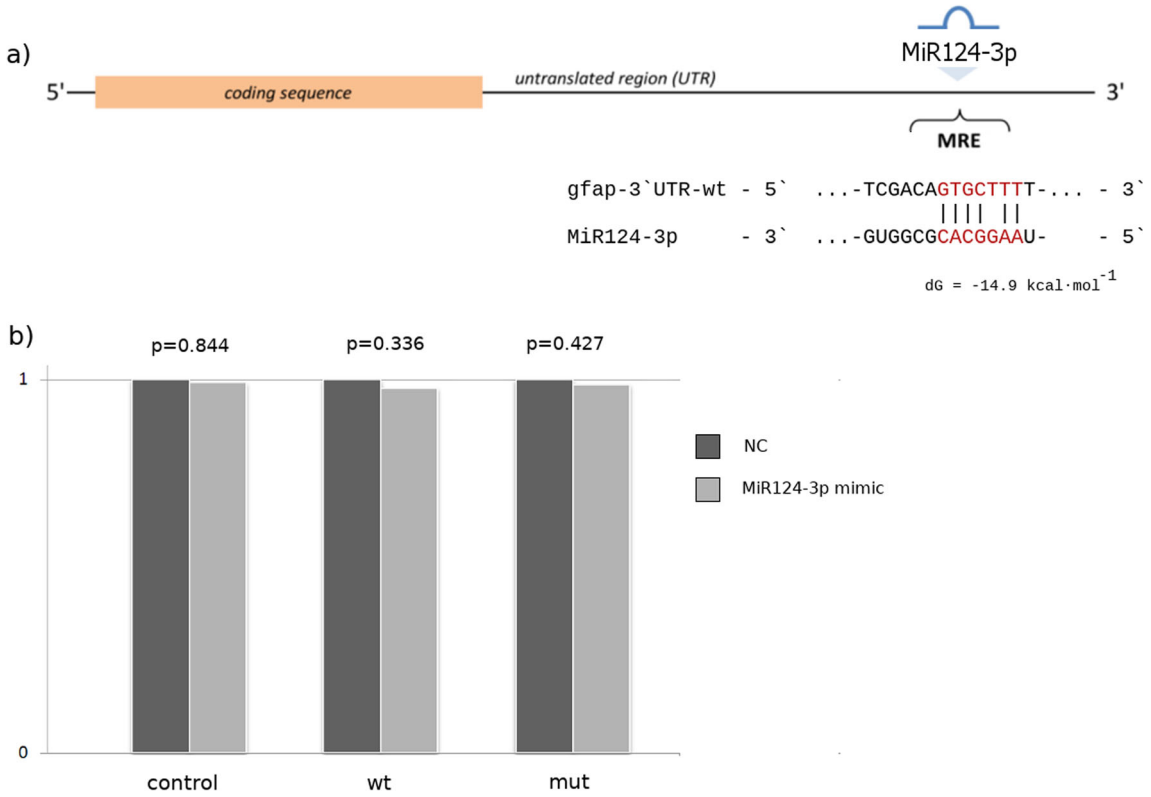


Fig. 3 Whitefish gfap 3′UTR is not a functional target of MiR124-3p in vitro. **a** Diagram of the MiR124-3p putative binding sites in the 3′UTR of *gfap*. **b** Effects of MiR124-3p mimic on the expression of gfap 3′-UTR-containing reporter genes (wt, wild type; mut, mutant type). Each luciferase activity was normalized to the value obtained in the cells transfected with NC mimics. Results were represented as mean ± S.D. from three independent experiments, each prepared in quadruplicate

and increased expression of Gfap protein, which indicated that astrocytes actively respond to the toxicity of MCs (Li et al. 2014). Reactive astrocytes not only secrete inflammatory mediators and chemokines that contribute to inflammation-mediated CNS damage (Meeuwsen et al. 2003) but also produce inflammatory cytokines and chemokines that contribute to reparative processes in the early stages of neuroinflammation (Sharma et al. 2007). Similarly, in the liver of whitefish exposed to MC-LR, numerous macrophages were present on the 7th day of the exposure period, indicating that cell debris from cell damage were being removed and that liver regeneration was beginning (Woźny et al. 2016). Activated macrophages produce cytokines, such as TNF-a, which is mainly involved in the systemic inflammation response, but also in apoptosis, cell proliferation, and cell differentiation (Hehlgans and Pfeffer 2005). Besides inflammation, MC-LR exerts whole brain cytotoxicity (Feurstein et al. 2009), inducing neuronal apoptosis and degrading the neurite network (Feurstein et al. 2011). As shown recently in rats' astrocytes, cytoskeletal disruption seen by the degradation of GFAP occurred after exposure to various MC variants (Bulc Rozman et al. 2017). Similarly, in the liver of whitefish, cytotoxicity was revealed in disruption of endoplasmic reticulum, chromatin, and cytoskeleton (Woźny et al. 2016). Although the current study does not include ultrastructural images of whitefish brain, it was reasonable to assume, based on the above-mentioned studies, that similar effects could have emerged. The present study demonstrates that repeated intraperitoneal injection of MC-LR induced neuronal toxicity was depicted in elevated *gfap* expression, which could be associated with inflammatory reactions in the midbrain.

Although *gfap* mRNA expression in the brain was elevated at the 7th day of exposure period, MiR124-3p remained unchanged. This suggests no functional correlation between *gfap* and MiR124-3p expression levels in MC-LR triggered toxicity in whitefish. MiR124-3p seems to play a crucial role in brain development as well it is enriched in mature brain tissue. Besides important roles in neuronal regulation, MiR124 is closely associated with the development of some CNS diseases. Abnormal expression of MiR124 has been shown to be implicated in many CNS diseases, like Alzheimer's disease, brain tumor, cerebral ischemic stroke, and Parkinson's disease (Sun et al. 2015). In Parkinson's disease, MiR124-3p prevented various pathological processes including neurotoxicity, neuronal apoptosis, neuroinflammation, and oxidative stress (Geng et al. 2017). MiR124-3p overexpression attenuated neuronal injury (displayed as increased cell viability and superoxide dismutase activity), as well as reduced cell apoptosis, Caspase-3 activity, lactate dehydrogenase activity,

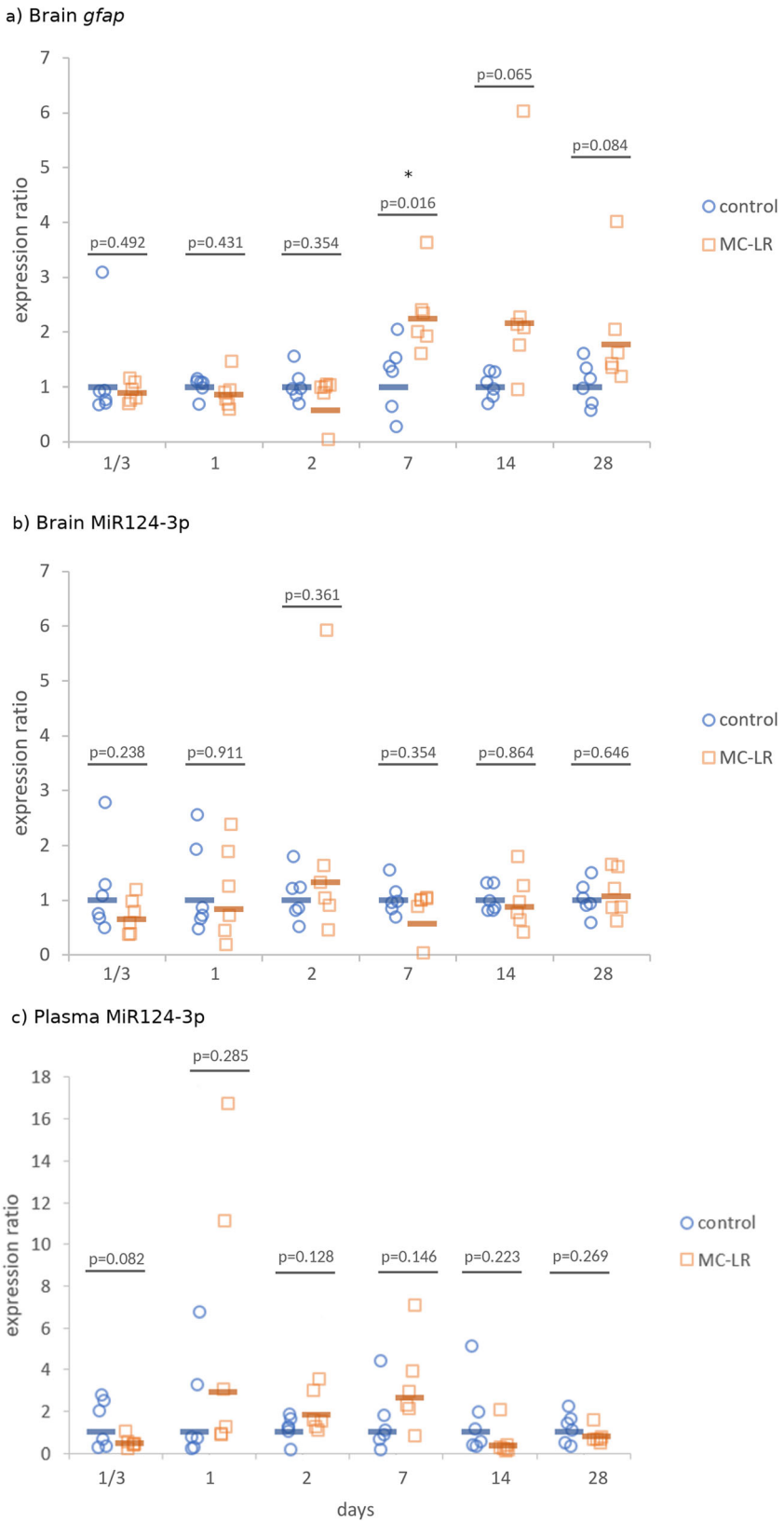


Fig. 4 Expression ratio of **a** *gfap* in midbrain, **b** MiR124-3p in midbrain, and **c** MiR124-3p in plasma of whitefish exposed for 28 days to microcystin (MC-LR) at a dose of 100 μg kg^{-1} (orange squares), relative to control (blue circles). Intraperitoneal injections of MC-LR were given on days 0, 7, 14, and 21. Points present values obtained from individual fish within a specific group, whereas horizontal lines indicate mean values ($n = 6$ per group) relative to control at the respective exposure period. Asterisks indicate significant differences from the control group at that time (treatment-dependent changes; $^*p < 0.05$)

inflammatory factors TNF-α and IL-1β levels, and reactive oxygen species generation (Geng et al. 2017). Possible regulation of the glial scar by MiR124 has been reported by Doeppner et al. (2013) and more recently by Hamzei Taj et al. (2016). MiR124 participated in this process, by increasing expression of Arg-1 or TGF-β in microglia and

macrophages, which in turn modulated the reactive astrocytes by the secretion of cytokines and chemokines. On the other hand, MiR124 effectively silenced human *GFAP* promoter expression by targeting its 3′UTR (Taschenberger et al. 2017). Moreover, it has been shown that MiR124 overexpression indirectly suppressed the expression of GFAP (Jiao et al. 2017). Our results showed an unchanged expression profile of MiR124-3p during the exposure period, proving that MC-LR-induced changes in *gfap* expression in whitefish is not correlated with participation of this miRNA.

It is accepted that circulating miRNAs are either byproducts of microvesicle secretion or cell death. Extracellular circulating miRNAs are mostly microvesicles free and associated with the RNA-binding Argonaute proteins (Ago), which are thought to be released into the circulation from the cytoplasm of necrotic cells due to disruption of cellular membranes (Sohel 2016). Thus, tissue-specific miRNAs are promising biomarkers of monitoring tissue injury. In this study, plasma levels of MiR124-3p in MC-LR exposed whitefish were unchanged during exposure period which excludes this miRNA as a biomarker of brain injury in fish. Both acetaminophen (APAP) and MC-LR induce acute liver injury in mammals and fish. Drug-induced liver injury can be monitored through traditional blood enzymes (ALT, AST) or more sensitively through miRNA quantification. Our previous study on whitefish exposed to MC-LR showed increased liver-specific miRNA plasma levels in fish, which is similar to the outcome acetaminophen induced in mammals (Florczyk et al. 2016). MiR122-5p levels were elevated as early as 8 h after exposure. This following study aimed to examine if MC-LR-induced brain injury could also be monitored using brain-specific MiR124-3p. Recent study on evaluating MiR124 as a marker of acetaminophen-induced brain injury in pigs demonstrated increased levels of this miRNA in blood (Baker et al. 2015). However, the release of MiR124 into the plasma was likely to be due to relative ischemia, as increased levels of MiR124 were significantly elevated only when cerebral perfusion pressure (CPP) fell below 30 mmHg. This could be related to indirect acetaminophen-induced brain injury caused by ischemia and general organ failure (Baker et al. 2015). In the present study, repeated exposure of whitefish to a subacute dose of MC-LR could not induce similar changes.

Luciferase reporter assay confirmed the lack of interaction in vitro which shows that MiR124-3p is unlikely to regulate *gfap* expression. This is the first study to investigate whether whitefish *gfap* is negatively regulated by MiR124-3p; however, our prediction of potential MiR124-3p target sites in 3′UTR of *gfap* could have been not accurate. For our analysis, we used miRNA prediction tool developed by Segal Lab, which has found only one moderate-stringent seed class MiR124-3p binding site. This miRNA seed class is considered as a weaker binding site than most commonly used in reporter assays 7-mer-m8 seed class. Therefore for our in vitro analysis, with only one binding site present, we have used the whole whitefish gfap 3′UTR sequence.

This prevented any false negative results even if our prediction was not completely correct and stronger MiR124-3p binding sites are present in *gfap* 3′UTR.

In conclusion, our study demonstrates that the exposure of whitefish to MC-LR-induced expression of *gfap* mRNA but did not involve any changes in expression of MiR124-3p in whitefish brain, contributing to our understanding of the mechanistic role of miRNAs in MC-LR neurotoxicity. In addition, we show that the expression of MiR124-3p in whitefish brain and plasma is not correlated with the changes of *gfap* mRNA expression and thus cannot be considered as a biomarker of brain injury induced by MC-LR. Furthermore, by using luciferase reporter assay, we confirmed the lack of interaction between 3′UTR of *gfap* mRNA and MiR124-3p, which rules out the possibility of their direct regulatory relationship. Further research focusing on regulation of astrocyte reactivity could provide better understanding of molecular background underlying MC-LR-induced neurotoxicity and perhaps hold promise for prevention strategy for MC-LR intoxication.

Acknowledgements We thank Prof. Stefan Dobosz from the Department of Salmonid Research in Rutki, Inland Fisheries Institute in Olsztyn, Poland, for his excellent technical assistance during hatchery operations. The authors also thank Mark Leonard for proofreading the manuscript. The study was supported by research grant from National Science Centre (Poland) No. DEC-2014/15/N/NZ9/01471.

Funding This study was funded by the National Science Centre (Poland) (grant number DEC-2014/15/N/NZ9/01471).

Compliance with Ethical Standards

Ethical Approval All applicable international, national, and/or institutional guidelines for the care and use of animals were followed.

Conflict of Interest The authors declare that they have no conflict of interest.

Open Access This article is distributed under the terms of the Creative Commons Attribution 4.0 International License (http://creativecommons.org/licenses/by/4.0/), which permits unrestricted use, distribution, and reproduction in any medium, provided you give appropriate credit to the original author(s) and the source, provide a link to the Creative Commons license, and indicate if changes were made.

References

Abidin SZ, Leong J-W, Mahmoudi M, Nordin N, Abdullah S, Cheah P-S, Ling K-H (2017) In silico prediction and validation of Gfap as an miR-3099 target in mouse brain. Neurosci Bull 33:373–382. https://doi.org/10.1007/s12264-017-0143-0

Arukwe A (2006) Toxicological housekeeping genes: do they really keep the house? Environ Sci Technol 40:7944–7949

Baganz D, Staaks G, Steinberg C (1998) Impact of the cyanobacteria toxin, microcystin-LR on behaviour of zebrafish, Danio rerio. Water Res 32:948–952

Baganz D, Staaks G, Pflugmacher S, Steinberg CEW (2004) Comparative study of microcystin-LR-induced behavioral changes of two fish species, Danio rerio and Leucaspius delineatus. Environ Toxicol 19:564–570. https://doi.org/10.1002/tox.20063

Baker LA, Lee KCL, Palacios Jimenez C, Alibhai H, Chang Y-M, Leckie PJ, Mookerjee RP, Davies NA, Andreola F, Jalan R (2015) Circulating microRNAs reveal time course of organ injury in a porcine model of acetaminophen-induced acute liver failure. PLoS One 10:e0128076. https://doi.org/10.1371/journal.pone.0128076

Bartel DP (2004) MicroRNAs: genomics, biogenesis, mechanism, and function. Cell 116:281–297. https://doi.org/10.1016/S0092-8674(04)00045-5

Biggar KK, Wu CW, Storey KB (2014) High-throughput amplification of mature microRNAs in uncharacterized animal models using polyadenylated RNA and stem-loop reverse transcription polymerase chain reaction. Anal Biochem 462:32–34. https://doi.org/10.1016/j.ab.2014.05.032

Brenner M (2014) Role of GFAP in CNS injuries. Neurosci Lett 565:7–13. https://doi.org/10.1016/j.neulet.2014.01.055

Brzuzan P, Woźny M, Wolińska L, Piasecka A (2012) Expression profiling in vivo demonstrates rapid changes in liver microRNA levels of whitefish (Coregonus lavaretus) following microcystin-LR exposure. Aquat Toxicol 122–123:188–196. https://doi.org/10.1016/j.aquatox.2012.07.001

Brzuzan P, Florczyk M, Łakomiak A, Woźny M (2016) Illumina sequencing reveals aberrant expression of microRNAs and their variants in whitefish (Coregonus lavaretus) liver after exposure to microcystin-LR. PLoS One 11:e0158899. https://doi.org/10.1371/journal.pone.0158899

Bulc Rozman K, Jurič DM, Šuput D (2017) Selective cytotoxicity of microcystins LR, LW and LF in rat astrocytes. Toxicol Lett 265:1–8. https://doi.org/10.1016/j.toxlet.2016.11.008

Cazenave J, Nores ML, Miceli M, Díaz MP, Wunderlin DA, Bistoni MA (2008) Changes in the swimming activity and the glutathione S-transferase activity of Jenynsia multidentata fed with microcystin-RR. Water Res 42:1299–1307. https://doi.org/10.1016/j.watres.2007.09.025

Chang T-H, Huang H-Y, Hsu JB-K, Weng S-L, Horng J-T, Huang H-D (2013) An enhanced computational platform for investigating the roles of regulatory RNA and for identifying functional RNA motifs. BMC Bioinformatics 14:S4–S8. https://doi.org/10.1186/1471-2105-14-S2-S4

Doeppner TR, Doehring M, Bretschneider E, Zechariah A, Kaltwasser B, Müller B, Koch JC, Bähr M, Hermann DM, Michel U (2013) MicroRNA-124 protects against focal cerebral ischemia via mechanisms involving Usp14-dependent REST degradation. Acta Neuropathol (Berl) 126:251–265. https://doi.org/10.1007/s00401-013-1142-5

Feurstein D, Holst K, Fischer a DDR (2009) Oatp-associated uptake and toxicity of microcystins in primary murine whole brain cells. Toxicol Appl Pharmacol 234:247–255. https://doi.org/10.1016/j.taap.2008.10.011

Feurstein D, Stemmer K, Kleinteich J, Speicher T, Dietrich DR (2011) Microcystin congener- and concentration-dependent induction of murine neuron apoptosis and neurite degeneration. Toxicol Sci Off J Soc Toxicol 124:424–431. https://doi.org/10.1093/toxsci/kfr243

Florczyk M, Łakomiak A, Woźny M, Brzuzan P (2014) Neurotoxicity of cyanobacterial toxins. Environ Biotechnol 10:26–43. https://doi.org/10.14799/ebms246

Florczyk M, Brzuzan P, Krom J, Woźny M, Łakomiak A (2016) miR-122-5p as a plasma biomarker of liver injury in fish exposed to microcystin-LR. J Fish Dis 39:741–751. https://doi.org/10.1111/jfd.12406

Friedman RC, Farh KK-H, Burge CB, Bartel DP (2009) Most mammalian mRNAs are conserved targets of microRNAs. Genome Res 19:92–105. https://doi.org/10.1101/gr.082701.108

Gasteiger E, Hoogland C, Gattiker A, Duvaud S, Wilkins MR, Appel RD, Bairoch A (2005) Protein identification and analysis tools on the ExPASy server. In: The proteomics protocols handbook. Humana Press, pp 571–607

Geng L, Liu W, Chen Y (2017) miR-124-3p attenuates MPP+-induced neuronal injury by targeting STAT3 in SH-SY5Y cells. Exp Biol Med Maywood NJ 242:1757–1764. https://doi.org/10.1177/1535370217734492

Guo L, Sun B, Sang F, Wang W, Lu Z (2009) Haplotype distribution and evolutionary pattern of miR-17 and miR-124 families based on population analysis. PLoS One 4:e7944. https://doi.org/10.1371/journal.pone.0007944

Hamzei Taj S, Kho W, Riou A, Wiedermann D, Hoehn M (2016) MiRNA-124 induces neuroprotection and functional improvement after focal cerebral ischemia. Biomaterials 91:151–165. https://doi.org/10.1016/j.biomaterials.2016.03.025

Hehlgans T, Pfeffer K (2005) The intriguing biology of the tumour necrosis factor/tumour necrosis factor receptor superfamily: players, rules and the games. Immunology 115:1–20. https://doi.org/10.1111/j.1365-2567.2005.02143.x

Jiao S, Liu Y, Yao Y, Teng J (2017) miR-124 promotes proliferation and differentiation of neuronal stem cells through inactivating Notch pathway. Cell Biosci 7:68. https://doi.org/10.1186/s13578-017-0194-y

Kapsimali M, Kloosterman WP, de Bruijn E, Rosa F, RH a P, Wilson SW (2007) MicroRNAs show a wide diversity of expression profiles in the developing and mature central nervous system. Genome Biol 8:R173. https://doi.org/10.1186/gb-2007-8-8-r173

Lagos-Quintana M, Rauhut R, Yalcin A, Meyer J, Lendeckel W, Tuschl T (2002) Identification of tissue-specific microRNAs from mouse. Curr Biol 12:735–739. https://doi.org/10.1016/S0960-9822(02)00809-6

Łakomiak A, Brzuzan P, Jakimiuk E, Florczyk M, Woźny M (2016) miR-34a and bcl-2 expression in whitefish (Coregonus lavaretus) after microcystin-LR exposure. Comp Biochem Physiol B Biochem Mol Biol 193:47–56. https://doi.org/10.1016/j.cbpb.2015.12.005

Landgraf P, Rusu M, Sheridan R, Sewer A, Iovino N, Aravin A, Pfeffer S, Rice A, Kamphorst AO, Landthaler M, Lin C, Socci ND, Hermida L, Fulci V, Chiaretti S, Foà R, Schliwka J, Fuchs U, Novosel A, Müller R-U, Schermer B, Bissels U, Inman J, Phan Q, Chien M, Weir DB, Choksi R, de Vita G, Frezzetti D, Trompeter HI, Hornung V, Teng G, Hartmann G, Palkovits M, di Lauro R, Wernet P, Macino G, Rogler CE, Nagle JW, Ju J, Papavasiliou FN, Benzing T, Lichter P, Tam W, Brownstein MJ, Bosio A, Borkhardt A, Russo JJ, Sander C, Zavolan M, Tuschl T (2007) A mammalian microRNA expression atlas based on small RNA library sequencing. Cell 129:1401–1414. https://doi.org/10.1016/j.cell.2007.04.040

Larkin MA, Blackshields G, Brown NP, Chenna R, McGettigan PA, McWilliam H, Valentin F, Wallace IM, Wilm A, Lopez R, Thompson JD, Gibson TJ, Higgins DG (2007) Clustal W and Clustal X version 2.0. Bioinformatics 23:2947–2948. https://doi.org/10.1093/bioinformatics/btm404

Letunic I, Doerks T, Bork P (2015) SMART: recent updates, new developments and status in 2015. Nucleic Acids Res 43:D257–D260. https://doi.org/10.1093/nar/gku949

Li X-B, Zhang X, Ju J, Li Y, Yin L, Pu Y (2014) Alterations in neurobehaviors and inflammation in hippocampus of rats induced by oral administration of microcystin-LR. Environ Sci Pollut Res 21:12419–12425. https://doi.org/10.1007/s11356-014-3151-x

Marchler-Bauer A, Derbyshire MK, Gonzales NR, Lu S, Chitsaz F, Geer LY, Geer RC, He J, Gwadz M, Hurwitz DI, Lanczycki CJ, Lu F,

Marchler GH, Song JS, Thanki N, Wang Z, Yamashita RA, Zhang D, Zheng C, Bryant SH (2015) CDD: NCBI's conserved domain database. Nucleic Acids Res 43:D222–D226. https://doi.org/10.1093/nar/gku1221

Meeuwsen S, Persoon-Deen C, Bsibsi M, Ravid R, Noort JMV (2003) Cytokine, chemokine and growth factor gene profiling of cultured human astrocytes after exposure to proinflammatory stimuli. Glia 43:243–253. https://doi.org/10.1002/glia.10259

Middeldorp J, Hol EM (2011) GFAP in health and disease. Prog Neurobiol 93:421–443. https://doi.org/10.1016/j.pneurobio.2011.01.005

Mishima T, Mizuguchi Y, Kawahigashi Y, Takizawa T, Takizawa T (2007) RT-PCR-based analysis of microRNA (miR-1 and -124) expression in mouse CNS. Brain Res 1131:37–43. https://doi.org/10.1016/j.brainres.2006.11.035

Mitchell A, Chang H-Y, Daugherty L, Fraser M, Hunter S, Lopez R, McAnulla C, McMenamin C, Nuka G, Pesseat S, Sangrador-Vegas A, Scheremetjew M, Rato C, Yong S-Y, Bateman A, Punta M, Attwood TK, Sigrist CJA, Redaschi N, Rivoire C, Xenarios I, Kahn D, Guyot D, Bork P, Letunic I, Gough J, Oates M, Haft D, Huang H, Natale DA, Wu CH, Orengo C, Sillitoe I, Mi H, Thomas PD, Finn RD (2015) The InterPro protein families database: the classification resource after 15 years. Nucleic Acids Res 43:D213–D221. https://doi.org/10.1093/nar/gku1243

Moxon S, Jing R, Szittya G, Schwach F, Pilcher RLR, Moulton V, Dalmay T (2008) Deep sequencing of tomato short RNAs identifies microRNAs targeting genes involved in fruit ripening. Genome Res 18:1602–1609. https://doi.org/10.1101/gr.080127.108

Pfaffl MW, Horgan GW, Dempfle L (2002) Relative expression software tool (REST) for group-wise comparison and statistical analysis of relative expression results in real-time PCR. Nucleic Acids Res 30:e36–e336

Pogue AI, Cui JG, Li YY, Zhao Y, Culicchia F, Lukiw WJ (2010) Micro RNA-125b (miRNA-125b) function in astrogliosis and glial cell proliferation. Neurosci Lett 476:18–22. https://doi.org/10.1016/j.neulet.2010.03.054

Saito T, Sætrom P (2010) MicroRNAs—targeting and target prediction. New Biotechnol 27:243–249. https://doi.org/10.1016/j.nbt.2010.02.016

Saraiva C, Paiva J, Santos T, Ferreira L, Bernardino L (2016) MicroRNA-124 loaded nanoparticles enhance brain repair in Parkinson's disease. J Control Release 235:291–305. https://doi.org/10.1016/j.jconrel.2016.06.005

Saul N, Chakrabarti S, Stürzenbaum SR, Menzel R, Steinberg CEW (2014) Neurotoxic action of microcystin-LR is reflected in the transcriptional stress response of Caenorhabditis elegans. Chem Biol Interact 223:51–57. https://doi.org/10.1016/j.cbi.2014.09.007

Sharma V, Mishra M, Ghosh S, Tewari R, Basu A, Seth P, Sen E (2007) Modulation of interleukin-1beta mediated inflammatory response in human astrocytes by flavonoids: implications in neuroprotection. Brain Res Bull 73:55–63. https://doi.org/10.1016/j.brainresbull.2007.01.016

Sofroniew MV, Vinters HV (2010) Astrocytes: biology and pathology. Acta Neuropathol (Berl) 119:7–35. https://doi.org/10.1007/s00401-009-0619-8

Sohel MH (2016) Extracellular/circulating microRNAs: release mechanisms, functions and challenges. Achiev Life Sci 10:175–186. https://doi.org/10.1016/j.als.2016.11.007

Spachmo B, Arukwe A (2012) Endocrine and developmental effects in Atlantic salmon (Salmo salar) exposed to perfluorooctane sulfonic or perfluorooctane carboxylic acids. Aquat Toxicol 108:112–124. https://doi.org/10.1016/j.aquatox.2011.07.018

Sun Y, Luo Z-M, Guo X-M, Su D-F, Liu X (2015) An updated role of microRNA-124 in central nervous system disorders: a review. Front Cell Neurosci 9. https://doi.org/10.3389/fncel.2015.00193

Tamura K, Stecher G, Peterson D, Filipski A, Kumar S (2013) MEGA6: molecular evolutionary genetics analysis version 6.0. Mol Biol Evol 30:2725–2729. https://doi.org/10.1093/molbev/mst197

Taschenberger G, Tereshchenko J, Kügler S (2017) A microRNA124 target sequence restores astrocyte specificity of gfaABC1D-driven transgene expression in AAV-mediated gene transfer. Mol Ther - Nucleic Acids 8:13–25. https://doi.org/10.1016/j.omtn.2017.03.009

Wang M, Chan LL, Si M, Hong H, Wang D (2010) Proteomic analysis of hepatic tissue of zebrafish (Danio rerio) experimentally exposed to chronic microcystin-LR. Toxicol Sci Off J Soc Toxicol 113:60–69. https://doi.org/10.1093/toxsci/kfp248

Wang C-Y, Yang S-H, Tzeng S-F (2015) MicroRNA-145 as one negative regulator of astrogliosis: role of mir-145 in astrocytic dynamics. Glia 63:194–205. https://doi.org/10.1002/glia.22743

Wheeler DL, Church DM, Edgar R, Federhen S, Helmberg W, Madden TL, Pontius JU, Schuler GD, Schriml LM, Sequeira E, Suzek TO, Tatusova TA, Wagner L (2004) Database resources of the National Center for Biotechnology Information: update. Nucleic Acids Res 32:D35–D40. https://doi.org/10.1093/nar/gkh073

Woźny M, Lewczuk B, Ziółkowska N, Gomułka P, Dobosz S, Łakomiak A, Florczyk M, Brzuzan P (2016) Intraperitoneal exposure of whitefish to microcystin-LR induces rapid liver injury followed by regeneration and resilience to subsequent exposures. Toxicol Appl Pharmacol 313:68–87. https://doi.org/10.1016/j.taap.2016.10.014

International Journal of
Molecular Sciences

MDPI

Article

De Novo Profiling of Long Non-Coding RNAs Involved in MC-LR-Induced Liver Injury in Whitefish: Discovery and Perspectives

Maciej Florczyk *, Paweł Brzuzan and Maciej Woźny

Department of Environmental Biotechnology, Faculty of Geoengineering, University of Warmia and Mazury in Olsztyn, ul. Słoneczna 45G, 10-709 Olsztyn, Poland; brzuzan@uwm.edu.pl (P.B.); maciej.wozny@uwm.edu.pl (M.W.)

* Correspondence: maciej.florczyk@uwm.edu.pl

Abstract: Microcystin-LR (MC-LR) is a potent hepatotoxin for which a substantial gap in knowledge persists regarding the underlying molecular mechanisms of liver toxicity and injury. Although long non-coding RNAs (lncRNAs) have been extensively studied in model organisms, our knowledge concerning the role of lncRNAs in liver injury is limited. Given that lncRNAs show low levels of sequence conservation, their role becomes even more unclear in non-model organisms without an annotated genome, like whitefish (*Coregonus lavaretus*). The objective of this study was to discover and profile aberrantly expressed polyadenylated lncRNAs that are involved in MC-LR-induced liver injury in whitefish. Using RNA sequencing (RNA-Seq) data, we de novo assembled a high-quality whitefish liver transcriptome. This enabled us to find 94 differentially expressed (DE) putative evolutionary conserved lncRNAs, such as MALAT1, HOTTIP, HOTAIR or HULC, and 4429 DE putative novel whitefish lncRNAs, which differed from annotated protein-coding transcripts (PCTs) in terms of minimum free energy, guanine-cytosine (GC) base-pair content and length. Additionally, we identified DE non-coding transcripts that might be 3′ autonomous untranslated regions (3′UTRs) of mRNAs. We found both evolutionary conserved lncRNAs as well as novel whitefish lncRNAs that could serve as biomarkers of liver injury.

Keywords: lncRNAs; autonomous 3′UTRs; de novo; MALAT1; non-coding RNAs; ceRNAs; drug-induced liver injury; biomarker; liver transcriptome

check for updates

Citation: Florczyk, M.; Brzuzan, P.; Woźny, M. De Novo Profiling of Long Non-Coding RNAs Involved in MC-LR-Induced Liver Injury in Whitefish: Discovery and Perspectives. *Int. J. Mol. Sci.* **2021**, *22*, 941. https://doi.org/10.3390/ijms22020941

Received: 30 October 2020
Accepted: 15 January 2021
Published: 19 January 2021

Publisher's Note: MDPI stays neutral with regard to jurisdictional claims in published maps and institutional affiliations.

Copyright: © 2021 by the authors. Licensee MDPI, Basel, Switzerland. This article is an open access article distributed under the terms and conditions of the Creative Commons Attribution (CC BY) license (https://creativecommons.org/licenses/by/4.0/).

1. Introduction

A substantial gap in knowledge persists regarding the role of microcystins (MCs) in the underlying molecular mechanisms of organ toxicity and injury. MCs are a group of cyclic heptapeptide hepatotoxins, of which microcystin-LR (MC-LR) is one of the most widely distributed and potent variants. MC-LR is absorbed, transported and accumulated predominantly in liver [1], and it causes drug-induced liver injury (DILI). Studies on the transcriptomic level have revealed various protein coding transcripts (PCTs) involved in the response and progression of MC-LR-induced liver injury in different species [2,3]. In addition to PCTs, various non-coding RNA transcripts (ncRNAs, NCTs) have been implicated in the responses to various stressors, including DILI [4]. MC-LR alters the expression levels of small regulatory ncRNAs (shorter than 200 nt) like microRNAs (miRNAs), piwi-associated RNAs (piRNAs) and small interfering RNAs (siRNAs) [5] in various types of tissues and cells [6,7].

In comparison to knowledge about small regulatory ncRNAs, our understanding of the functions and mechanism of action of long non-coding RNAs (longer than 200 nt; lncRNAs) is still limited. Unlike miRNAs, lncRNAs are poorly conserved among species [8], which hinders research on their function and evolution. However, it has been shown that lncRNAs are involved in a variety of biological processes such as cell proliferation, apoptosis and dif-

ferentiation [9] by regulating gene expression via a variety of mechanisms, including binding (sponging) miRNAs. In sponging, lncRNA competitively binds to miRNA, resulting in changes in the protein level of coding genes at the post-transcriptional level [10]. LncRNAs may function as competing endogenous RNAs (ceRNAs) that share common miRNA-response elements with PCTs [11]. For example, the recently characterized metastasis-associated-in-lung-adenocarcinoma transcript-1 (MALAT1), a well-conserved lncRNA that is implicated in diseases in humans, was shown to bind MiR34a in melanoma cells, thereby lowering MiR34a levels [12]. However, the role of MALAT1 in DILI has not yet been elucidated, and in general, our knowledge concerning the role of lncRNAs in DILI is still limited even in mammals [13].

Successful applications of RNA sequencing (RNA-Seq) technology for resolving problems pertinent to fish biology and immunology prompted us to use RNA-based methods to investigate patterns of MC-LR-induced liver injury in a teleost fish, the whitefish (*Coregonus lavaretus*). Our previous results showed that repeated exposure of whitefish to MC-LR results in severe liver damage, followed by an unexpected resilience to further exposures to the toxin and regeneration of the damaged liver structure [14]. We showed that in these adaptations, MC-LR regulates several hepatic miRNA signaling pathways and alters the expression profiles of miRNAs over the short-term [15] and long-term [16], suggesting extensive transcriptome rebuilding during these processes. Because lncRNAs have been implicated in species-specific adaptations (e.g., adaptation of zebrafish to cold [17]), a similar adaptation to MC-LR exposure that involved novel lncRNAs may have occurred in the whitefish.

Biologically active lncRNAs are present in zebrafish [18] and rainbow trout [19,20], however, these are species with well-established annotated genomes, and reference genome is not available for the majority of species. In the absence of an annotated genome, separating NCTs from PCTs requires a more challenging bioinformatic approach. As the foundation for our approach to profile lncRNAs in MC-LR-induced liver injury, we de novo assembled a whitefish liver transcriptome. Using a step-by-step pipeline designed to filter out redundant contigs, we were able to identify transcripts without coding potential, which were differentially expressed in whitefish liver after exposure to MC-LR. We identified a list of putative lncRNA transcripts, both novel and orthologous to known lncRNAs in other species. In addition, we showed that treatment of fish with MC-LR may affect levels of non-coding transcripts that may be 3′ autonomous untranslated regions of mRNAs. Furthermore, by showing how MC-LR changes expression patterns of putative lncRNAs, including MALAT1, we extended our knowledge regarding the underlying mechanisms of liver injury in whitefish. Our findings contribute to better understanding of the role of ncRNA in the molecular response to MC-LR-induced liver injury in fish.

2. Results

2.1. Sequencing Results

The number of raw reads in samples ranged from 50,797,688 to 70,885,836. The effective rate ranged from 95.88 to 99.25% ([Clean reads/Raw reads] × 100%), with a stable base error rate at 0.03% in all samples. Content of GC base pairs ranged from 47.23 to 50.50%. Detailed statistics on the quality of sequencing data for each sample are presented in Supplementary Table S1.

2.2. Assessing the Quality of the De Novo Assembled Liver Transcriptome

The number of detected transcripts in our raw de novo assembled liver transcriptome was 1,136,890, with an average length of 367 base pairs. After the assembly, we mapped the trimmed reads back to the assembled liver transcriptome. The fraction of aligned reads was between 97% and 98% per sample. The final assembly, which was used in further analyses, was obtained by filtering out too short, redundant and lowly expressed transcripts. The number of transcripts in our final assembly was 420,280 transcripts, with an

average length of 594 base pairs. The detailed statistics of the final assembly are presented in Supplementary Table S2.

The Benchmarking Universal Single-Copy Orthologs (BUSCO) analysis pipeline revealed that of the 3640 Actinopterygian single-copy orthologs searched, our final assembly completely recovered 74.9% and partially recovered 7.5% (Table 1), while 17.6% of the single-copy orthologs were reported missing from our liver transcriptome.

Table 1. Summary of the complete, duplicated, fragmented and missing orthologs inferred from the Benchmarking Universal Single-Copy Orthologs (BUSCO) search against the orthologs for *Actinopterygii*.

BUSCO Statistic	Whitefish Liver; OrthoDBv10 (This Study)	European Whitefish Whole Transcriptome; OrthoDBv10 [21]
Complete BUSCOs (C)	2725 (74.9%)	2786 (76.6%)
Complete and single-copy BUSCOs (S)	1780 (48.9%)	1713 (47.1%)
Complete and duplicated BUSCOs (D)	945 (26.0%)	1073 (29.5%)
Fragmented BUSCOs (F)	272 (7.5%)	320 (8.8%)
Missing BUSCOs (M)	643 (17.6%)	534 (14.6%)
Total BUSCO groups searched	3640	3640

2.3. De Novo Transcriptome Assembly Allowed Discovery and Classification of Non-Coding RNAs in Whitefish Exposed to MC-LR

Using the procedure for identifying ncRNAs in non-model species first described by Harris et al., we managed to first separate protein-coding transcripts (148,646 contigs) and then discover various long non-coding transcripts in whitefish (209,270) [22]. Subsequent filtering steps allowed us to separate these transcripts into three non-overlapping groups. The first group contained non-coding transcripts that showed homology to sequences deposited in the Rfam database (the group of known non-coding transcripts: 20,272 contigs). The second group contained NCTs that had homology with non-coding 3′ untranslated regions (3′UTR) of mRNA sequences deposited in the RefSeq database and had associated PCTs (autonomous 3′UTR/PCT group: 104,024 contigs). The third contained NCTs with no homology to any tested database (putative novel long non-coding RNAs: 84,974 contigs). Our filtering process is summarized in the workflow diagram (Figure 1B).

2.4. MC-LR Exposure Altered Expression of Evolutionary Conserved lncRNAs

To obtain the list of evolutionary conserved lncRNAs, transcripts left after removing PCTs were additionally checked for coding potential with the support-vector machine (SVM) based Coding Potential Calculator. Non-coding transcripts were further compared with sequences of transcripts deposited in the Rfam database. This produced a list of 20,272 contigs, which were counted and analyzed for differential expression (Figure 2A–D). Among 4238 differentially expressed (DE) evolutionary conserved non-coding RNAs, there were 94 known, putatively conserved DE lncRNAs identified, including MALAT1, HOXA transcript at the distal tip (HOTTIP), HOX transcript antisense RNA (HOTAIR) and highly up-regulated in liver cancer lncRNA (HULC) (Figure 2E–H). To show similarities in sequence conservation between whitefish and 17 other species, including human, we aligned the sequence of our putative MALAT1 transcript with seed sequences of MALAT1 deposited in the Rfam database (Supplementary Figure S1).

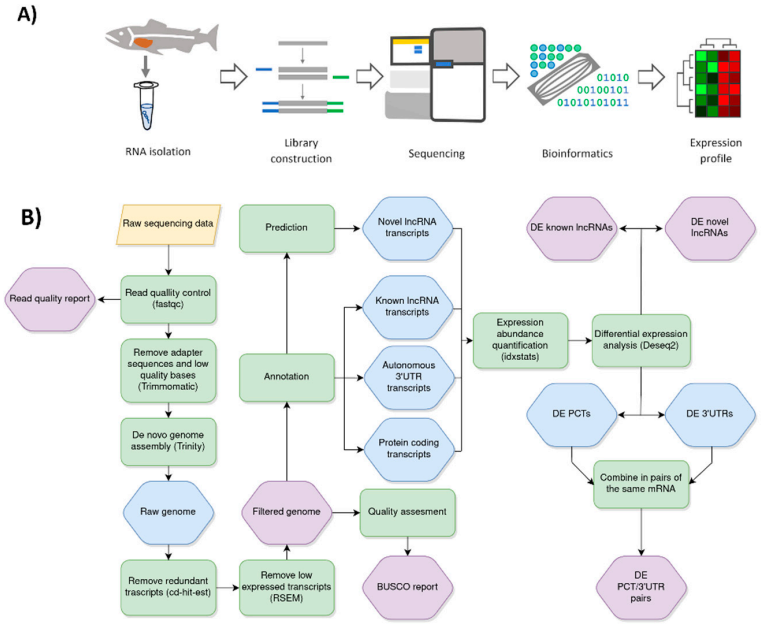


Figure 1. Schematic representation of pipeline used to profile changes in expression of putative long non-coding RNAs (lncRNAs) in microcystin-LR (MC-LR)-induced liver damage in whitefish. (**A**) Overview of the experimental procedure. (**B**) Bioinformatic analysis workflow. Yellow shapes indicate pipeline input, green shapes indicate action step taken in analysis, blue shapes indicate output of an action, purple shapes indicate final output. DE, differentially expressed; PCTs, protein coding transcripts.

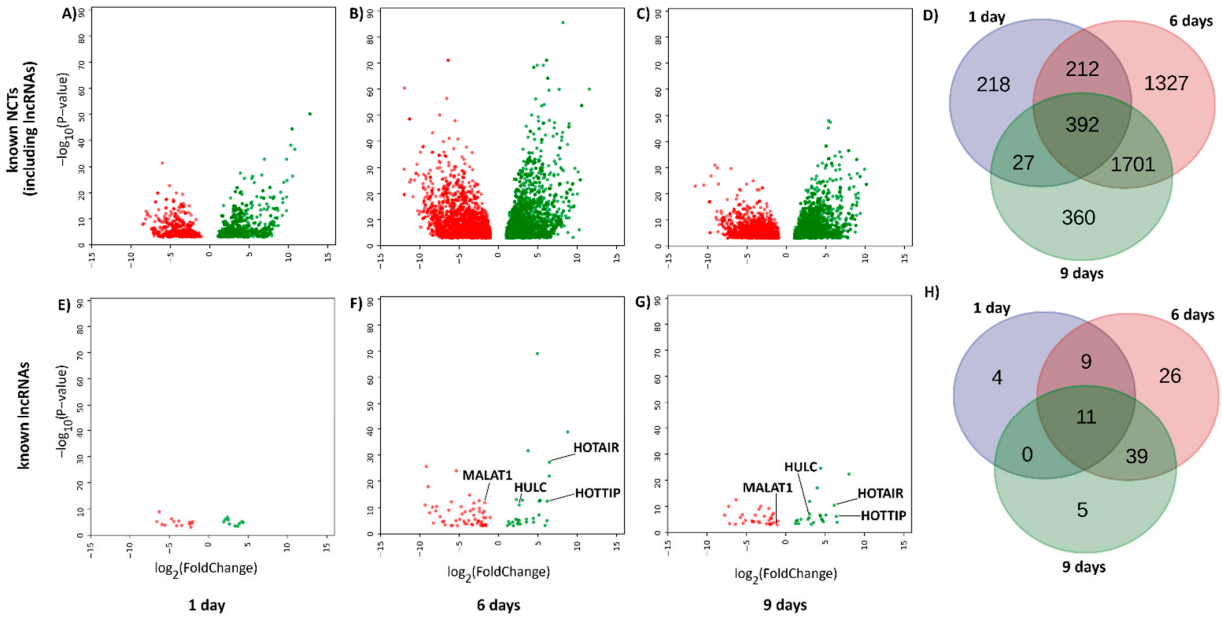


Figure 2. Differentially expressed putative known non-coding RNAs after MC-LR exposure. (**A**–**D**) Volcano plots and Venn diagram of differentially expressed (DE) transcripts with homology to any transcript deposited in the Rfam database (including lncRNAs). (**E**–**H**) Volcano plots and Venn diagram of DE transcripts with homology to transcripts labeled as lncRNAs in the Rfam database. Data points represent downregulated (red) or upregulated (green) putative known ncRNAs. Expression of putative metastasis-associated-in-lung-adenocarcinoma transcript-1 (MALAT1) transcript was downregulated at 6 and 9 days of microcystin-LR (MC-LR) exposure. Thresholds of a log2 fold-change > |2| and an adjusted p-value < 0.001 were used to filter out contigs with the smaller and less statistically significant differences between groups.

2.5. Co-Expression of Autonomous 3′UTRs and Their Associated PCTs after MC-LR Exposure

To investigate the effects of MC-LR exposure on the expression of non-coding contigs identified as autonomous 3′UTRs, we first set them together with corresponding PCTs of the same mRNA. Then, using the DESeq2 package from Bioconductor, we separately calculated the differential expression of the putative autonomous 3′UTRs and their associated PCTs. Finally, we compared the percentages of the corresponding contigs that were both up- or down-regulated, and those that were regulated in opposing directions (Figure 3). We found that, in the majority of cases, if a putative autonomous 3′UTR was DE, the associated PCT was also DE in the same direction. After 1 day of the experiment, over 82% of the transcript pairs were upregulated and only 11% were downregulated. In contrast, after 6 and 9 days, up- and down-regulated pairs were present in about the same proportions (around 40%). Moreover, we checked whether the pattern of changes in expression of co-expressed PCT/3′UTR pairs was reflected in the pattern of changes in expression of all PCTs (paired with 3′UTRs and unpaired). We found that both expression patterns were similar but not identical (data not shown).

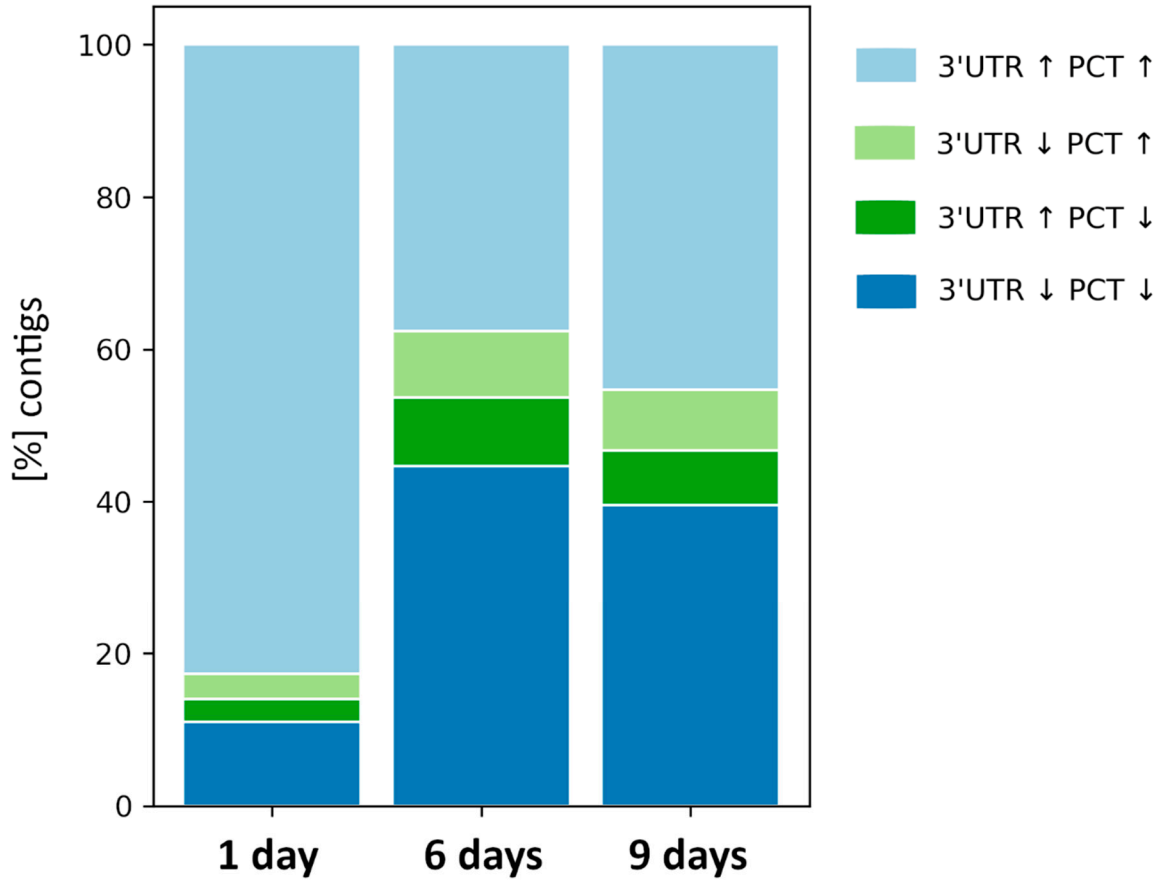


Figure 3. Pairs of differentially expressed (DE) putative autonomous 3′ untranslated regions (3′UTRs) and protein coding transcripts (PCTs) from the same mRNA in whitefish liver after microcystin-LR (MC-LR) exposure. Bars show percentages of DE contigs from the same mRNA that were both upregulated (light blue) or downregulated (dark blue), as well as those with opposing expression profiles (light and dark green). Arrows in the figure legend shows direction of expression changes (up- or down-regulated).

Gene ontology (GO) analysis indicated similarities in terms of the pairs that were simultaneously upregulated or downregulated after 6 and 9 days of MC-LR exposure (Supplementary Figure S2). In contrast, upregulated pairs at 1 day were enriched in transcription regulator activity and DNA-binding transcription factor activity transcripts when compared with upregulated pairs at 6 and 9 days (Figure 4). Downregulated pairs at

1 day were depleted in transcripts involved in enzyme regulator activity processes when compared with downregulated pairs at 6 and 9 days of exposure. GO analysis of DE contigs from the same mRNA after 1 day of the experiment that were both upregulated or downregulated, as well as those with opposing expression profiles, are shown in detail in Supplementary Figure S3.

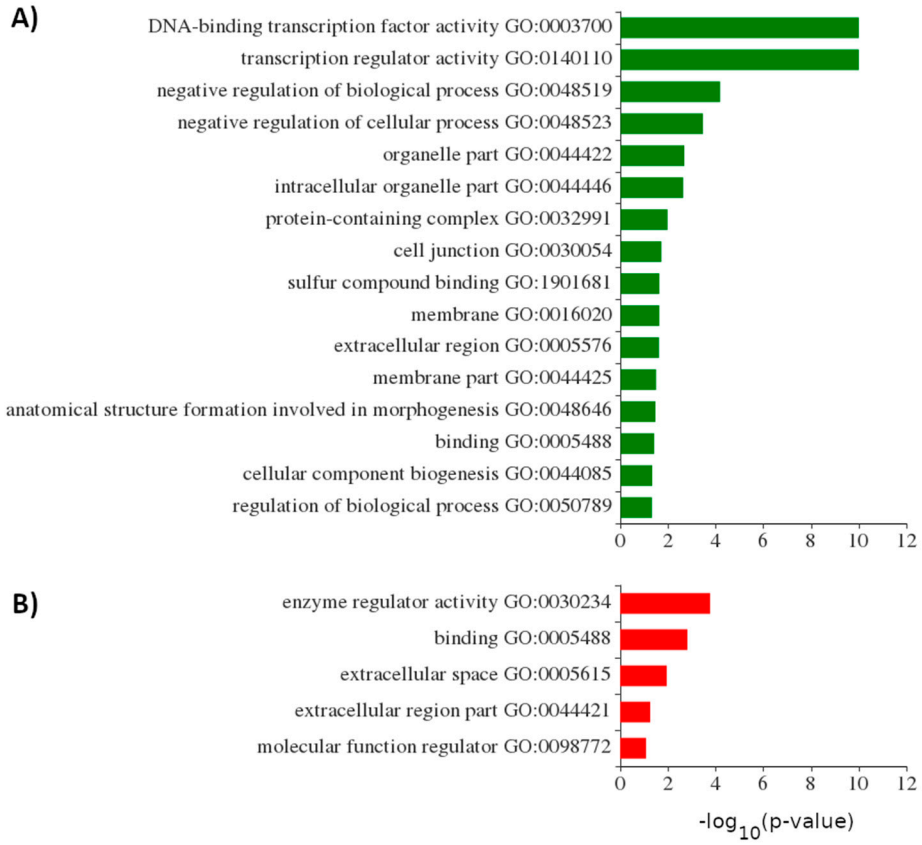


Figure 4. Gene ontology (GO) of co-expressed pairs of putative autonomous 3′UTRs and protein coding transcripts (PCTs) from the same mRNA that were upregulated (**A**) or downregulated (**B**) after microcystin-LR (MC-LR) exposure. Figure shows enriched (**A**) or depleted (**B**) gene ontology terms for pairs that were upregulated (**A**) or downregulated (**B**) at 1 day compared to 6 and 9 days. Horizontal bars represent the corresponding *p*-values of each regulated transcript pairs, $p < 0.05$.

2.6. MC-LR Produced Opposing Expression Profiles of Some Autonomous 3′UTRs and Their Associated PCTs

In addition, we found that MC-LR exposure caused contrasting changes in the expression of some 3′UTRs and their associated PCTs (Figure 3, light and dark green bars). The proportion of these to all DE transcripts was lowest after 1 day of MC-LR exposure (7%), and higher at 6 and 9 days (19% and 16% accordingly). On the other hand, the proportions of both groups with the opposite expression profiles to each other remained at a similar level throughout all the days of exposure. In the group with 3′UTRs downregulated and PCTs upregulated, gene ontology terms again showed similarities on days 6 and 9, whereas on day 1, the transcripts were comparatively enriched in terms like 'signaling' or 'response to stimulus'. In contrast, in the group with 3′UTRs upregulated and PTCs downregulated, transcripts involved in 'cell', 'cell part', 'membrane' and 'membrane part' were enriched on days 6 and 9.

2.7. Putative Novel lncRNAs and PCTs Differed in Terms Minimum Free Energy, GC Base-Pair Content and Length

To determine if the novel whitefish lncRNA candidates differed from PCTs in terms of a minimum free-energy (MFE), we used the RNAfold algorithm from the ViennaRNA package. The free energy values of the secondary structures were corrected for the lengths of the sequences (Figure 5A). The mean length-corrected MFE of the putative lncRNAs was significantly higher than that of the annotated protein coding transcripts (-0.237 kcal/mol/nt $\pm$ 0.038758 vs. -0.289 kcal/mol/nt $\pm$ 0.059464 kcal/mol/nt respectively, t(3999) = 46.65, $p < 0.001$, 95% [0.04963723, 0.05399174]. Moreover, the mean content of GC base pairs was significantly higher in PCTs (t(3999) = 56.16, $p < 0.001$, [0.06915164, 0.06448719]) (Figure 5B). Finally, the distribution of transcript lengths differed between the putative lncRNAs and the annotated PCTs, with more PCTs with longer sequence lengths (Figure 5C). In summary, structural differences between the putative lncRNAs and the annotated PCTs validated our methodology for discovery of lncRNAs in whitefish.

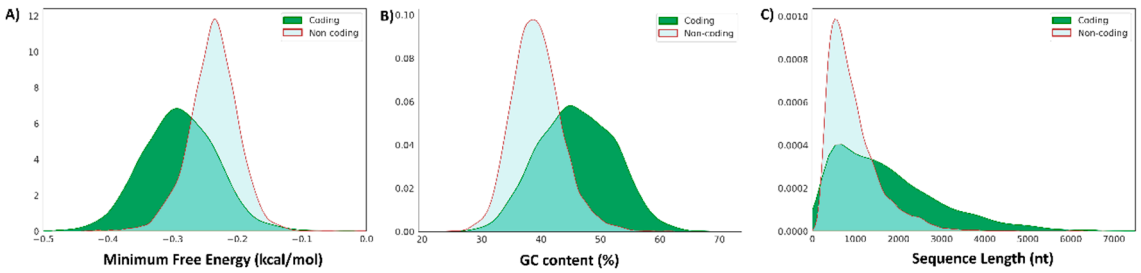


Figure 5. Distributions of length-corrected minimum free energy, content of guanine-cytosine (GC) base pairs and transcript lengths differ between protein coding transcripts (PCTs) and putative novel lncRNAs. (**A**) lncRNA transcripts have a higher mean length-corrected minimum free energy (-0.237 kcal/mol/nt) than PCTs (-0.289 kcal/mol/nt). (**B**) lncRNA transcripts have a lower mean GC base pair content (0.393) than PCTs (0.460). (**C**) Distribution of sequence lengths differ between lncRNAs and PCTs. Note that the distribution of PCT sequence lengths includes many longer sequence lengths.

2.8. MC-LR Altered the Expression Profiles of the Identified Putative Novel lncRNAs

Using the DESeq2 package of Bioconductor, we investigated whether MC-LR induced changes in the expression profiles of the putative novel lncRNAs discovered in this study. Using an adjusted *p*-value of 0.001 and a log2 fold-change of 2 as cutoffs, we identified 1739 and 2689 transcripts that were either up- or down-regulated by MC-LR exposure, respectively. Figure 6 shows volcano plots of up- and down-regulated putative novel lncRNAs (Figure 6A–C) and Venn diagrams with number of transcripts specific to each time period, as well as those which overlap between days of exposure to MC-LR (Figure 6D,E). In terms of changes in the expression of the identified transcripts, day 6 and day 9 were more similar to each other than to day 1: 31.0% and 34.8% of all up- and down-regulated lncRNA transcripts, respectively, were downregulated on both day 6 and day 9, but not on day 1 of the exposure (Figure 6D,E).

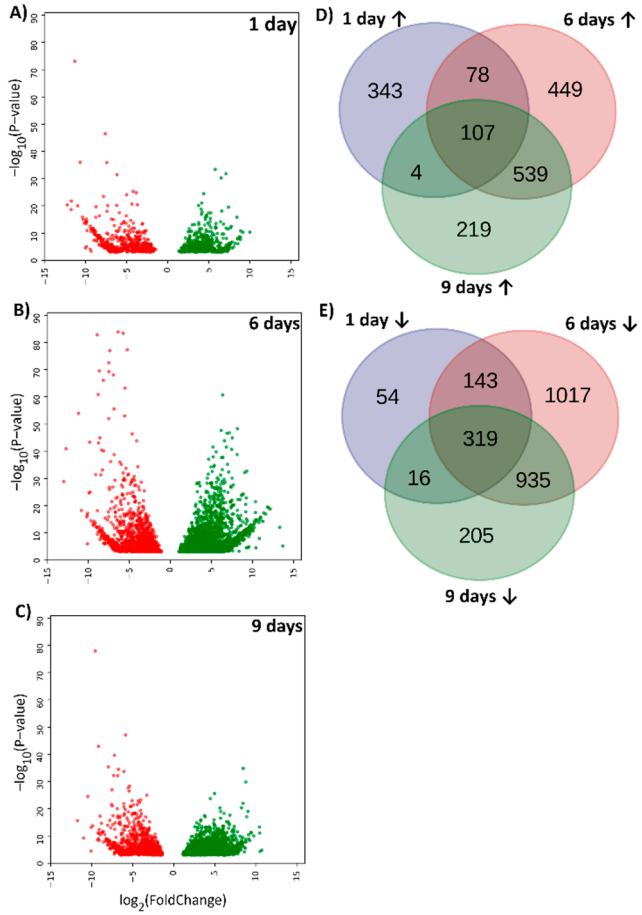


Figure 6. Microcystin-LR (MC-LR) induced differentially expressed (DE) putative novel lncRNAs in whitefish liver. Volcano plots after 1 day (**A**), 6 days (**B**) and 9 days (**C**) of exposure; data points represent downregulated (red) or upregulated (green) putative novel lncRNAs. Venn diagrams of upregulated (**D**) and downregulated (**E**) putative novel lncRNAs after MC-LR exposure. Note that days 6 and 9 are more similar to each other than to day 1 in terms of which lncRNAs were DE on those days. Thresholds of a log2 fold-change > |2| and an adjusted *p*-value < 0.001 were used to filter out contigs with the smaller and less statistically significant differences between groups.

2.9. Real-Time polymerase chain reaction (RT-PCR) Confirmed Aberrant Expression of Selected Transcripts

To validate the RNA-Seq data, we selected three known lncRNAs (Figure 7) and 10 putative novel lncRNAs (five upregulated and five downregulated, Supplementary Figure S4) and designed a RT-PCR study that re-analyzed their levels. The qPCR data indicated statistically significant changes in the expression of all selected transcripts, except MALAT1 transcripts.

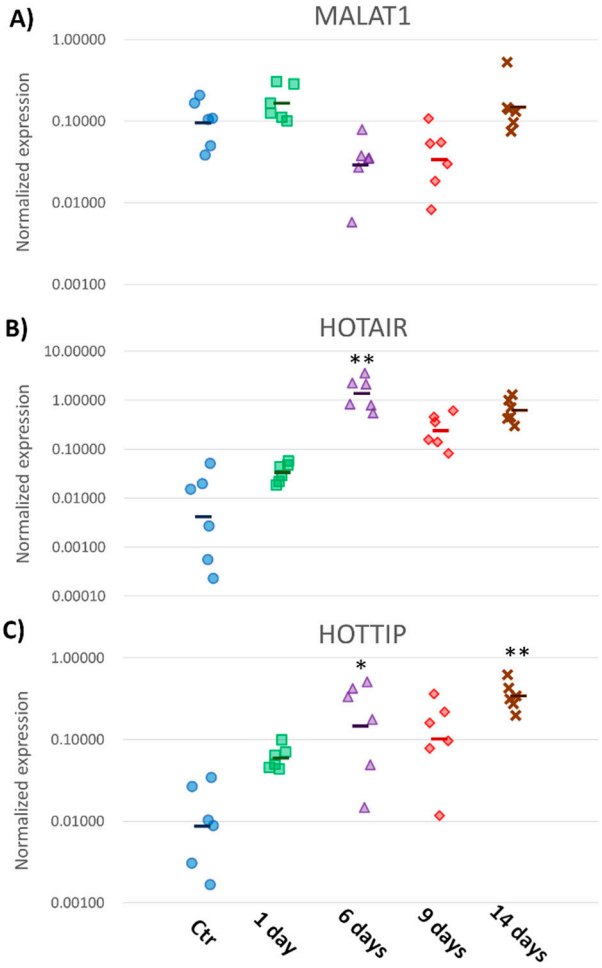


Figure 7. Expression of putative metastasis-associated-in-lung-adenocarcinoma transcript-1 (MALAT1) (**A**), HOX transcript antisense RNA (HOTAIR) (**B**) and HOXA transcript at the distal tip (HOTTIP) (**C**) in whitefish liver after 1, 6, 9 and 14 days of MC-LR exposure quantified using Real-Time polymerase chain reaction (RT-PCR). * $p < 0.05$; ** $p < 0.01$. Ctr—control, unchallenged group. Points represent individual fish in respective experimental group.

3. Discussion

In this study, using RNA-Seq data, we identified a list of putative lncRNA transcripts involved in MC-LR-induced liver injury in whitefish, a non-model species without a reference genome. Further qPCR validation of selected putative lncRNA candidates confirmed the participation of these transcripts in MC-LR-induced liver injury in whitefish. We showed that the altered expression profiles of lncRNAs could serve as potential biomarkers of liver injury in whitefish.

The lack of standardized methodologies for discovery of lncRNAs poses a challenge for the analysis and interpretation of RNA-sequencing data. The outcome of pipelines designed to discover lncRNAs in RNA-Seq data strongly depends on factors which precede in silico analysis, such as RNA isolation or the method of preparing sequencing libraries [23]. Therefore, methods designed for enriching polyadenylated protein-coding mRNAs may not be optimal for recovering lncRNAs that are present at low levels. On the other hand, designing a large-scale RNA-Seq experiment with a large set of samples is demanding and usually some trade-offs must be made [24]. Because the main aim of our RNA-Seq experiment was to analyze the profiles of protein-coding genes, Illumina's TruSeq Stranded mRNA protocol was chosen (Brzuzan et al., in preparation). However, this protocol can also be used for lncRNA discovery [23]. In fact, the majority of biologically functional lncRNAs reported to date are polyadenylated [25], thus approaches based on enriching

polyadenylated transcripts to discover functional lncRNAs are common in pipelines based on annotated genomes, as well as those based on de novo assembled transcriptomes. For example 54,503 putative lncRNAs were discovered in rainbow trout [19] and 122,969 putative lncRNAs were reported in *Rhinella arenarum* [26]. Our pipeline based on the de novo assembly of the liver transcriptome allowed us to obtain 209,270 non-coding transcripts longer than 200 nt, of which 84,974 were labeled as putative novel lncRNAs (see further discussion, page 14).

Difficulties in comparing results of RNA-Seq in silico analysis based on de novo assembled transcriptomes may be attributed to multiple factors. For example, poor reproducibility of de novo-based analyses [27] could come from the source of the reference genome (i.e., selection of tissues), in addition to the methodologies used in preparation of the sequencing libraries. Last but not least, to obtain reliable and comparable results in discovery of lncRNAs, sequencing depth should be considered. It is estimated that, in human samples, >200 million paired-end reads are required to detect the full range of transcripts, including all possible isoforms [28]. However, this number can be much lower for differential expression analyses. For example, if the expectation is that the expression of abundant transcripts changes across conditions, 36 million reads per sample may be sufficient [24]. Because it was expected that (i) MC-LR will drastically change expression profiles of transcripts [16] and (ii) polyadenylated lncRNAs are expressed at higher abundances than non-polyadenylated lncRNAs [29], we sequenced our liver samples with 50 million reads per sample, which was sufficient to identify evolutionary conserved and novel transcripts.

In organisms without a conclusively proven reference genome, good-quality de novo assembled transcripts are a prerequisite for obtaining meaningful results in downstream analysis, such as discovery of novel transcripts [30]. We assembled whitefish liver transcriptome from 52 liver samples that originated from different experimental groups, including some that were part of another study, which extended the scope of available transcripts used for the assembly (Brzuzan et al., in preparation, Supplementary Table S1). BUSCO analysis, which estimates assembly quality based on evolutionary-informed expectations of gene content from orthologues selected from OrthoDB, showed 74.9% completeness of Actinopterygian core genes (OrthoDB v10). For comparison, the current best assembly of a whitefish full-length transcriptome based on a whole fish homogenate showed only slightly higher completeness (76.6%, OrthoDB v10, Table 1) [21]. Importantly, BUSCO recovery estimates tend to be higher in full organism assemblies than in those assembled from a set of separate tissues. For example, a whitefish tissue-based full-length transcriptome deposited in the PhyloFish database showed only 26% completeness [21]. Because our assembly of a whitefish liver transcriptome showed completeness similar to the current best whitefish whole transcriptome assemblies, we believe that it not only provided a solid foundation for our analysis, but it could also extend the completeness of current and future assemblies of whitefish transcriptomes.

Designing an accurate step-by-step pipeline for discovery of lncRNAs is an essential step for producing high-quality results. This is even more important for non-model species without a reference genome, as redundancy tends to be higher in those analyses. As a consensus state-of-the-art integrated pipeline does not yet exist, we decided to base our pipeline on a previously described pipeline for identification of lncRNAs in non-model species [22]. The core aim of this pipeline was to remove known PCTs and ncRNAs in a sequence of filtration steps. As a result, the pipeline predicts novel lncRNAs, then uses software that employs Support Vector Machine in an attempt to validate the novel transcripts by assessing protein-coding potential. Unfortunately, as both the pipeline and the validation process use BLAST results with varying levels of confidence, this validation is in fact only pseudo-independent, and thus the presented transcripts are predictions at best, and only experimental evidence can validate their true function [22]. However, a lack of an assessment of the sensitivity or the specificity of a pipeline is common among current

studies aiming to classify novel lncRNA transcripts, particularly in non-model species without well-annotated genomes.

Here, we show that the putative lncRNAs differ substantially from the PCTs in terms of minimum length-corrected free energy, GC content and distribution of transcripts lengths (Figure 5). Minimum free energy is considered crucial for RNA secondary-structure stability [31]. Previous studies reported that lncRNAs have a higher free-energy level than PCTs [32–34], which is in line with our data. Moreover, previous findings showed that lncRNAs are less folded than PCTs due to the lower content of GC base pairs than PCTs [22,34], which was also reflected in our results. Additionally, previous studies, including studies of fish, have revealed that lncRNAs were overall enriched for shorter transcripts [19,22], which was confirmed in our study. Additionally, to validate the results of our pipeline, we performed a successful qPCR validation of selected putative lncRNA transcripts (Supplementary Figure S4).

Based on the similarity of our transcripts to the non-coding sequences deposited in the Rfam database, we identified putative whitefish liver lncRNAs whose expression was changed after MC-LR administration (known differentially expressed lncRNAs). We found that MC-LR altered expression of potent regulators of genes, such as HOTAIR, HOTTIP, HULC or MALAT1 (Figure 2E–H). Generally, lncRNAs are poorly conserved among species [8], but some of them, for example MALAT1, are conserved in mammals [35] as well as in other vertebrates, such as zebrafish [36], suggesting that they have important conserved biological roles. Moreover, MALAT1 is one of the most abundantly expressed lncRNAs in normal tissues [35,37], even similar in this regard to many protein-coding genes, such as glyceraldehyde 3-phosphate dehydrogenase (GAPDH) [38]. MALAT1 expression has been shown to be either upregulated (lung cancer, hepatocellular carcinoma) or downregulated (colorectal cancer, breast cancer) [37], indicating that its role is either cancer-promoting or tumor-suppressing. At the functional level, MALAT1 has been shown to bind various miRNAs, which promoted [39,40] or decreased cancer progression [41]. For example, knocking down MALAT1 in melanoma cells significantly upregulated the expression of tumor-suppressing MiR34a [42]. Interestingly, previous results demonstrated that MiR34a was upregulated in whitefish liver after MC-LR exposure [43,44].

Because our RNA-Seq and qPCR results showed that MALAT1 was present at a high level in normal whitefish liver, and most likely its expression was downregulated at 6 and 9 days after MC-LR exposure, this could indicate that decreased abundance of MALAT1 may also be linked with upregulated levels of MiR34a in whitefish liver after MC-LR exposure. Although the qPCR data on MALAT1 was not statistically conclusive, it was consistent with the RNA-Seq data, in that both techniques suggested or indicated, respectively, downregulation of this transcript 6 and 9 days after MC-LR exposure. Although it is too soon to speculate on whether and how this effect could potentially underlie the molecular mechanisms of MC-LR-induced liver injury, this finding adds to the little that is known about possible lncRNA and miRNA interactions in liver cells.

Previous research on MALAT1 variability has demonstrated that the majority of its transcripts are not polyadenylated [45]. However, it has been revealed that, in mammals, MALAT1 not only has a highly abundant short isoform that lacks a poly(A) tail, but also has a long isoform that is present at a much lower level and has a genomically encoded poly(A) tract. The longer isoform is further processed by RNAse P and RNAse Z to the shorter isoform. In this study, using a library preparation method that enriched only polyadenylated transcripts, we might have detected mainly polyadenylated MALAT1 transcripts, thus confirming the presence of that isoform in fish. To better study the biological function of these lncRNA, further research is required to investigate both the structural diversity and gene regulation of MALAT1.

After removal of PCTs and known NCTs, a large group of the remaining NCTs still mapped to the mRNAs deposited in the Reference Sequence database (RefSeq). However, after closer examination of particular BLAST hits, we noticed that the vast majority of our remaining NCTs mapped not to the coding parts of matched mRNA sequences, but to

their non-coding 3′UTR regions. The presence of autonomous 3′UTR transcripts separated from their associated mRNAs has been documented in studies on mouse and human cells [46–48]. Because 3′UTR regions that were considered to be a part of the canonical transcripts are in fact biologically significant autonomous units participating in post-transcriptional regulation [48], we analyzed how expression of our putative autonomous 3′UTR transcripts corresponded to that of the PCT from the same mRNA. We found that, in the normal (unchallenged) condition, almost the same number of mRNAs had a significantly higher number of 3′UTR transcripts (48% of differentially expressed (DE) mRNAs) as those which had a higher number of PCTs (52% of DE mRNAs). This may indicate that, in normal whitefish liver, expression of those transcripts remains in a stable relationship. Moreover, we showed that exposure to MC-LR increased the abundance of PCTs while decreasing that of 3′UTR transcripts from the same mRNA (Figure 3). In pairs in which expression was changed after MC-LR exposure, 60% of the pairs had more PCTs than 3′UTR transcripts. In contrast, the same DE pairs showed the opposite pattern of expression in the control samples (i.e., 60% of the same pairs had more 3′UTR transcripts), indicating that MC-LR changed the PCT/3′UTR ratio in about 20% of DE mRNAs (depending on the duration of exposure). This also indicated that, after MC-LR exposure, expression of our putative 3′UTR transcripts changed independently of PCTs expression.

In the majority of cases, if a putative autonomous 3′UTR was DE after MC-LR exposure, the associated PCT was also DE in the same direction. Our results show that, out of all DE PCT/3′UTR pairs after 1 day of MC-LR exposure, over 82% of the paired transcripts were upregulated (Figure 3). In contrast, at after 6 and 9 days of exposure, there was no longer a majority of PCT/3′UTR pairs that were DE in the same direction. Moreover, gene ontology terms analysis showed that, after 1 day of exposure, the co-upregulated pairs were enriched in transcription regulators, suggesting that these transcripts play roles in regulating the response to severe liver damage (Figure 4A). For example, this group included both ATF3 and FOS, the subunits of the AP-1, a pro-apoptotic transcription factor. This is in line with recently published results of transcriptomic profiling of microcystin-LR in human hepatocyte cell line [49]. On the other hand, after 1 day of exposure, the co-downregulated pairs were depleted in enzyme regulators, including phosphatases, which is the canonical mode of action of microcystins [50] (Figure 4B).

Additionally, our results show that DE PCT/3′UTR pairs at 6 and 9 days of exposure are similar in terms of function and direction of expression changes (Supplementary Figure S2). The observed changes in the liver transcriptome between the 1st and the 6th or 9th day of exposure may support our previous finding that challenging whitefish with MC-LR results in severe liver damage, which is followed by resilience to further exposures to the toxin, allowing for regeneration of the damaged organ [14]. It should be investigated whether this apparent shift in the transcriptome profile reflects remodeling of liver cell processes for repair of the tissue.

Moreover, we also found that, in response to MC-LR exposure, some putative autonomous 3′UTRs and PCTs from the same mRNA were differently expressed in opposite directions, i.e., one was upregulated while the other was downregulated (Figure 3, light and dark green bars). We were particularly interested in pairs where the 3′UTR transcripts were upregulated and the PCTs were downregulated, as this could be attributed to a recently discovered mechanism in which the 3′UTR is cleaved and shortened [48]. The discoverers of that mechanism hypothesized that it serves as a global regulatory tool that works by increasing the effectiveness of miRNA binding sites upstream of the cleavage site. This would cause levels of 3′UTRs to rise after cleavage, while levels of the corresponding PCTs would drop as a result of more effective miRNA binding. Previous studies showed that miRNAs that play roles in transcription regulation are also aberrantly expressed after exposure to MC-LR [5,16,51,52]. Because there is a possible crosstalk between various types of NCTs participating in post-transcriptional regulation of PCTs in MC-LR-induced liver injury, our results suggest the necessity of adopting a wider perspective when investigating the effects of MC-LR-induced liver damage. Researchers looking to discover all aspects

of transcriptome regulation by ncRNAs in MC-LR toxicity should focus on decoding the crosstalk between NCTs and PCTs, i.e., competition between endogenous RNAs [53]. It has been shown recently that this strategy can be applied to successfully investigate mechanisms of MC-LR toxicity in other tissues. For example, Meng et al. showed a transcriptomic regulatory network of miRNAs, piRNAs, circular RNAs, lncRNAs and mRNAs that were simultaneously involved in the cytotoxicity of MC-LR in testicular tissues in mice [5].

Gene ontology terms analysis of pairs where the 3′UTR transcripts were upregulated and the PCTs were downregulated (Supplementary Figure S3D) showed genes involved in the catalytic activity and binding processes, particularly mapk3 (non-specific serine/threonine protein kinase) involved in mitogen activated protein kinase (MAPK) signaling. MAPK signaling is induced by MC-LR, which inhibits PP2A phosphatases [54]. Active MAPKs stimulate the synthesis and phosphorylation of transcription factors, which leads to an increase in cellular proliferation and tumor promotion [55]. Because it was shown that mapk3 is regulated by MIR550a-3p in breast cancer [56], it may be possible that increased MAPK signaling is compensated by the mechanism of shortening of 3′UTRs. Similarly, we also observed enriched transcripts involved in the metabolic pathways, for example, GTP cyclohydrolase 1 encoded by the GCH1 gene, which is responsible for the hydrolysis of guanosine triphosphate (GTP). In a recent study, GCH1 was found enriched in human hepatocellular carcinoma [57]. GCH1 gene expression is regulated post-translationally, e.g., by phosphorylation [58], but it was also shown that GCH1 mRNA is a target of miR-133a in endothelial cells [59].

Although we showed that the putative 3′UTR contigs were expressed independently of PCTs, some of the autonomous 3′UTRs paired with PCTs from the same mRNA could in fact be fragmented or incomplete mRNAs which were not assembled properly. However, even if a de novo transcriptome assembly approach for detecting various types of non-coding RNAs is not without flaws, it can be used as an extension to analyses based on annotated genomes. Because the detection of autonomous 3′UTR transcripts using an annotated genome needs additional enrichment of 3′UTR transcripts in the RNA isolation or library preparation steps, it requires additional sequencing runs. Alternatively, pipelines designed to analyze autonomous 3′UTRs based on the de novo assembled transcriptome may be used in a preliminary research, eventually leading to more focused sequencing runs. Furthermore, the huge collection of deposited transcriptomic data may be reused for additional de novo analysis by teams seeking direction for their studies on non-coding RNAs.

The aforementioned group of 84,974 putative novel lncRNAs contained transcripts longer than 200 nucleotides with no homology to any tested database. We showed that MC-LR upregulated expression levels of 1739 putative novel lncRNAs and downregulated 2690 (Figure 6). We found that MC-LR-induced change in expression of putative novel lncRNAs was also reflected in change in expression of PCTs (data not shown). Because, as for now, co-expression of lncRNAs with PCTs is the most common approach for identifying potential target genes of lncRNAs [12], this will allow to identify potential target genes of lncRNAs, and to investigate their biological function in MC-LR-induced liver injury in whitefish. Moreover, putative novel lncRNAs might also serve as potential biomarkers for early detection of severe liver injury in whitefish (1 day), as well as the fish's recovery from exposure to the toxin, including regeneration of liver tissues (6 and 9 days). As demonstrated in certain types of cancers [60], lncRNAs have highly specific expression patterns and relatively stable secondary structures, and are efficiently detected in blood, plasma and urine. With these properties, they have the potential to serve as novel noninvasive biomarkers for drug-induced liver injury [13,61,62]. Additionally, our previous results suggests that the non-coding MiR122 can be a non-invasive biomarker for detecting liver damage in fish, and a promising alternative to current gold-standard hepatotoxicity markers [63].

The adverse effects of MC-LR in whitefish are not limited only to the liver. For example, we previously showed that MC-LR caused brain injury in whitefish [64]. Although plasma levels of brain-specific MiR124-3p were not altered, it is possible that some brain-specific lncRNAs could serve as biomarkers of brain injury. Interestingly, MALAT1 shows

relatively high expression in the brain, where it is involved in regulating synaptogenesis [65]. MALAT1 was downregulated in glioma [66] and is able to regulate levels of MiR124 in various diseases, including Parkinson's disease [67]. Future studies will advance understanding of the roles of lncRNAs in MC-LR toxicity and will likely reveal novel biomarkers and targets for treatment. It will also be important to determine whether the aberrantly expressed lncRNAs detected in this study can be detected in noninvasively collected samples.

4. Materials and Methods

4.1. Fish Maintenance and Exposure

This study is a part of larger project which aimed to examine changes in the liver transcriptome of whitefish exposed to MC-LR and the effects of intervention with the use of microRNA 92b-3p synthetic analogs (mimic and inhibitor) on the transcriptome. Experimental details concerning maintenance and exposure of the individuals used in this project will be described in separate papers (Brzuzan et al., Woźny et al., in preparation). In the current study, a total number of 52 individuals from the RNA-Seq of the whole project were used in order to assemble the reference transcriptome (Supplementary Table S1). However, only 30 individuals from the project were used to assess MC-LR effects on expression of non-coding transcripts.

Fish maintenance and exposure were conducted at the Department of Salmonid Research in Rutki (Inland Fisheries Institute in Olsztyn, Poland). The department also provided fish for this study. All animal-related procedures were approved by the Local Ethics Committee for Experiments on Animals in Olsztyn, Poland (resolution No. 44/2016 of 30 November 2016). Juvenile whitefish (mean ± standard deviation (SD): 29.9 ± 1.6 g, 17.0 ± 0.4 cm) were kept in flow-through tanks supplied with well (underground) water. Water temperature in the tanks was 9.3 ± 0.2 °C and oxygen level was 10.3 ± 0.6 mg·L^{-1}. Throughout the experiment, all the fish were fed with a minimal feeding procedure dependent on the water temperature, caloric content of the feed and predicted fish mass. However, 1–2 days prior to exposure (intraperitoneal injections) or collection of samples, the fish were deprived of food.

The dose of MC-LR (100 µg·kg^{-1} of body mass) and the treatment periods (1, 6, 9 and 14 days) were based on our previous studies on molecular and physiological responses of whitefish to this toxin [14,16,68]. MC-LR (purity ≥ 95%; high-performance liquid chromatography, HPLC) was obtained from Enzo Life Sciences (Enzo Biochem, Inc.; Farmingdale, NY, USA) and dissolved in phosphate buffer saline (PBS) as a solvent vehicle. Prior to exposure, randomly selected individuals from each group were anesthetized by immersion in MS-222 solution, and then they received an intraperitoneal injection of the MC-LR solution. To maintain continuous exposure, the MC-LR injection (100 µg·kg^{-1} of body mass) was repeated after 7 days of the experiment. Fish that received an intraperitoneal injection with pure PBS served as a negative control group. Throughout the exposure period, fish from the different groups were kept in separate tanks. Each experimental group (PBS or MC-LR) in each treatment period (1, 6, 9 and 14 days) consisted of n = 6 individuals, thus in total, 30 individuals were used in our MC-LR-treatment study. The number of fish in each experimental group was estimated based on our previous work [16], where we demonstrate that this group size is sufficient to observe a distinct effect of MC-LR on ncRNA expression pattern.

After each exposure period, randomly selected individuals from each group were euthanized by the MS-222 anesthetic overdosing (immersion in 300 ppm solution) and fragments of their livers were collected and preserved in RNAlater solution according to the manufacturer's recommendations (Sigma-Aldrich, St. Louis, MO, USA). All the fish used in this study were euthanized via an overdose of MS-222.

4.2. RNA Isolation, Sequencing and Initial De Novo Assembly

Total RNA was extracted from the RNAlater-preserved liver fragments (approximately 20 mg) using a PureLink RNA Mini Kit (Life Technologies, Carlsbad, CA, USA) according to the manufacturer's protocol. To remove the genomic DNA residue, the extracted samples were incubated with TURBO DNAse (Invitrogen, Carlsbad, CA, USA) and then purified using the PureLink RNA Mini Kit. RNA integrity was evaluated with an Agilent Bioanalyzer 2100 with an Agilent 6000 Nano Kit and the samples with mean RNA integrity number (RIN) > 8 were taken for library preparation with the Illumina TruSeq Stranded mRNA Library Prep protocol. The libraries were sequenced with an Illumina HiSeq4000 sequencer (250–300 bp insert cDNA size, PE150, 50 M reads, 15 Gb).

The workflow used to profile changes in expression of putative ncRNAs in MC-LR-induced liver injury in whitefish is shown in Figure 1. Quality control of raw sequencing reads was performed with FastQC, version 0.11.8. To remove adapter sequences and low-quality bases, the reads were processed using Trimmomatic, version 0.36 [69]. After quality trimming, every 6th read (starting from the 6th) was selected for downstream analysis. Selected reads were assembled into a reference genome using Trinity, version 2.5.1, with the default parameters [70]. Trimmed reads were mapped back to the reference genome using Bowtie2, version 2.3.5.1 [71].

4.3. ncRNA Identification Pipeline

The following pipeline was based on Reference [22]. First, the Trinity de novo assembled genome was filtered for redundant transcripts using the cd-hit-est algorithm of CD-HIT [72], with a sequence identity threshold of 0.9. Filtering by expression was executed with RSEM [73] implemented by the Trinity-provided perl script 'align_and_estimate_abundance'. Transcripts with expression levels below FPKM = 1.50 (fragments per kilobase of transcript per million mapped reads) were filtered out from the dataset.

To assess the quality of the filtered de novo assembled transcriptome, we quantified its completeness by comparing it with a set of highly conserved single-copy orthologs. Using the BUSCO v2 pipeline [74], we compared our assembly with the predefined set of 3640 Actinopterygian single-copy orthologs from the OrthoDB v10 database [75]. BUSCO analysis calculated the number of orthologs, whose length was within two standard deviations of the mean length of the given BUSCO (complete BUSCOs, C), complete BUSCOs represented by single-copy transcript (single-copy BUSCOs, S), complete BUSCOs evidenced by more than one transcript (duplicated BUSCOs, D), partially recovered BUSCOs (fragmented BUSCOs, F) and not recovered BUSCOs (missing BUSCOs, M). To verify our assembly, we repeated exactly the same procedure with the most complete whitefish whole transcriptome available to date [21].

Next, the transcripts were searched for open reading frames (ORFs) by Transdecoder, version 2.0.1 [76]. To identify protein coding transcripts, ORFs and transcripts were searched against the UniProt-Swiss-Prot and Atlantic salmon proteins reference databases (GCF_000233375.1) using blastp and blastx from the BLAST+ suite with a threshold E-value of 1×10^{-3} [77]. Protein family searches were performed with the Pfam 32.0 database [78] using the ORF protein sequences in HMMER, version 3.2.1. Finally, the top BLAST hit based on the bit score, E-value and percent alignment, and all HMMER hits were loaded into Trinotate, version 3.2.1, to generate an annotation report [79]. Based on the report, transcripts that were not PCTs were then filtered against the RFAM database, version 12.0 [80], by the cmscan algorithm implemented by Infernal, version 1.1.3 [81]. Any hit that Infernal considered significant using the default parameters was filtered out (and labeled as a known ncRNA). All remaining putative novel NCTs were further validated by calculating coding potential using Coding Potential Calculator (CPC) [82].

To further verify that the remaining contigs were completely separated from mRNAs, putative novel non-coding transcripts were subjected to a blastn search against the Reference RNA Sequences database (NCBI, refseq_rna). Any transcript that was identified as "mRNA" was set together in a pair with corresponding PCT of the same mRNA. Only

transcripts which had a corresponding PCT were subjected to further analysis (putative autonomous 3′UTRs).

At this point, all transcripts that were considered to be either known ncRNAs or putative novel ncRNAs, as well as transcripts identified as Atlantic salmon proteins (PCTs) and putative autonomous 3′UTR transcripts, were counted in each sequenced sample using samtools idxstats (Figure 1B) [83].

4.4. Free-Energy Levels of Non-Coding Transcripts

The minimum free-energy of each transcript was calculated using the rnafold algorithm implemented by ViennaRNA, version 2.4.12 [84], using the following options: –p –d2 –noLP. The minimum free-energies of the transcripts were then compared to the minimum free-energies of a randomly selected set of protein coding transcripts (Figure 5A).

4.5. Functional Annotation of Putative Autonomous 3′UTRs and PCTs of the Same mRNA

GO analysis (http://www.geneontology.org) was performed to construct gene annotations. To retrieve GO IDs for particular proteins, we used the Retrieve/ID mapping tool from the UniProt website [85]. WEGO (Web Gene Ontology Annotation Plot) was used to visualize the results [86]. A p-value < 0.05 was considered to indicate a statistically significant difference.

4.6. Real-Time PCR

To profile known and putative novel lncRNA expression, reverse transcription (RT) was carried out using SuperScript IV Reverse Transcriptase (Thermo Scientific, Waltham, MA, USA). The reaction contained 1 µg total RNA, 4 µL 5× RT buffer, 1 µL 0.1 M DTT, 1 µL 10 mM dNTP mix, 1 µL Ribonuclease Inhibitor and SuperScript IV RT enzyme, and 1 µL 50 µM Oligo(dT)20 primer. The reaction was carried out at 23 °C for 10 min, 55 °C for 10 min and 80 °C for 10 min. Synthesized cDNA samples were diluted (20×), stored at −80 °C, and thawed only once, just before the amplification.

Real-time PCR was used to determine relative expression of known and putative novel lncRNAs in the cDNA samples. Reactions were carried out in final volumes of 20 µL, consisting of 10 µL Power SYBR Green PCR Master Mix (Life Technologies, USA), 0.25 µM of each primer (forward and reverse; Table S3), 1 µL cDNA template and 7 µL PCR-grade water. Amplification was performed with a Quant Studio 5 Real-time PCR System (Applied Biosystems; Foster City, CA, USA) with the following conditions: 95 °C for 10 min, then 45 cycles of 95 °C for 15 s and 60 °C for 1 min. The reaction for each sample was carried out in duplicate. No-template controls (NTCs) were included to test for the possibility of cross-contamination. To check the quality of each PCR product, melting curve analyses were performed after each run. For normalization of data from the treatment (MC-LR) and control (PBS) groups, "uncharacterized transcript" was used as a reference gene. This transcript was selected based on RNA-Seq results. Its stability was confirmed by Real-Time PCR (standard deviation (SD) of quantification cycle (Cq) ± 0.84).

4.7. Statistical Methods

Contigs that were differentially expressed (DE known and novel lncRNAs, DE 3′UTRs, DE PCTs) in the MC-LR-treated and the control (PBS) groups were indicated using the DESeq2 package, version 1.28.0 [87] for R, version 3.6.3 [88]. Adjusted p-values were calculated with Benjamini and Hochberg's method [89]. Thresholds of a log2 fold-change > |2| and an adjusted p-value < 0.001 were used to filter out contigs with the smaller and less statistically significant differences between groups.

Before assessing the differences in minimum free-energy and content of GC base pairs, we used histograms and normal Q-Q plots (shown in Supplementary Figure S5) to assess the distribution of the data. These methods indicated that, considering the large sample size, any deviations from normality were too small to be important. Thus, we assessed differences between groups using Welch's t-test, which is robust to violations of

the assumption of homoscedasticity. 95% confidence intervals for differences are shown in square brackets in the main text, e.g., [9.5, 11.7]. Statistical calculations were handled in Python's statistical modules (Sci-Py, StatsModels). Confidence intervals were calculated using the R Tidyverse package.

Statistical calculations for qPCR data were performed using GenEx 7.0. To assess the significance of difference between groups, one-way independent analysis of variance (ANOVA) was used after log-transforming the data, followed by Dunnett's post hoc test.

4.8. Data Availability

The raw data from this study have been submitted to the NCBI SRA database. The accession numbers for data from the individual samples are given in Supplementary Table S1. De novo assembled whitefish liver transcriptome and sequences of transcripts identified in this study have been deposited in The Dryad Digital Repository (https://datadryad.org).

5. Conclusions

In this study, we detected differentially expressed polyadenylated lncRNAs in whitefish exposed to MC-LR. To achieve this, we constructed an extensive liver transcriptome that can be used to complete the current whitefish genome assemblies or to curate ones that are developed in the future. We obtained a dataset that provides a starting point for future studies on the role of lncRNAs in MC-LR-induced liver injury and subsequent liver regeneration. Among the detected DE transcripts, we identified novel, uncharacterized contigs that could potentially be used as non-invasive biomarkers of MC-LR-induced liver injury in whitefish. In addition, we detected transcripts with homology to lncRNAs previously described in other species. Current understanding of lncRNAs is limited [90], and we believe that our work is a step toward better understanding lncRNA expression and functions in the context of MC-LR toxicity, and the mechanisms of MC-LR toxicity in general. Lastly, we believe that to fully understand the molecular functions of lncRNAs, studies should adopt a broader perspective, including simultaneous analysis of all aspects of the network of competing endogenous RNAs. For that purpose, a combination of different methods of library preparation for RNA sequencing should be considered, which also may allow new types of RNA to be uncovered.

Supplementary Materials: Supplementary Materials can be found at https://www.mdpi.com/1422-0067/22/2/941/s1. Table S1: Detailed statistics on the quality of sequencing data from all (52) samples used for de novo assembly of the whitefish liver transcriptome. Samples in bold were used in this study for quantitative analysis of lncRNA. Table S2: Contig metrics of the filtered de novo assembled liver transcriptome. All metrics were calculated using Transrate, version 1.0.3. Table S3: Sequences of primers used in RT-qPCR. Figure S1: Alignment of our putative MALAT1 transcript to the seed sequence of human MALAT1 deposited in the Rfam database. (A) Output of cmscan hit alignment. (B) ClustalO alignment. Figure S2: Comparison of gene ontology terms of co-upregulated (A) and co-downregulated (B) putative PCT/3′UTR transcript pairs at 6 days (red bars) and 9 days (gray bars) of MC-LR exposure. Figure S3: Gene Ontology terms of DE contigs from the same mRNA after 1 day of the experiment that were both upregulated (A) or downregulated (C), as well as those with opposing expression profiles (B,D). Figure S4: Expression of selected putative novel lncRNAs in whitefish liver after 1, 6, 9 and 14 days of microcystin-LR (MC-LR) exposure quantified using RT-qPCR. Transcripts were selected based on RNA-Seq results. * $p < 0.05$ and ** $p < 0.01$. Points represent individual fish in respective experimental group. Figure S5: Histograms and normal Q-Q plots of minimum free-energy (MFE), content of GC base pairs and sequence length in protein-coding transcripts (PCTs) and non-coding transcripts (NCTs).

Author Contributions: Wrote the manuscript: M.F.; designed the study: P.B. and M.W.; edited the manuscript: P.B. and M.W.; carried out experiments: P.B., M.W., and M.F.; data analysis: M.F. All authors have read and agreed to the published version of the manuscript.

Funding: The project was funded by the National Science Centre of Poland (NCN; decision number: 2016/21/B/NZ9/03566). Paweł Brzuzan was the main recipient (Principal Investigator) of the NCN

OPUS 11 research grant. The funder (NCN) was not involved in study design, collection and analysis of data, preparation of the manuscript, or decision to publish.

Institutional Review Board Statement: The animal-related procedures were approved by the Local Ethics Committee for Experiments on Animals in Olsztyn, Poland (resolution No. 44/2016 of 30th November 2016).

Informed Consent Statement: Not applicable.

Data Availability Statement: The raw data from this study have been submitted to the NCBI SRA database. The accession numbers for data from the individual samples are given in Supplementary Table S1. De novo assembled whitefish liver transcriptome and sequences of transcripts identified in this study have been deposited in The Dryad Digital Repository (https://datadryad.org). The results of gene expression have been submitted to the NCBI Gene Expression Omnibus database.

Acknowledgments: We thank Stefan Dobosz, Janusz Krom, Rafał Różyński, and Tomasz Zalewski for their excellent assistance in hatchery operations.

Conflicts of Interest: The authors declare no conflict of interest.

Abbreviations

ATF3	activating transcription factor 3
BLAST	Basic local alignment search tool
BUSCO	Benchmarking set of Universal Single-Copy Orthologs
bp	base pair
DE	Differentially expressed
DILI	Drug-induced liver injury
FOS	fos proto-oncogene
GCH1	GTP cyclohydrolase 1
GO	Gene ontology
HOTAIR	HOX transcript antisense RNA
HOTTIP	HOXA transcript at the distal tip
HULC	Highly up-regulated in liver cancer
lncRNA	long non-coding RNA
MAPK	mitogen activated protein kinase
MC	microcystin
MC-LR	microcystin-LR
NCBI	National Centre for Biotechnology Information
ncRNAs	non-coding RNAs
NCTs	non-coding transcripts
miRNA	microRNA
ORF	Open Reading frame
PCTs	protein-coding transcripts
piRNA	piwi-associated RNA
RIN	RNA integrity number
RT	Reverse transcription
siRNA	small interfering RNA
SVM	Support Vector Machine

References

1. Fischer, W.; Dietrich, D. Pathological and Biochemical Characterization of Microcystin-Induced Hepatopancreas and Kidney Damage in Carp (Cyprinus carpio). *Toxicol. Appl. Pharmacol.* **2000**, *164*, 73–81. [CrossRef] [PubMed]
2. Weng, D.; Lu, Y.; Wei, Y.; Liu, Y.; Shen, P. The role of ROS in microcystin-LR-induced hepatocyte apoptosis and liver injury in mice. *Toxicology* **2007**, *232*, 15–23. [CrossRef] [PubMed]
3. Wei, L.; Sun, B.; Song, L.; Nie, P. Gene expression profiles in liver of zebrafish treated with microcystin-LR. *Environ. Toxicol. Pharmacol.* **2008**, *26*, 6–12. [CrossRef] [PubMed]
4. Shah, N.; Nelson, J.E.; Kowdley, K.V. MicroRNAs in Liver Disease: Bench to Bedside. *J. Clin. Exp. Hepatol.* **2013**, *3*, 231–242. [CrossRef]

5. Meng, X.; Peng, H.; Ding, Y.; Zhang, L.; Yang, J.; Han, X. A transcriptomic regulatory network among miRNAs, piRNAs, circRNAs, lncRNAs and mRNAs regulates microcystin-leucine arginine (MC-LR)-induced male reproductive toxicity. *Sci. Total. Environ.* **2019**, *667*, 563–577. [CrossRef]
6. Feng, Y.; Ma, J.; Xiang, R.; Li, X.-Y. Alterations in microRNA expression in the tissues of silver carp (Hypophthalmichthys molitrix) following microcystin-LR exposure. *Toxicon* **2017**, *128*, 15–22. [CrossRef]
7. Xu, L.; Qin, W.; Zhang, H.; Wang, Y.; Dou, H.; Yu, D.; Ding, Y.; Yang, L.; Wang, Y.P. Alterations in microRNA expression linked to microcystin-LR-induced tumorigenicity in human WRL-68 Cells. *Mutat. Res. Toxicol. Environ. Mutagen.* **2012**, *743*, 75–82. [CrossRef]
8. Wang, J.; Zhang, J.; Zheng, H.; Li, J.; Liu, D.; Li, H. Neutral evolution of "non-coding" complementary DNAs. *Nature* **2004**, *431*, 1–2. [CrossRef]
9. Zhao, L.; Wang, W. miR-125b suppresses the proliferation of hepatocellular carcinoma cells by targeting Sirtuin7. *Int. J. Clin. Exp. Med.* **2015**, *8*, 18469–18475.
10. Paraskevopoulou, M.D.; Hatzigeorgiou, A.G. Analyzing MiRNA-LncRNA Interactions. In *Methods in Molecular Biology*; Humana Press: Clifton, NJ, USA, 2016; Volume 1402, pp. 271–286.
11. Beermann, J.; Piccoli, M.-T.; Viereck, J.; Thum, T. Non-coding RNAs in Development and Disease: Background, Mechanisms, and Therapeutic Approaches. *Physiol. Rev.* **2016**, *96*, 1297–1325. [CrossRef]
12. Li, G.; Shi, H.; Wang, X.; Wang, B.; Qu, Q.; Geng, H.; Sun, H. Identification of diagnostic long non-coding RNA biomarkers in patients with hepatocellular carcinoma. *Mol. Med. Rep.* **2019**, *20*, 1121–1130. [CrossRef] [PubMed]
13. Wen, C.; Yang, S.; Zheng, S.; Feng, X.; Chen, J.; Yang, F. Analysis of long non-coding RNA profiled following MC-LR-induced hepatotoxicity using high-throughput sequencing. *J. Toxicol. Environ. Health Part A* **2018**, *81*, 1165–1172. [CrossRef] [PubMed]
14. Woźny, M.; Lewczuk, B.; Ziółkowska, N.; Gomułka, P.; Dobosz, S.; Łakomiak, A.; Florczyk, M.; Brzuzan, P. Intraperitoneal exposure of whitefish to microcystin-LR induces rapid liver injury followed by regeneration and resilience to subsequent exposures. *Toxicol. Appl. Pharmacol.* **2016**, *313*, 68–87. [CrossRef] [PubMed]
15. Brzuzan, P.; Woźny, M.; Wolińska, L.; Piasecka, A. Expression profiling in vivo demonstrates rapid changes in liver microRNA levels of whitefish (Coregonus lavaretus) following microcystin-LR exposure. *Aquat. Toxicol.* **2012**, *122*, 188–196. [CrossRef]
16. Brzuzan, P.; Florczyk, M.; Łakomiak, A.; Woźny, M. Illumina Sequencing Reveals Aberrant Expression of MicroRNAs and Their Variants in Whitefish (Coregonus lavaretus) Liver after Exposure to Microcystin-LR. *PLoS ONE* **2016**, *11*, e0158899. [CrossRef] [PubMed]
17. Jiang, N.; Meng, X.; Mi, H.; Chi, Y.; Li, S.; Jin, Z.; Tian, H.; He, J.; Shen, W.; Tian, H.; et al. Circulating lncRNA XLOC_009167 serves as a diagnostic biomarker to predict lung cancer. *Clin. Chim. Acta* **2018**, *486*, 26–33. [CrossRef]
18. Pauli, A.; Valen, E.; Lin, M.F.; Garber, M.; Vastenhouw, N.L.; Levin, J.Z.; Fan, L.; Sandelin, A.; Rinn, J.L.; Regev, A.; et al. Systematic identification of long noncoding RNAs expressed during zebrafish embryogenesis. *Genome Res.* **2011**, *22*, 577–591. [CrossRef]
19. Al-Tobasei, R.; Paneru, B.; Salem, M. Genome-Wide Discovery of Long Non-Coding RNAs in Rainbow Trout. *PLoS ONE* **2016**, *11*, e0148940. [CrossRef]
20. Paneru, B.; Al-Tobasei, R.; Palti, Y.; Wiens, G.D.; Salem, M. Differential expression of long non-coding RNAs in three genetic lines of rainbow trout in response to infection with Flavobacterium psychrophilum. *Sci. Rep.* **2016**, *6*, 36032. [CrossRef]
21. Carruthers, M.; Yurchenko, A.A.; Augley, J.J.; Adams, C.E.; Herzyk, P.; Elmer, K.R. De novo transcriptome assembly, annotation and comparison of four ecological and evolutionary model salmonid fish species. *BMC Genom.* **2018**, *19*, 32. [CrossRef]
22. Harris, Z.N.; Kovacs, L.G.; Londo, J.P. RNA-seq-based genome annotation and identification of long-noncoding RNAs in the grapevine cultivar 'Riesling'. *BMC Genom.* **2017**, *18*, 1–12. [CrossRef] [PubMed]
23. Chao, H.-P.; Chen, Y.; Takata, Y.; Tomida, M.W.; Lin, K.; Kirk, J.S.; Simper, M.S.; Mikulec, C.D.; Rundhaug, J.E.; Fischer, S.M.; et al. Systematic evaluation of RNA-Seq preparation protocol performance. *BMC Genom.* **2019**, *20*, 1–20. [CrossRef] [PubMed]
24. Sims, D.W.; Sudbery, I.M.; Ilott, N.E.; Heger, A.; Ponting, C.P. Sequencing depth and coverage: Key considerations in genomic analyses. *Nat. Rev. Genet.* **2014**, *15*, 121–132. [CrossRef] [PubMed]
25. Zhang, Y.; Yang, L.; Chen, L.-L. Life without A tail: New formats of long noncoding RNAs. *Int. J. Biochem. Cell Biol.* **2014**, *54*, 338–349. [CrossRef]
26. Ceschin, D.G.; Pires, N.S.; Mardirosian, M.N.; Lascano, C.I.; Venturino, A. The Rhinella arenarum transcriptome: De novo assembly, annotation and gene prediction. *Sci. Rep.* **2020**, *10*, 1–8. [CrossRef]
27. Wolfien, M.; Rimmbach, C.; Schmitz, U.; Jung, J.J.; Krebs, S.; Steinhoff, G.; Robert, D.; Wolkenhauer, O. TRAPLINE: A standardized and automated pipeline for RNA sequencing data analysis, evaluation and annotation. *BMC Bioinform.* **2016**, *17*, 1–11. [CrossRef]
28. Tarazona, S.; García-Alcalde, F.; Dopazo, J.; Ferrer, A.; Conesa, A. Differential expression in RNA-seq: A matter of depth. *Genome Res.* **2011**, *21*, 2213–2223. [CrossRef]
29. Kashi, K.; Henderson, L.; Bonetti, A.; Carninci, P. Discovery and functional analysis of lncRNAs: Methodologies to investigate an uncharacterized transcriptome. *Biochim. Biophys. Acta (BBA) Gene Regul. Mech.* **2016**, *1859*, 3–15. [CrossRef]
30. Eldem, V.; Zararsiz, G.; Taşçi, T.; Duru, I.P.; Bakir, Y.; Erkan, M. Transcriptome Analysis for Non-Model Organism: Current Status and Best-Practices. In *Applications of RNA-Seq and Omics Strategies: From Microorganisms to Human Health*; Books on Demand: Norderstedt, Germany, 2017.
31. Zuker, M.; Stiegler, P. Optimal computer folding of large RNA sequences using thermodynamics and auxiliary information. *Nucleic Acids Res.* **1981**, *9*, 133–148. [CrossRef]

32. Mohammadin, S.; Edger, P.P.; Pires, J.C.; Schranz, M.E. Positionally-conserved but sequence-diverged: Identification of long non-coding RNAs in the Brassicaceae and Cleomaceae. *BMC Plant Biol.* **2015**, *15*, 217. [CrossRef]
33. Mu, C.; Wang, R.; Li, T.; Li, Y.; Tian, M.; Jiao, W.; Huang, X.; Zhang, L.; Hu, X.; Wang, S.; et al. Long Non-Coding RNAs (lncRNAs) of Sea Cucumber: Large-Scale Prediction, Expression Profiling, Non-Coding Network Construction, and lncRNA-microRNA-Gene Interaction Analysis of lncRNAs in Apostichopus japonicus and Holothuria glaberrima During LPS Challenge and Radial Organ Complex Regeneration. *Mar. Biotechnol.* **2016**, *18*, 485–499. [CrossRef]
34. Yang, J.-R.; Zhang, J. Human long noncoding RNAs are substantially less folded than messenger RNAs. *Mol. Biol. Evol.* **2015**, *32*, 970–977. [CrossRef] [PubMed]
35. Hutchinson, J.N.; Ensminger, A.W.; Clemson, C.M.; Lynch, C.R.; Lawrence, J.B.; Chess, A. A screen for nuclear transcripts identifies two linked noncoding RNAs associated with SC35 splicing domains. *BMC Genom.* **2007**, *8*, 1–16. [CrossRef] [PubMed]
36. Ulitsky, I.; Shkumatava, A.; Jan, C.H.; Sive, H.; Bartel, D.P. Conserved Function of lincRNAs in Vertebrate Embryonic Development despite Rapid Sequence Evolution. *Cell* **2011**, *147*, 1537–1550. [CrossRef] [PubMed]
37. Sun, Y.; Ma, L. New Insights into Long Non-Coding RNA MALAT1 in Cancer and Metastasis. *Cancers* **2019**, *11*, 216. [CrossRef]
38. Zhang, B.; Arun, G.; Mao, Y.S.; Lazar, Z.; Hung, G.; Bhattacharjee, G.; Xiao, X.; Booth, C.J.; Wu, J.; Zhang, C.; et al. The lncRNA Malat1 Is Dispensable for Mouse Development but Its Transcription Plays a cis-Regulatory Role in the Adult. *Cell Rep.* **2012**, *2*, 111–123. [CrossRef]
39. Chen, L.; Yao, H.; Wang, K.; Liu, X. Long Non-Coding RNA MALAT1 Regulates ZEB1 Expression by Sponging miR-143-3p and Promotes Hepatocellular Carcinoma Progression. *J. Cell. Biochem.* **2017**, *118*, 4836–4843. [CrossRef]
40. Zhao, L.; Lou, G.; Li, A.; Liu, Y. lncRNA MALAT1 modulates cancer stem cell properties of liver cancer cells by regulating YAP1 expression via miR-375 sponging. *Mol. Med. Rep.* **2020**, *22*, 1449–1457. [CrossRef]
41. Xia, C.; Liang, S.; He, Z.; Zhu, X.; Chen, R.; Chen, J. Metformin, a first-line drug for type 2 diabetes mellitus, disrupts the MALAT1/miR-142-3p sponge to decrease invasion and migration in cervical cancer cells. *Eur. J. Pharmacol.* **2018**, *830*, 59–67. [CrossRef]
42. Li, F.; Li, X.; Qiao, L.; Liu, W.; Xu, C.; Wang, X. MALAT1 regulates miR-34a expression in melanoma cells. *Cell Death Dis.* **2019**, *10*, 389. [CrossRef]
43. Łakomiak, A.; Brzuzan, P.; Jakimiuk, E.; Florczyk, M.; Woźny, M. Molecular characterization of the cyclin-dependent protein kinase 6 in whitefish (*Coregonus lavaretus*) and its potential interplay with miR-34a. *Gene* **2019**, *699*, 115–124. [CrossRef] [PubMed]
44. Zhao, Y.; Xie, P.; Fan, H. Genomic Profiling of MicroRNAs and Proteomics Reveals an Early Molecular Alteration Associated with Tumorigenesis Induced by MC-LR in Mice. *Environ. Sci. Technol.* **2011**, *46*, 34–41. [CrossRef] [PubMed]
45. Wilusz, J.E.; Freier, S.M.; Spector, D.L. 3′ end processing of a long nuclear-retained non-coding RNA yields a tRNA-like cytoplasmic RNA. *Cell* **2008**, *135*, 919–932. [CrossRef] [PubMed]
46. Mercer, T.R.; Wilhelm, D.; Dinger, M.E.; Soldà, G.; Korbie, D.J.; Glazov, E.A.; Truong, V.; Schwenke, M.; Simons, C.; Matthaei, K.I.; et al. Expression of distinct RNAs from 3′ untranslated regions. *Nucleic Acids Res.* **2010**, *39*, 2393–2403. [CrossRef]
47. Kocabas, A.; Duarte, T.; Kumar, S.; Hynes, M.A. Widespread Differential Expression of Coding Region and 3′ UTR Sequences in Neurons and Other Tissues. *Neuron* **2015**, *88*, 1149–1156. [CrossRef]
48. Malka, Y.; Steiman-Shimony, A.; Rosenthal, E.; Argaman, L.; Cohen-Daniel, L.; Arbib, E.; Margalit, H.; Kaplan, T.; Berger, M. Post-transcriptional 3´-UTR cleavage of mRNA transcripts generates thousands of stable uncapped autonomous RNA fragments. *Nat. Commun.* **2017**, *8*, 1–11. [CrossRef]
49. Biales, A.D.; Bencic, D.C.; Flick, R.W.; DeLaCruz, A.; Gordon, D.A.; Huang, W. Global transcriptomic profiling of microcystin-LR or -RR treated hepatocytes (HepaRG). *Toxicon X* **2020**, *8*, 100060. [CrossRef]
50. Yoshizawa, S.; Matsushima, R.; Watanabe, M.F.; Harada, K.-I.; Ichihara, A.; Carmichael, W.W.; Fujiki, H. Inhibition of protein phosphatases by microcystis and nodularin associated with hepatotoxicity. *J. Cancer Res. Clin. Oncol.* **1990**, *116*, 609–614. [CrossRef]
51. Qu, X.; Hu, M.; Shang, Y.; Pan, L.; Jia, P.; Fu, C.; Liu, Q.; Wang, Y. Liver Transcriptome and miRNA Analysis of Silver Carp (*Hypophthalmichthys molitrix*) Intraperitoneally Injected with Microcystin-LR. *Front. Physiol.* **2018**, *9*. [CrossRef]
52. Chen, H.-Q.; Zhao, J.; Li, Y.; He, L.-X.; Huang, Y.-J.; Shu, W.-Q. Gene expression network regulated by DNA methylation and microRNA during microcystin-leucine arginine induced malignant transformation in human hepatocyte L02 cells. *Toxicol. Lett.* **2018**, *289*, 42–53. [CrossRef]
53. Kartha, R.V.; Subramanian, S. Competing endogenous RNAs (ceRNAs): New entrants to the intricacies of gene regulation. *Front. Genet.* **2014**, *5*, 8. [CrossRef] [PubMed]
54. Gehringer, M.M. Microcystin-LR and okadaic acid-induced cellular effects: A dualistic response. *FEBS Lett.* **2003**, *557*, 1–8. [CrossRef]
55. Toivola, D.M.; Eriksson, J.E. Toxins Affecting Cell Signalling and Alteration of Cytoskeletal Structure. *Toxicol. Vitr.* **1999**, *13*, 521–530. [CrossRef]
56. Safa, A.; Abak, A.; Shoorei, H.; Taheri, M.; Ghafouri-Fard, S. MicroRNAs as regulators of ERK/MAPK pathway: A comprehensive review. *Biomed. Pharmacother.* **2020**, *132*, 110853. [CrossRef] [PubMed]
57. Li, C.; Zhang, W.; Yang, H.; Xiang, J.; Wang, X.; Wang, J. Integrative analysis of dysregulated lncRNA-associated ceRNA network reveals potential lncRNA biomarkers for human hepatocellular carcinoma. *PeerJ* **2020**, *8*, e8758. [CrossRef] [PubMed]

58. Li, L.; Rezvan, A.; Salerno, J.C.; Husain, A.; Kwon, K.; Jo, H. GTP Cyclohydrolase I Phosphorylation and Interaction with GTP Cyclohydrolase Feedback Regulatory Protein Provide Novel Regulation of Endothelial Tetrahydrobiopterin and Nitric Oxide. *Circ. Res.* **2010**, *106*, 328–336. [CrossRef] [PubMed]
59. Li, P.; Yin, Y.-L.; Guo, T.; Sun, X.-Y.; Ma, H.; Zhu, M.-L. Inhibition of Aberrant MicroRNA-133a Expression in Endothelial Cells by Statin Prevents Endothelial Dysfunction by Targeting GTP Cyclohydrolase 1 in Vivo. *Circulation* **2016**, *134*, 1752–1765. [CrossRef]
60. Yarmishyn, A.A.; Kurochkin, I.V. Long noncoding RNAs: A potential novel class of cancer biomarkers. *Front. Genet.* **2015**, *6*, 145. [CrossRef]
61. Zheng, S.; Wen, C.; Yang, S.; Yang, Y.; Yang, F. Circular RNA expression profiles following MC-LR treatment in human normal liver cell line (HL7702) cells using high-throughput sequencing analysis. *J. Toxicol. Environ. Health Part A* **2019**, *82*, 1103–1112. [CrossRef]
62. Zhou, J.; Li, Y.; Liu, X.; Long, Y.; Chen, J. LncRNA-Regulated Autophagy and its Potential Role in Drug-induced Liver Injury. *Ann. Hepatol.* **2018**, *17*, 355–363. [CrossRef]
63. Florczyk, M.; Brzuzan, P.; Krom, J.; Woźny, M.; Łakomiak, A. miR-122-5p as a plasma biomarker of liver injury in fish exposed to microcystin-LR. *J. Fish Dis.* **2015**, *39*, 741–751. [CrossRef] [PubMed]
64. Florczyk, M.; Brzuzan, P.; Łakomiak, A.; Jakimiuk, E.; Woźny, M. Microcystin-LR-Triggered Neuronal Toxicity in Whitefish Does Not Involve MiR124-3p. *Neurotox. Res.* **2018**, *35*, 29–40. [CrossRef] [PubMed]
65. Bernard, D.; Prasanth, K.V.; Tripathi, V.; Colasse, S.; Nakamura, T.; Xuan, Z.; Zhang, M.Q.; Sedel, F.; Jourdren, L.; Coulpier, F.; et al. A long nuclear-retained non-coding RNA regulates synaptogenesis by modulating gene expression. *EMBO J.* **2010**, *29*, 3082–3093. [CrossRef] [PubMed]
66. Han, Y.; Wu, Z.; Wu, T.; Huang, Y.; Cheng, Z.; Li, X.; Sun, T.; Xie, X.; Zhou, Y.; Du, Z. Tumor-suppressive function of long noncoding RNA MALAT1 in glioma cells by downregulation of MMP2 and inactivation of ERK/MAPK signaling. *Cell Death Dis.* **2016**, *7*, e2123. [CrossRef] [PubMed]
67. Liu, W.; Zhang, Q.; Zhang, J.; Pan, W.; Zhao, J.; Xu, Y. Long non-coding RNA MALAT1 contributes to cell apoptosis by sponging miR-124 in Parkinson disease. *Cell Biosci.* **2017**, *7*, 1–9. [CrossRef]
68. Brzuzan, P.; Woźny, M.; Ciesielski, S.; Łuczyński, M.K.; Gora, M.; Kuźmiński, H.; Dobosz, S. Microcystin-LR induced apoptosis and mRNA expression of p53 and cdkn1a in liver of whitefish (*Coregonus lavaretus* L.). *Toxicon* **2009**, *54*, 170–183. [CrossRef]
69. Bolger, A.M.; Lohse, M.; Usadel, B. Trimmomatic: A flexible trimmer for Illumina sequence data. *Bioinformatics* **2014**, *30*, 2114–2120. [CrossRef]
70. Grabherr, M.G.; Haas, B.J.; Yassour, M.; Levin, J.Z.; Thompson, D.A.; Amit, I. Trinity: Reconstructing a full-length transcriptome without a genome from RNA-Seq data. *Nat. Biotechnol.* **2011**, *29*, 644–652. [CrossRef]
71. Langmead, B.; Salzberg, S.L. Fast gapped-read alignment with Bowtie 2. *Nat. Methods* **2012**, *9*, 357–359. [CrossRef]
72. Fu, L.; Niu, B.; Zhu, Z.; Wu, S.; Li, W. CD-HIT: Accelerated for clustering the next-generation sequencing data. *Bioinformatics* **2012**, *28*, 3150–3152. [CrossRef]
73. Li, B.; Dewey, C.N. RSEM: Accurate transcript quantification from RNA-Seq data with or without a reference genome. *BMC Bioinform.* **2011**, *12*, 323. [CrossRef] [PubMed]
74. Simão, F.A.; Waterhouse, R.M.; Ioannidis, P.; Kriventseva, E.V.; Zdobnov, E.M. BUSCO: Assessing genome assembly and annotation completeness with single-copy orthologs. *Bioinformatics* **2015**, *31*, 3210–3212. [CrossRef] [PubMed]
75. Kriventseva, E.V.; Kuznetsov, D.; Tegenfeldt, F.; Manni, M.; Dias, R.; A Simão, F.; Zdobnov, E. OrthoDB v10: Sampling the diversity of animal, plant, fungal, protist, bacterial and viral genomes for evolutionary and functional annotations of orthologs. *Nucleic Acids Res.* **2019**, *47*, D807–D811. [CrossRef] [PubMed]
76. Haas, B.J.; Papanicolaou, A.; Yassour, M.; Grabherr, M.; Blood, P.D.; Bowden, J.; Couger, M.B.; Eccles, D.; Li, B.; Lieber, M.; et al. De novo transcript sequence reconstruction from RNA-seq using the Trinity platform for reference generation and analysis. *Nat. Protoc.* **2013**, *8*, 1494–1512. [CrossRef]
77. Camacho, C.E.; Coulouris, G.; Avagyan, V.; Ma, N.; Papadopoulos, J.S.; Bealer, K.; Madden, T.L. BLAST+: Architecture and applications. *BMC Bioinform.* **2009**, *10*, 421. [CrossRef]
78. El-Gebali, S.; Mistry, J.; Bateman, A.; Eddy, S.R.; Luciani, A.; Potter, S.C.; Qureshi, M.; Richardson, L.J.; Salazar, G.A.; Smart, A.; et al. The Pfam protein families database in 2019. *Nucleic Acids Res.* **2018**, *47*, D427–D432. [CrossRef]
79. Bryant, D.M.; Johnson, K.; DiTommaso, T.; Tickle, T.; Couger, M.B.; Payzin-Dogru, D.; Lee, T.J.; Leigh, N.D.; Kuo, T.-H.; Davis, F.G.; et al. A Tissue-Mapped Axolotl De Novo Transcriptome Enables Identification of Limb Regeneration Factors. *Cell Rep.* **2017**, *18*, 762–776. [CrossRef]
80. Kalvari, I.; Argasinska, J.; Quinones-Olvera, N.; Nawrocki, E.P.; Rivas, E.; Eddy, S.R.; Bateman, A.; Finn, R.D.; Petrov, A.I. Rfam 13.0: Shifting to a genome-centric resource for non-coding RNA families. *Nucleic Acids Res.* **2018**, *46*, D335–D342. [CrossRef]
81. Nawrocki, E.P.; Eddy, S.R. Infernal 1.1: 100-fold faster RNA homology searches. *Bioinformatics* **2013**, *29*, 2933–2935. [CrossRef]
82. Kong, L.; Zhang, Y.; Ye, Z.-Q.; Liu, X.-Q.; Zhao, S.-Q.; Wei, L.; Gao, G. CPC: Assess the protein-coding potential of transcripts using sequence features and support vector machine. *Nucleic Acids Res.* **2007**, *35*, W345–W349. [CrossRef]
83. Li, H.; Xie, P.; Li, G.; Hao, L.; Xiong, Q. In vivo study on the effects of microcystin extracts on the expression profiles of proto-oncogenes (*c-fos*, *c-jun* and *c-myc*) in liver, kidney and testis of male Wistar rats injected i.v. with toxins. *Toxicon* **2009**, *53*, 169–175. [CrossRef] [PubMed]

84. Lorenz, R.; Bernhart, S.H.; Zu Siederdissen, C.H.; Tafer, H.; Flamm, C.; Stadler, P.F.; Hofacker, I.L. ViennaRNA Package 2.0. *Algorithms Mol. Biol.* **2011**, *6*, 26. [CrossRef] [PubMed]
85. Consortium, T.U. UniProt: A worldwide hub of protein knowledge. *Nucleic Acids Res.* **2019**, *47*, 506–515. [CrossRef] [PubMed]
86. Ye, J.; Fang, L.; Zheng, H.; Zhang, Y.; Chen, J.; Zhang, Z.; Wang, J.M.; Li, S.; Li, R.; Bolund, L. WEGO: A web tool for plotting GO annotations. *Nucleic Acids Res.* **2006**, *34*, 293–297. [CrossRef] [PubMed]
87. Love, M.I.; Huber, W.; Anders, S. Moderated estimation of fold change and dispersion for RNA-seq data with DESeq2. *Genome Biology.* **2014**, *15*, 1–21. [CrossRef] [PubMed]
88. R Core Team. R: A Language and Environment for Statistical Computing. 2020. Available online: www.r-project.org (accessed on 29 February 2020).
89. Benjamini, Y.; Hochberg, Y. Controlling the False Discovery Rate—A Practical and Powerful Approach to Multiple Testing. *J. R. Stat. Soc. Ser. B Methodol.* **1995**, *57*, 289–300. [CrossRef]
90. Hezroni, H.; Koppstein, D.; Schwartz, M.G.; Avrutin, A.; Bartel, D.P.; Ulitsky, I. Principles of Long Noncoding RNA Evolution Derived from Direct Comparison of Transcriptomes in 17 Species. *Cell Rep.* **2015**, *11*, 1110–1122. [CrossRef]

Oświadczenia współautorów

Mgr Janusz Krom

Zakład Hodowli Ryb Łososiowatych w Rutkach
Instytut Rybactwa Śródlądowego
83-330 Żukowo

Rutki, dnia 5 kwietnia 2022 r.

OŚWIADCZENIE

Oświadczam, że w pracy Florczyk M, Brzuzan P, Krom J, Woźny M, Łakomiak A. *miR-122-5p as a plasma biomarker of liver injury in fish exposed to microcystin-LR*. Journal of Fish Diseases. 2016;39:741–51 mój udział polegał na wykonaniu części prac związanych z przygotowaniem doświadczenia z wykorzystaniem siei, a także asystowanie przy przeprowadzaniu ekspozycji siei na toksynę oraz pomoc przy pobieraniu materiału do badań. Swój udział szacuję na 8%.

Podpis

Janusz Krom

Dr Jakimiuk Ewa
Katedra Prewencji Weterynaryjnej i Higieny Pasz
Wydział Medycyny Weterynaryjnej
Uniwersytet Warmińsko-Mazurski w Olsztynie
10-719 Olsztyn

Olsztyn, dnia 14 kwietnia 2022 r.

O Ś W I A D C Z E N I E

Oświadczam, że w pracy Florczyk M, Brzuzan P, Łakomiak A, Jakimiuk E, Woźny M. *Microcystin-LR-Triggered Neuronal Toxicity in Whitefish Does Not Involve MiR124-3p.* Neurotoxicity Research. 2019;35:29–40 mój udział polegał na przystosowaniu laboratorium do prowadzenia hodowli komórkowej oraz prowadzeniu instruktażu hodowli komórek eukariotycznych HEK-293T. Swój udział szacuję na 8%.

Podpis

Ewa Jakimiuk

Dr Alicja Łakomiak

Olsztyn, dnia 13 kwietnia 2022 r.

OŚWIADCZENIA

Oświadczam, że w pracy Florczyk M, Brzuzan P, Krom J, Woźny M, Łakomiak A. *miR-122-5p as a plasma biomarker of liver injury in fish exposed to microcystin-LR*. Journal of Fish Diseases. 2016;39:741–51 mój udział polegał na przeprowadzeniu optymalizacji metody RT-PCR. Swój udział szacuję na 2%.

W pracy Florczyk M, Brzuzan P, Łakomiak A, Jakimiuk E, Woźny M. *Microcystin-LR-Triggered Neuronal Toxicity in Whitefish Does Not Involve MiR124-3p*. Neurotoxicity Research. 2019;35:29–40 mój udział polegał na wykonaniu części prac doświadczalnych, do których zaliczało się przeprowadzenie optymalizacji transfekcji komórek HEK293T. Swój udział szacuję na 2%.

A. Łakomiak

Podpis

Prof. dr hab. Paweł Brzuzan
Katedra Biotechnologii w Ochronie Środowiska
Wydział Geoinżynierii
Uniwersytet Warmińsko-Mazurski w Olsztynie
10-709 Olsztyn

Olsztyn, dnia 14 kwietnia 2022 r.

O Ś W I A D C Z E N I A

Oświadczam, że w pracy Florczyk M, Brzuzan P, Krom J, Woźny M, Łakomiak A. *miR-122-5p as a plasma biomarker of liver injury in fish exposed to microcystin-LR*. Journal of Fish Diseases. 2016;39:741–51 mój udział polegał na przygotowaniu koncepcji pracy, nadzorze merytorycznym, interpretacji uzyskanych wyników, odpowiedzi na rezenzje oraz kierowaniu projektem naukowym obejmującym badania opisane w pracy. Swój udział szacuję na 12%.

W pracy Florczyk M, Brzuzan P, Łakomiak A, Jakimiuk E, Woźny M. *Microcystin-LR-Triggered Neuronal Toxicity in Whitefish Does Not Involve MiR124-3p.* Neurotoxicity Research. 2019;35:29–40 mój udział polegał na przygotowaniu koncepcji pracy, nadzorze merytorycznym, interpretacji uzyskanych wyników, odpowiedzi na recenzje. Swój udział szacuję na 12%.

W pracy Florczyk M, Brzuzan P, Woźny M. *De Novo Profiling of Long Non-Coding RNAs Involved in MC-LR-Induced Liver Injury in Whitefish: Discovery and Perspectives.* International Journal of Molecular Sciences. 2021;22:941 mój udział polegał na przygotowaniu koncepcji pracy, nadzorze merytorycznym, interpretacji uzyskanych wyników, odpowiedzi na recenzje oraz kierowaniu projektem naukowym obejmującym badania opisane w pracy. Swój udział szacuję na 10%.



Podpis

Dr hab. inż Maciej Woźny, prof. UWM
Katedra Biotechnologii w Ochronie Środowiska
Wydział Geoinżynierii
Uniwersytet Warmińsko-Mazurski w Olsztynie
10-709 Olsztyn

Olsztyn, dnia 14 kwietnia 2022 r.

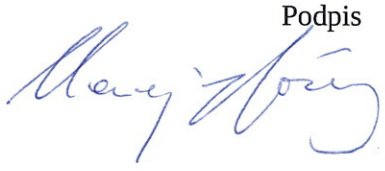
O Ś W I A D C Z E N I A

Oświadczam, że w pracy Florczyk M, Brzuzan P, Krom J, Woźny M, Łakomiak A. *miR-122-5p as a plasma biomarker of liver injury in fish exposed to microcystin-LR*. Journal of Fish Diseases. 2016;39:741–51 mój udział polegał na zaplanowaniu i przeprowadzeniu doświadczeń z wykorzystaniem ryb, poborze prób do badań, interpretacji uzyskanych wyników i odpowiedzi na recenzje. Swój udział szacuję na 10%.

W pracy Florczyk M, Brzuzan P, Łakomiak A, Jakimiuk E, Woźny M. *Microcystin-LR-Triggered Neuronal Toxicity in Whitefish Does Not Involve MiR124-3p*. Neurotoxicity Research. 2019;35:29–40 mój udział polegał na zaplanowaniu i przeprowadzeniu doświadczeń z wykorzystaniem ryb, poborze prób do badań, interpretacji uzyskanych wyników i odpowiedzi na recenzje. Swój udział szacuję na 10%.

W pracy Florczyk M, Brzuzan P, Woźny M. *De Novo Profiling of Long Non-Coding RNAs Involved in MC-LR-Induced Liver Injury in Whitefish: Discovery and Perspectives.* International Journal of Molecular Sciences. 2021;22:941 mój udział polegał na zaplanowaniu i przeprowadzeniu doświadczeń z wykorzystaniem ryb, poborze prób do badań, interpretacji uzyskanych wyników i odpowiedzi na recenzje. Swój udział szacuję na 10%.

Podpis



Mgr Maciej Florczyk
Katedra Biotechnologii w Ochronie Środowiska
Wydział Geoinżynierii
Uniwersytet Warmińsko-Mazurski w Olsztynie
10-709 Olsztyn

Olsztyn, dnia 14 kwietnia 2022 r.

O Ś W I A D C Z E N I A

Oświadczam, że w pracy Florczyk M, Brzuzan P, Krom J, Woźny M, Łakomiak A. *miR-122-5p as a plasma biomarker of liver injury in fish exposed to microcystin-LR*. Journal of Fish Diseases. 2016;39:741–51 mój udział polegał na pobieraniu osocza do badań, izolacji RNA z osocza, przeprowadzeniu reakcji odwrotnej transkrypcji, wykonaniu rekcji RT-PCR, analizie i interpretacji wyników badań, przygotowaniu manuskryptu oraz odpowiedzi na recenzje. Swój udział szacuję na 68%.

W pracy Florczyk M, Brzuzan P, Łakomiak A, Jakimiuk E, Woźny M. *Microcystin-LR-Triggered Neuronal Toxicity in Whitefish Does Not Involve MiR124-3p.* Neurotoxicity Research. 2019;35:29–40 mój udział polegał na poznaniu i analizie sekwencji cDNA genu *gfap* u siei, przygotowaniu konstruktów opartych na wektorze plazmidowym pmirGLO, zbadaniu funkcji regulacyjnej MiR124-3p względem gfap z zastosowaniem metody reporterowej, profilowaniu ekspresji, analizie statystycznej, interpretacji wyników, przygotowaniu manuskryptu, odpowiedzi na recenzje i kierowaniu projektem naukowym obejmującym badania opisane w pracy. Swój udział szacuję na 68%.

W pracy Florczyk M, Brzuzan P, Woźny M. *De Novo Profiling of Long Non-Coding RNAs Involved in MC-LR-Induced Liver Injury in Whitefish: Discovery and Perspectives.* International Journal of Molecular Sciences. 2021;22:941 mój udział polegał na wykonaniu szeregu analiz bioinformatycznych zmierzających do identyfikacji sekwencji długich niekodujących RNA u siei oraz profilowaniu ich ekspresji, jak również analizie statystycznej, analizie i interpretacji wyników, przygotowaniu manuskryptu oraz odpowiedzi na recenzje. Swój udział szacuję na 80%.

Podpis

Maciej Florczyk